Geomechanical dynamics in granite-dominated deep geothermal drilling: From mineral-scale thermal damage to macroscopic mechanical responses

Author(s): Lu, Shuaiyi; Ma, Yinlong; Yu, Ziwang; Cong, Lianghan; Zeng, Lingtao

Title: Geomechanical dynamics in granite-dominated deep geothermal drilling: From mineral-scale thermal damage to macroscopic mechanical responses

Year: 2026

Version: Accepted manuscript

Please cite the original version:

Lu, S., Ma, Y., Yu, Z., Cong, L., & Zeng, L. (2026). Geomechanical dynamics in granite-dominated deep geothermal drilling: From mineral-scale thermal damage to macroscopic mechanical responses. *Renewable and Sustainable Energy Reviews, 244,* 117393. https://doi.org/10.1016/j.rser.2026.117393

Geomechanical dynamics in granite-dominated deep geothermal drilling: From mineral-scale thermal damage to macroscopic mechanical responses

Shuaiyi Lu[a], Yinlong Ma[a*], Ziwang Yu[a], Lianghan Cong[b], Lingtao Zeng[a]

a State Key Laboratory of Deep Earth Exploration and Imaging, College of Construction Engineering, Jilin University, Changchun 130026, China

b Department of Energy Technology, University of Vaasa, P.O.Box 700, FIN-65101, Vaasa, Finland

Abstract

Deep geothermal energy is a stable, clean, and renewable resource vital to the transition to sustainable energy systems. However, extreme temperatures and hard rock formations in deep reservoirs pose geomechanical challenges to efficient and safe drilling. This paper reviews advances in geomechanical research for deep geothermal reservoir drilling, with the quantitative treatment centerd on granite and other crystalline basement reservoirs, for which the evidence base is most complete. First, it examines high-temperature mechanisms, including thermal expansion anisotropy in rock minerals and microcrack development associated with quartz phase transitions. It details the resulting degradation of rock strength, the brittle-ductile transition, and the staged nonlinear evolution of permeability and thermal conductivity. Next, addressing low rock-breaking efficiency caused by high confining pressure-induced suppression of crack propagation and enhanced ductility at elevated temperatures, the review summarizes the evolution from conventional mechanical breaking to advanced techniques such as combined axial-torsional impact, thermal stress assistance, and directed energy methods. It contrasts physics-based and data-driven models for drilling performance evaluation and parameter prediction, assessing their suitability for geothermal drilling conditions. From the thermo-hydro-mechanical (THM) multi-field

[*] Corresponding author.

E-mail address: ylma@jlu.edu.cn

coupling perspective, the review analyzes how drilling fluid cooling-induced transient thermal stresses cause wellbore wall tensile failure, triggering a feedback loop of lost circulation, cooling, and fracture propagation. It further evaluates wellbore stability failure criteria and dynamic lost circulation control strategies optimized for complex conditions. Finally, the review identifies key geomechanical challenges in deep geothermal drilling and outlines future directions, including intelligent evaluation systems, dynamic multi-field coupling models, and integrated engineering efficiency optimization.

Keywords: Deep geothermal drilling; THM coupling; High-temperature rock mechanics; Rock-breaking efficiency; Wellbore stability

---

1 Introduction

The continued large-scale consumption of fossil fuels such as coal and oil has driven a continuous rise in atmospheric CO_2 concentration, leading to global warming, a challenge shared across the world [1, 2]. To address this crisis, nations are actively pursuing energy transitions and have committed under the Paris Agreement to limiting global average temperature rise to well below 2 °C above pre-industrial levels. Achieving this target is widely recognized as requiring coordinated strategies: reducing existing emissions through carbon capture, utilization, and storage (CCUS) while vigorously developing renewable energy to replace fossil fuels, thereby progressively achieving deep decarbonization of the energy system [3-5]. Within this framework, geothermal energy is recommended by the Intergovernmental Panel on Climate Change (IPCC) as one of the important options for advancing the energy transition and mitigating climate change. With vast reserves, high stability, and low environmental impact, geothermal energy plays a key role in building diversified green energy systems [6, 7]. Global geothermal development is shifting from shallow hydrothermal systems to deep hot dry rock (HDR) and enhanced geothermal systems (EGS), with target depths typically ranging from 3 km to 6 km or greater. Typical HDR reservoirs exceed 150 °C, while in extreme fields such as Krafla in Iceland, encountered temperatures can surpass 900 °C [8, 9]. Although deep geothermal resources offer immense potential for power generation and heating, current technical bottlenecks in efficient and safe drilling under extreme conditions hinder the large-scale utilization needed to meet global climate goals.

Although deep geothermal drilling has partially borrowed technical approaches from conventional oil and gas drilling, the geomechanical responses encountered are far more complex. This complexity arises because geothermal reservoirs differ fundamentally from sedimentary oil and gas reservoirs in lithological characteristics, dominant physical field mechanisms, and engineering objectives. Deep geothermal development typically targets highly abrasive crystalline basement rocks. The mechanical behavior of these rocks is no longer dominated by pore pressure alone but is strongly influenced by thermal stresses induced by extreme temperature fields and the brittle-ductile transition. Moreover, geothermal well construction must account for the exceptionally high demands that subsequent high-pressure reservoir stimulation places on wellbore integrity. Although geothermal drilling also considers reservoir damage, its core engineering objective has shifted from protecting matrix porosity in conventional oil and gas wells to preserving and pre-stimulating natural and engineered fracture networks. To clearly illustrate the unique characteristics of deep geothermal drilling and the scientific challenges it faces, Table 1 provides a systematic comparison between deep geothermal drilling and conventional oil and gas drilling across target formations, dominant physical field characteristics, and key geomechanical responses.

Table 1. Comparison of key features and geomechanical responses between deep geothermal drilling and conventional oil and gas drilling

Characteristic	Conventional oil & gas drilling	Deep geothermal drilling	Key geomechanical-response difference
Target formation	Mainly sedimentary rocks (sand, mud, shale), burial depth 1–5 km	Mainly crystalline hard rock (granite, metamorphic rock), burial depth 3–6 km	Poor rock drillability; higher MSE for rock breaking
Formation temperature	Usually below 120 °C	Above 150 °C	Induces mineral phase transitions and thermal-damage cracks
Rock compressive strength	Sedimentary rocks (sandstone, mudstone/shale) relatively low	Intact crystalline hard rock higher; further weakened in deep high-temperature environments	Higher overall strength; superimposed high temperature induces additional damage
Reservoir permeability	Conventional reservoirs mD to D	Several orders of magnitude lower; requires hydraulic-fracturing stimulation	Extremely low natural productivity; completion must prepare wellbore integrity for high-pressure stimulation
Pressure characteristics	Often accompanied by overpressure, requiring strict pressure control	Large-scale lost circulation occurs	Causes a “loss–cooling” thermal-stress feedback loop
Drilling fluid	Water-based fluids stable to 150 °C	At high temperature additives degrade and rheology changes abruptly; oil-based fluids or air/foam often used	Fluid properties degrade at high temperature and wellbore temperature-field prediction is more difficult

Dominant wellbore-instability mechanism	Mainly shear failure from pore-pressure imbalance, with mudstone/shale hydration	Cooling-induced transient tensile thermal-stress fractures; high-temperature plastic creep and borehole shrinkage	Shifts from M–C coupling dominance to T–M coupling dominance
Drilling-stage objective	Penetrate and connect hydrocarbon-bearing formations	Reach high-temperature formations and provide access for reservoir stimulation	Geothermal drilling must prepare wellbore integrity for subsequent high-pressure fracturing
Expectation for the formation	Protect porosity; prevent drilling-fluid damage to the producing layer	Protect natural fracture channels or pre-induce micro-fractures	Induced fracture development may damage the reservoir, reducing productivity

Because geothermal reservoirs possess these distinctive characteristics, research advances from conventional oil and gas drilling do not fully transfer. The extreme conditions in deep geothermal wells frequently trigger engineering incidents well beyond those typically expected [10]. Regarding wellbore stability [11, 12], frequent stuck-pipe incidents due to wellbore collapse and cuttings accumulation have occurred in Kenya's Olkaria geothermal field, with well OWGBDV sidelined for 109 days as a result [13]. Similarly, China’s Tianjin SR-28 geothermal well experienced severe tool sticking caused by complex formation collapse [14, 15]. In terms of bottom-hole pressure balance and completion safety, encountering extreme high-temperature and high-pressure reservoirs readily triggers blowout risks [16, 17]. At New Zealand’s Wairakei field, drilling well WK204 penetrated a high-temperature, high-pressure fracture zone with inadequate pressure control, resulting in a massive blowout that lasted 13 years and formed a 70 m diameter crater [18]. A blowout during drilling in the Hawaii geothermal project severely undermined the region's geothermal development prospects, underscoring the critical importance of pressure management in high-temperature geothermal operations [19, 20]. The 2017 Mw 5.4 earthquake in Pohang, South Korea, is to date the largest induced seismic event in the history of EGS; it was caused by reservoir hydraulic stimulation activating a critically stressed fault, resulted in significant casualties and economic losses, and led to the permanent shutdown of the Pohang EGS project [21, 22]. Drilling can also directly induce seismic activity. In Switzerland’s St. Gallen geothermal well, high-concentration methane influx was followed by high-pressure injection of large volumes of drilling fluid to control the gas kick, disturbing in-situ stresses and triggering earthquakes, an event that ultimately led to project termination [23, 24]. Beyond these incidents, lost circulation during drilling can directly impair reservoir properties, causing irreversible declines in productivity [25, 26]. Surveys of deep geothermal exploration in Henan Province, China, indicate that over 70% of wells in the 1200 to 3800 m depth interval failed to achieve expected water production due to reservoir damage, resulting in high abandonment rates [27]. The reservoir in New Mexico's Baca geothermal field exhibits pronounced underpressure, leading to severe lost circulation issues during drilling, where drilling fluids and cuttings invaded productive fractures and significantly impaired well performance [28, 29].

These representative engineering incidents clearly highlight the urgent need for research on geomechanical responses during deep geothermal well drilling. Deep drilling is not merely a mechanical rock-breaking process but a dynamic process governed by coupled thermo-hydro-mechanical (THM) interactions. Although existing studies have conducted extensive engineering investigations into rate-of-penetration enhancement and lost circulation control in geothermal development, and related progress has been organized in several reviews, these reviews tend to be topic-specific. For example, Song et al.[30] systematically organized geothermal drilling and completion tools, drilling fluids, and rock-breaking technologies; Kumari and Ranjith [7] reviewed THMC coupling and fracture management in EGS at the reservoir scale; and Isania and Elahifar [31] summarized progress in machine-learning methods for rates of penetration (ROP) and wellbore-stability prediction. However, these works are largely single-theme reviews of process optimization, reservoir management, or algorithmic prediction, and a systematic review of the mechanical evolution path from mineral-scale thermal damage to wellbore and bit response in geothermal drilling is still lacking. The essence of deep geothermal drilling lies in the nonlinear mechanical response of the rock mineral framework to energy disturbances under extreme conditions. Furthermore, geomechanical problems manifest not only in isolated sudden risks but more critically in strong feedback loops between evolving rock properties and engineering hazards (Fig. 1). For example, high-temperature-induced nonlinear rock damage and plastic creep are underlying causes of borehole shrinkage and stuck pipe [32, 33], while transient thermal stresses from drilling fluid cooling represent the core mechanical mechanism driving tensile fracture propagation and uncontrolled lost circulation [34, 35]. The evolution mechanisms from thermodynamic mismatch among mineral components to macroscopic engineering responses remain poorly understood, resulting in risk predictions under complex conditions that lack a solid physical foundation. Therefore, in-depth analysis of high-temperature-induced nonlinear rock damage mechanisms and the development of dynamic evaluation systems accounting for multi-field coupling are essential. Using these insights to optimize bit rock-breaking methods and drilling fluid circulation patterns is critical for ensuring wellbore integrity and extraction efficiency in deep geothermal operations. From an economic standpoint, drilling cost is a central bottleneck constraining the commercialization of deep geothermal energy. In geothermal projects, drilling and completion expenditures typically account for 30%–60% of total investment [36, 37]. Moreover, at the same depth the drilling cost of a geothermal well is usually substantially higher than that of an oil and gas well and increases nonlinearly with depth [38, 39]. This makes the geomechanical problems reviewed in this paper (rock-breaking efficiency, wellbore stability, and lost circulation control) not only engineering-safety concerns but also core issues that directly determine the economic viability of a project.

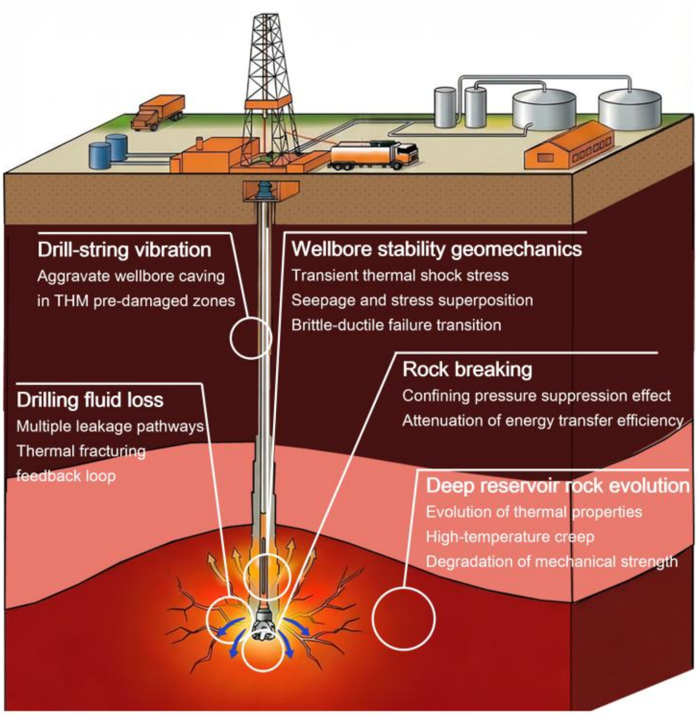

Fig. 1. Overview of geomechanical issues in deep geothermal well drilling

Based on this, the present paper systematically reviews progress in micro-scale thermal damage evolution of deep geothermal reservoir rocks, macroscopic rock-breaking mechanisms, and wellbore stability studies. The aim is to establish a conceptual link in geothermal drilling from mineral-scale thermal damage to macroscopic mechanical responses, thereby providing geomechanical support for the efficient and safe development of deep geothermal energy. First, it examines the evolution of mechanical, hydraulic, and thermal properties of deep geothermal reservoir rocks under high temperatures. Second, it provides a detailed account of rock-breaking mechanisms and efficient drilling technologies for deep geothermal reservoirs. Third, it reviews the thermal evolution of the drilling fluid, the mechanisms of lost circulation, and the corresponding control strategies, which together define the thermal and hydraulic boundary conditions acting on the wellbore. Fourth, on this basis, it summarizes the geomechanical response of the wellbore under cooling cycles and multi-field coupling, covering failure criteria and instability-evolution mechanisms. Finally, it identifies the key challenges in geomechanical research for deep geothermal drilling and outlines future research directions and prospects. On this basis, the cross-scale review framework established here comprises four levels (mineral, microstructure, rock-sample testing, and wellbore/drilling system) together with their transfer mechanisms, as detailed in Appendix A1. Reservoir stimulation after drilling involves reservoir-scale geomechanical problems such as fracture propagation and inter-fracture stress interference; such studies have been reviewed elsewhere and have a different emphasis from the drilling mechanics addressed in this paper. A second boundary follows from the evidence base rather than from subject matter: the quantitative results compiled below are drawn mainly from granite, whereas carbonate, basalt and andesite reservoirs are covered where quantitative results exist, with the remaining gaps identified rather than filled by extrapolation.

2 Methodology

To improve the reproducibility and scientific rigor of this review, a systematic retrieval workflow based on the PRISMA framework was adopted. The literature search covered three databases with broad coverage of geothermal and geomechanical research: Web of Science (WoS), Scopus, and EI (Engineering Index). The search window was primarily 2010–2026 to reflect recent progress, while a number of earlier classic references were retained. The search terms were organized around three themes. The first concerned high-temperature rock mechanical behavior, with key terms including high-temperature rock mechanics, thermal damage, brittle–ductile transition, thermal cycling, and hot dry rock. The second concerned geothermal drilling and rock-breaking technologies, including geothermal drilling, PDC bit, hard-rock drilling, rate of penetration, liquid-nitrogen jet, and thermal-assisted rock-breaking. The third concerned deep wellbore stability and lost circulation control, including wellbore stability, thermo-hydro-mechanical coupling, failure criterion, lost circulation, and induced seismicity.

The initial search returned 4,390 records. After combined keyword retrieval and time-window screening, 3,215 records remained. Subsequent screening of titles and abstracts further excluded records whose full text was unavailable, duplicate records, items unrelated to deep geothermal drilling and completion, and some purely review-type papers, yielding a final set of 318 references as the analytical basis for this review. The literature search and screening procedure was documented following the PRISMA framework, as shown in Fig. 2.

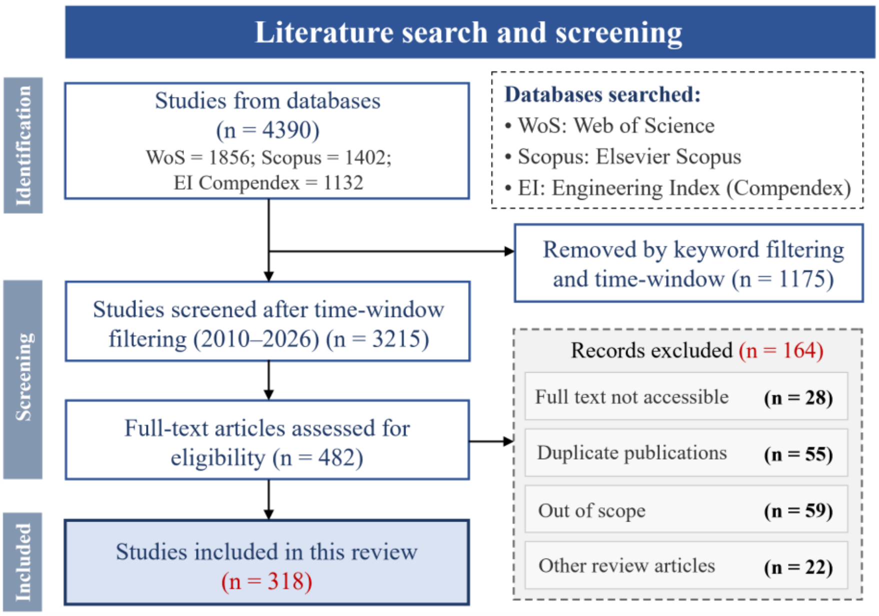

Fig. 2. Flowchart of the literature search and screening process

3 Physical and mechanical properties of geothermal reservoir rocks

Geothermal resources are primarily hosted in deep formations and classified into several types based on geological characteristics, including hydrothermal, HDR, geopressured, and magma systems [40]. The term "deep geothermal drilling" in this review refers to high-temperature geothermal systems at depths greater than 3 km with reservoir temperatures of no less than 150 °C, encompassing deep hydrothermal resources and HDR/EGS. Typical HDR reservoirs are located at depths of 3 km to 6 km and defined as high-temperature rock masses with temperatures exceeding 150 °C, characterized by dense, impermeable structures containing virtually no natural fluids [41-43]. Under certain extreme geological conditions, such as magmatic systems in volcanic regions, temperatures within 7 km depth can exceed 650 °C. For instance, in Iceland's Krafla high-temperature geothermal field, conventional production temperatures reach approximately 350 °C. During drilling of the IDDP-1 deep well, magma was encountered at temperatures of approximately 900 °C, with measured wellhead fluid temperatures exceeding 450 °C [44, 45]. Fig. 3 shows the depth and temperature of selected geothermal wells worldwide.

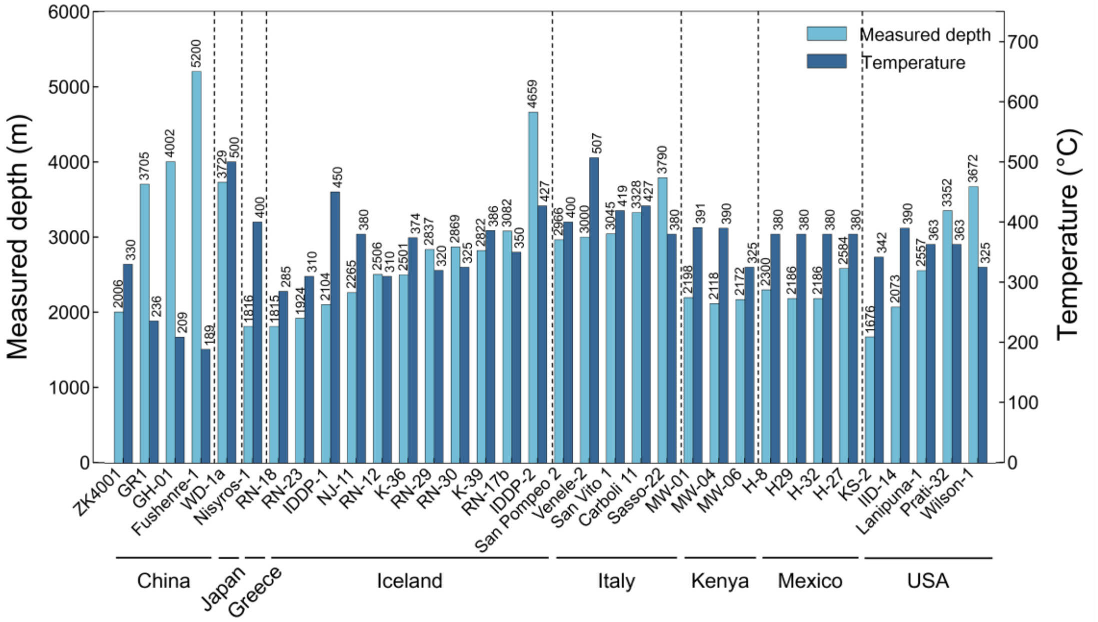

Fig. 3. Measured depth (left axis) and temperature (right axis) of selected geothermal wells worldwide. Detailed information for each well and the specific data sources are provided in Table S1 of the supplementary materials.

In terms of lithology, the primary targets for deep geothermal reservoir development worldwide are crystalline basement rocks, such as granites and metamorphic rocks [46-48]. In volcanically active regions, volcanic rocks such as basalt and andesite also constitute important reservoirs: the reservoir of the Reykjanes geothermal field in Iceland is dominated by basaltic lavas and hyaloclastites [49], while the Rotokawa geothermal field in the Taupo Volcanic Zone of New Zealand is hosted in andesite [50]. In addition, deep high-temperature carbonate rocks and even shales have been shown to possess potential for geothermal resource development [51], and large-scale development precedents already exist: geothermal fields such as Kizildere in Turkey's Büyük Menderes graben produce from limestone and marble reservoirs with temperatures of up to 242 °C [52], and at Larderello in Tuscany, Italy, the world's first geothermal power producer, the shallow reservoir likewise consists of carbonate-evaporite formations [53]. This lithological diversity is the direct reason why the thermo-mechanical thresholds in the following sections are characterized separately by lithology. Regarding hydraulic properties, increasing burial depth leads to compaction and cementation, significantly reducing matrix porosity and permeability in the rock, resulting in marked densification and low porosity-permeability characteristics. Under these conditions, the degree of fracture system development and their effective aperture under the in-situ stress field are critical factors determining reservoir physical properties and development potential [54, 55]. Consequently, fluid migration and heat exchange rely not on matrix pores but mainly on natural fracture networks that are oriented at high angles or vertically under in-situ stress [56, 57]. This fracture-dominated reservoir structure, combined with extreme high-temperature and high-pressure conditions, causes strong nonlinear coupled evolution in the mechanical, hydraulic, and thermal properties of the rock under drilling disturbances, posing severe challenges to deep well drilling operations. Unless stated otherwise, the threshold temperatures and property changes quoted throughout this review were determined in the laboratory on small specimens under unconfined or low-confinement conditions. Where such values are compared with, or extrapolated to, deep in-situ conditions, this is stated explicitly and the associated confinement correction is discussed.

3.1 Rock mechanical properties at high temperatures

3.1.1 Evolution of rock mechanical properties under heating

In the extreme conditions of deep geothermal well drilling, the physical and mechanical properties of reservoir rocks are not constant but exhibit strong temperature dependence and nonlinear evolution. These changes are critical for bit selection and wellbore stability prediction [58, 59]. A key physical cause of strength degradation and damage evolution in deep hard rocks is the thermal-expansion mismatch among minerals that develops as temperature rises. This mechanism stems primarily from the heterogeneity of mineral composition and the anisotropy of crystal structures [60]. For example, crystalline rocks such as granite, which are widely distributed in geothermal reservoirs, are formed by the tight cementation of various mineral grains such as quartz, feldspar, and mica, and the thermal expansion coefficients of these minerals differ markedly; for instance, K-feldspar is 8.7×10^{-6} K^{-1}, plagioclase is 14.1×10^{-6} K^{-1}, quartz is 24.3×10^{-6} K^{-1}, and mica is 3.0×10^{-6} K^{-1} [61]. During heating, these differences cause inconsistent volumetric expansion rates between adjacent grains. Constrained by surrounding material, grains cannot deform freely, generating substantial local tensile or shear thermal stresses at grain boundaries. When these thermal stresses exceed the tensile strength of intergranular cement or the cleavage strength within grains, intergranular micro-cracks initiate and propagate [62, 63]. Moreover, even within the same mineral, thermal expansion coefficients often vary along different crystallographic axes, intensifying stress concentrations inside grains and promoting intragranular micro-cracks [64]. In quartz-rich rocks, reaching the α/β quartz phase transition temperature triggers rapid lattice reorganization in quartz crystals, accompanied by a sharp volume increase. This sudden expansion can instantaneously connect internal fracture networks, causing irreversible damage to the rock's dense structure [65, 66]. Fig. 4 illustrates the thermal damage mechanisms in granite, a common rock in geothermal reservoirs. Moreover, the lithology of geothermal reservoirs is not limited to quartz-rich granite, and the thermal response differs markedly with the dominant mineral assemblage. In feldspar-dominated rocks, feldspar grain-boundary cracking replaces feldspar–quartz boundary cracking as the dominant thermal-damage pathway above 330 °C [67]. In carbonate reservoirs, the strong anisotropy of axial calcite expansion, superimposed on decarbonation reactions above 600 °C, jointly drives pore-network reshaping and strength decay [68]. In clay-bearing interlayers that may be present, the smectite-to-illite transformation under hydrothermal conditions is accompanied by interlayer-water expulsion and volumetric contraction, significantly changing the boundary conditions for wellbore stability in geothermal drilling [69, 70]. These differences indicate that the thermo-mechanical response of deep geothermal reservoirs depends on the dominant mineral assemblage and must be analyzed specifically in light of the reservoir's principal minerals.

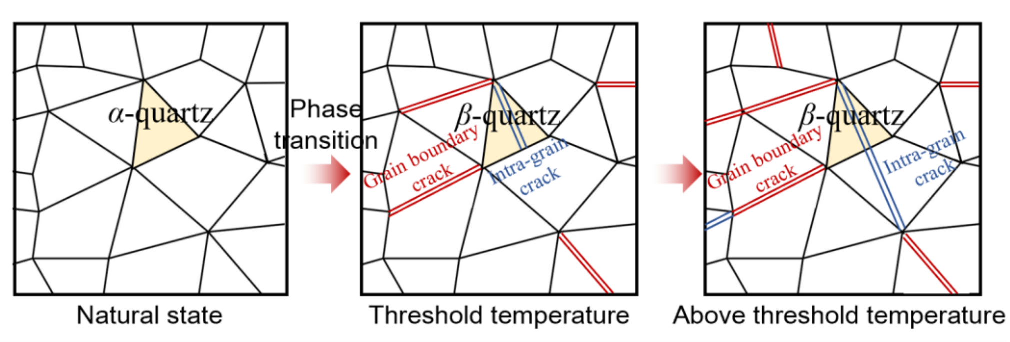

Fig. 4. Thermal damage mechanisms in granite modified from Wang et al. [71]. When the temperature exceeds the α/β quartz transition threshold, the volume mismatch before and after the transition simultaneously activates two crack types in the mineral framework: grain-boundary cracks (red), developing along quartz–matrix interfaces and driven mainly by thermal-expansion mismatch among minerals; and intragranular cracks (blue), propagating within quartz grains along the transition orientation and produced directly by the lattice distortion of the phase transition.

Specifically, as temperature rises from ambient levels, rock modulus and strength generally decline, but this process exhibits distinct staged characteristics. During the low-temperature heating stage, some granites may experience a slight increase or stabilization in peak strength and elastic modulus due to closure and compaction of pre-existing micro-cracks. At this stage, the removal of adsorbed water reduces frictional damping between grains, which can transiently raise the measured stiffness and strength. However, once a critical threshold temperature is exceeded, significant differences in thermal expansion coefficients and anisotropy among rock-forming minerals such as quartz and feldspar cause intense local thermal stress concentrations at grain boundaries, leading to rapid initiation and propagation of intergranular micro-cracks [71, 72]. Thermally induced mechanical degradation exhibits lithology-dependent critical-temperature thresholds and degradation patterns. For granite, about 300 °C is the key threshold at which compressive and tensile strength begin to drop sharply; beyond it, strength and elastic modulus fall markedly as grain boundaries soften, minerals lose water, and micro-cracks propagate, while the α/β quartz transition, accompanied by a sudden volume increase, further promotes micro-crack growth and strength loss [73]. By comparison, the P-wave velocity of sandstone decays more nearly linearly with temperature and its temperature–confining-pressure response threshold is lower than that of granite; Deng et al. [74] measured logarithmic and linear P-wave-velocity declines of 24.3% and 29.7% for granite and sandstone, respectively. This degradation is highly coupled across multiple parameters: elastic modulus decreases, stiffness softens, Poisson's ratio increases with crack propagation, and P-wave velocity drops markedly due to acoustic attenuation in the cracked medium, all strongly correlated with strength parameters [75-77]. For hot-dry-rock samples, Gao et al. [78] observed substantial P- and S-wave velocity attenuation as early as 120–180 °C, with the P-wave velocity dropping by about 500 m/s, indicating that crystalline hard rocks can undergo significant elastic degradation at lower temperatures. Thus, critical thresholds and degradation patterns are governed by the dominant mineral assemblage, and predictions of permeability and strength evolution should be characterized piecewise according to the principal lithology; meanwhile, the strong correlation between wave velocity and strength parameters makes velocity a viable basis for non-destructive monitoring of downhole thermal damage.

In the high-temperature and high-pressure conditions of deep geothermal reservoirs, rock mechanical behavior markedly deviates from the linear elasticity observed at room temperature, exhibiting a pronounced brittle-ductile transition [79, 80]. This transition is primarily driven by intergranular thermal stresses arising from the anisotropy in mineral thermal expansion coefficients. These stresses activate micro-crack initiation and damage evolution, transforming the rock structure from dense and brittle to porous and ductile [81]. In terms of failure modes, this transition shifts rock failure from brittle splitting at room temperature to shear or semi-ductile failure at high temperatures, and the transition temperature depends on the rock type. Under confining pressure, carbonate rocks can show a tendency toward plastic transition at relatively low temperatures; Wang et al. [82] using high-temperature triaxial acoustic-emission tests and particle-flow simulations on marble, found that between 30 and 150 °C the total number of internal cracks increased, the proportion of shear cracks decreased, grain-displacement activity intensified, and ductile features became progressively pronounced with rising temperature. Zhu et al. [72] likewise observed that granite exhibits clear ductile behavior only around 600 °C, with a gentler post-peak stress–strain drop and a failure process changing from sudden instability to progressive failure. Both indicate that the transition threshold rises with the thermal stability and cementation of the dominant minerals: the brittle–ductile transition temperature of quartz-rich hard rock is markedly higher than that of carbonates, so rock-breaking and wellbore-instability criteria must calibrate this threshold separately by reservoir lithology.

Across the high-temperature experiments discussed in this section, the vast majority adopt a procedure of heating the sample and then loading it after cooling to room temperature; the measured reductions in strength, elastic modulus, and wave velocity reflect the micro-crack network accumulated during thermal treatment and persisting after cooling, which can be regarded as the rock's thermal pre-damage response. In actual geothermal drilling, however, the rock is in a coupled state in which high temperature and confining pressure are applied simultaneously; here, thermally activated plastic deformation and damage accumulation occur concurrently, constituting an in-situ thermo-mechanical coupling behavior distinct from thermal pre-damage. In other words, the mechanical degradation measured at room temperature cannot be simply extrapolated to deep drilling efficiency, because the suppression of crack propagation by confining pressure and the efficiency of energy transfer under dynamic loading also affect the rock-breaking response under in-situ geothermal conditions; this point is developed further in Section 4.1.1.

3.1.2 Mechanical response under cooling and cyclic cooling shock

During deep geothermal drilling, reservoir rocks experience not only the inherent high-temperature and high-pressure conditions but also the cooling induced by circulating drilling fluids. This rapid temperature variation significantly alters rock mechanical behavior, often causing greater strength degradation than steady high-temperature heating alone [83, 84]. Existing experimental studies show that cooling rate, cooling medium type, and number of thermal cycles are key factors determining the extent of strength reduction and changes in failure modes. Fig. 5 shows the fragmentation of granite subjected to impact loading under different cooling media and different temperatures. Naturally cooled specimens exhibit the fewest cracks and the most intact fragments, followed by water-cooled specimens, whereas liquid-nitrogen-treated specimens show the densest secondary fractures and the finest debris; moreover, the higher the initial temperature, the more pronounced the differences among the three.

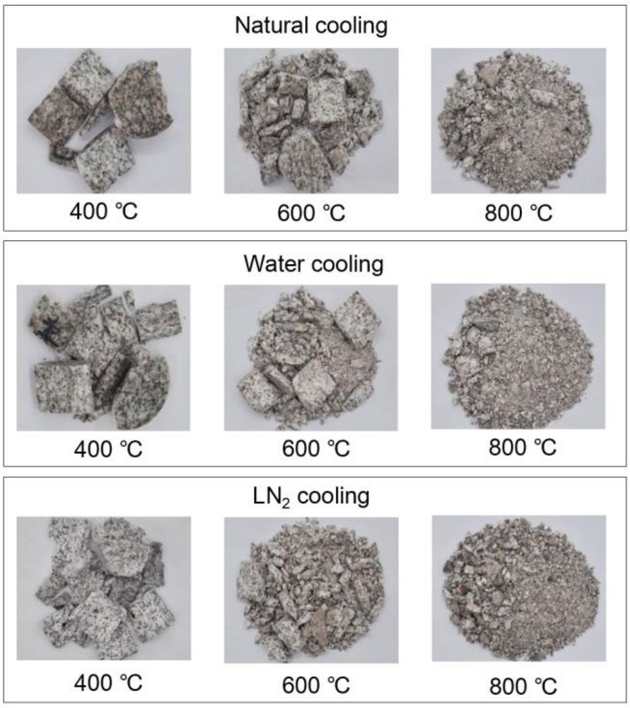

Fig. 5. Effects of different cooling methods on fragmentation characteristics of granite [85].

First, the cooling rate decisively influences the strength deterioration of rock. Natural cooling has the lowest cooling rate, producing a gentle temperature gradient between the interior and exterior of the specimen and allowing thermal stresses to be released fully. In contrast, water or drilling-fluid cooling involves a heat-transfer coefficient markedly higher than that of natural convection in air, causing the surface layer to cool sharply within a short time and generating a steep transient temperature gradient and strong tensile thermal stresses, which substantially reduce the load-bearing capacity of the rock [86, 87]. Liquid nitrogen, owing to its extremely low temperature, produces the largest temperature difference between the surface and interior and the fastest cooling rate, and therefore induces the most severe thermal-stress damage. In comparative tests on calcarenite, Brotóns et al. [88] found that after exposure to 600 °C, the reduction in uniaxial compressive strength was significantly greater for water-cooled specimens than for air-cooled ones, and the loss of elastic modulus caused by water cooling was also more severe. Garrido et al. [89] further identified 400 °C as a threshold temperature at which rock strength undergoes a drastic transition, and reported that after heating to 900 °C followed by water cooling, the UCS of carbonate rock decreased by up to 95%. For more extreme cooling media, Fan et al. [90] systematically compared three cooling paths, namely natural cooling, water cooling, and liquid-nitrogen cooling, and showed that the higher the heat-transfer coefficient of the cooling medium, the more severe the thermal-stress damage within the rock. Cooling tests on granite by Zhu et al. [91] confirmed that the ultra-low temperature of liquid nitrogen induces a denser network of cracks within the rock, increasing permeability by a factor of 5.24 and reducing compressive strength by 13.6%, while the failure mode shifts from brittle axial splitting at room temperature to a complex shear-tensile mixed or fragmentation failure, demonstrating that liquid-nitrogen treatment generates far more pervasive micro-cracks than water cooling. Fig. 5 confirms this trend: granite specimens fragmented after LN_2 treatment exhibit more secondary cracks and finer debris than those cooled in water or naturally, particularly at higher initial temperatures.

Second, the fluid circulation during drilling is accompanied by periodic temperature fluctuations, and the cumulative damage caused by such cyclic cooling shocks cannot be neglected. As the number of cooling cycles increases, the plastic deformation accumulated within the rock grows progressively, and both the elastic modulus and compressive strength decay exponentially, with the most pronounced strength reduction occurring during the initial cycles [71]. Fracture-toughness tests by Feng et al. [92] support this view, showing that the rock's resistance to fracture drops sharply within the first five cycles. However, Liu et al. [93] observed an unusual phenomenon in direct-shear tests: after about 15 cooling cycles, the direct-shear strength of granite exhibited a temporary recovery, because fine mineral particles spalled from the shear surface filled and compacted the pores. This finding reveals that under cyclic cooling shocks the rock is governed not only by a strength-weakening mechanism but also, under certain conditions, by a competing particle-filling strengthening mechanism. At the microscopic level, the above degradation of macroscopic mechanical performance is attributed to thermal-gradient stresses that promote the rapid coalescence and propagation of intergranular micro-cracks. Using CT and optical microscopy, Zhu et al. [94] confirmed that the rapid temperature drop induced by water cooling intensifies the non-uniform contraction among mineral grains, particularly after the quartz phase-transition temperature is exceeded, damaging the rock skeleton and causing physical parameters such as P-wave velocity and thermal conductivity to decrease linearly or exponentially with increasing temperature. This temperature-difference-induced cooling damage has practical implications for deep geothermal drilling: on the one hand, it effectively reduces the strength of bottomhole rock, which is favorable for improving rock-breaking efficiency and provides a theoretical basis for controlled cyclic-cooling-shock-assisted rock breaking; on the other hand, if the cooling-induced cracks propagate too deeply into the wellbore wall, they will markedly degrade the integrity of the surrounding rock and increase the risk of wall spalling and collapse in deep formations.

3.2 Evolution of hydraulic properties

Under the high-temperature and high-pressure conditions of deep geothermal reservoirs, the hydraulic properties of rocks are no longer static constants but depend strongly on the stress and temperature states [95, 96]. The dynamic evolution of reservoir permeability fundamentally results from the combined action of multiple mechanisms: effective stress-induced fracture closure, pore throat compression due to matrix thermal expansion, thermal stress-induced fracture opening, and changes in fluid properties [97, 98].

First, high in-situ stress in deep environments significantly suppresses permeability in fracture-dominated reservoirs. As confining pressure increases, initially open micro-fractures close, causing permeability to decrease nonlinearly in an exponential or concave manner [99, 100]. In the low-temperature heating stage, permeability is dominantly controlled by stress and does not increase with rising temperature; instead, it remains stable or slightly decreases. This occurs because, under confining pressure, thermal expansion of mineral grains occupies pore space, narrowing effective flow channels [101, 102]. Modified versions of the classic Kozeny-Carman equation, incorporating temperature variables, can theoretically quantify permeability evolution caused by matrix thermal expansion and microstructural changes [103]. Addressing volumetric deformation in THM coupling, Ran and Li [104] derived a dynamic permeability model based on volumetric strain theory that includes a temperature term. The model posits that thermal expansion of rock grains directly occupies pore space, reducing permeability:

$$\frac{k}{k_0} = \frac{1}{1+\epsilon_v}\left[1 + \frac{\epsilon_v}{\phi_0} - \frac{\gamma \Delta T(1-\phi_0)}{\phi_0}\right]^3 \tag{1}$$

where k_0 and ϕ_0 are the initial permeability and porosity, respectively; ϵ_v is the volumetric strain due to rock deformation; γ is the volumetric thermal expansion coefficient of the rock skeleton; and ΔT is the temperature change. All of the above parameters can be obtained directly from conventional experiments, and this model is applicable to the low-temperature heating stage dominated by matrix thermal expansion squeezing the pore space, i.e., temperatures below the critical threshold for thermal-crack development. This equation clearly quantifies the suppressive effect of matrix thermal expansion on permeability during the low-temperature heating stage, explaining why permeability often decreases with rising temperature before macroscopic thermal fracturing occurs.

As described in Section 3.1, structural damage induced by the α/β quartz phase transition causes rapid interconnection of previously isolated micro-pores within the rock [105-107]. Evolving from microscopic thermal damage at grain boundaries to macroscopic fracture-network connectivity, this process not only reduces rock strength but also directly promotes the development of fluid-flow pathways in the reservoir. As a result, permeability exhibits dramatic, orders-of-magnitude increases once a critical temperature threshold is reached. As shown in Fig. 6, SEM observations reveal that below 200 °C the matrix remains dense and cracks are rare, grain-boundary cracking becomes identifiable from 400 °C, and connected damage bands develop between 600 and 800 °C. CT reconstruction likewise shows almost no internal fractures at 300 °C, isolated micro-fractures appearing at 400 °C, and coalescence into a directional macroscopic fracture network between 500 and 700 °C. Results from both scales and both imaging methods indicate that the emergence of cracks and connected networks exhibits a well-defined temperature threshold. These observations were obtained on heat-treated specimens under unconfined laboratory conditions, so the threshold temperatures identified here should be read as laboratory lower bounds rather than as in-situ values.

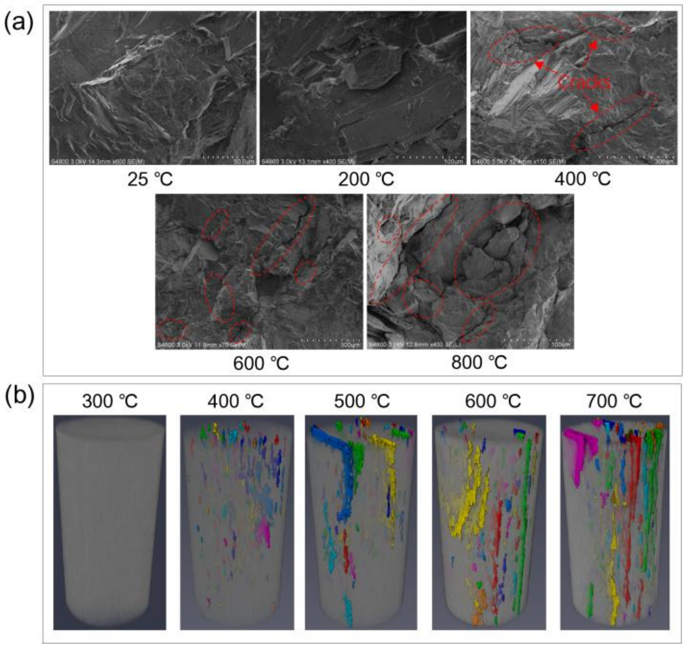

Fig. 6. Multi-scale evolution of thermal damage in rock. (a) Evolution of microscopic SEM morphology of thermal damage [81], with red arrows and dashed regions; (b) extraction results of internal fractures by CT reconstruction [101].

The threshold temperature for the pore-to-fracture permeability transition differs markedly with lithology. For granite, primary micro-pore closure and compaction dominate from room temperature to about 300 °C; intergranular micro-cracks initiate from about 300 °C, and above approximately 573–600 °C (near the quartz phase-transition point) the pore–fracture network becomes connected, producing an order-of-magnitude jump in permeability [108, 109]. It must be emphasized that the above threshold and jump magnitude were obtained under low confining pressures of only a few MPa, whereas under in-situ effective stresses of 50–200 MPa at depth, thermally induced micro-cracks with micron-scale apertures will be substantially closed. Fracture hydraulic aperture decays by orders of magnitude with increasing effective normal stress and exhibits hysteresis [110]. Matrix permeability likewise decreases with increasing effective confinement [38]. The temperature threshold for pore–fracture network connection will therefore shift toward higher temperatures, and the magnitude of the permeability jump will also be suppressed. The permeability-transition threshold temperature obtained under low confinement should accordingly be regarded as a lower bound of the in-situ threshold temperature; extrapolation to deep conditions requires in-situ stress corrections, and measured studies of permeability evolution under coupled real-time high temperature and high confinement remain very limited. The critical temperature of sandstone is generally lower than that of granite, commonly around 400 °C, above which dehydration and decomposition of the cement phase together with micro-crack coalescence drive an exponential permeability increase [111]. In carbonate reservoirs, limestone shows significant threshold changes in porosity, wave velocity, and strength as early as 340 °C [112], and calcite decomposition near 800 °C further drives macroscopic reshaping of the pore–fracture network [113].

This indicates that the activation thresholds for the pore-to-fracture permeability transition differ substantially among lithologies, so permeability-evolution predictions for deep geothermal reservoirs must be characterized piecewise according to the principal reservoir lithology.

These thresholds are not in conflict once measurement conditions are separated. Values obtained after a full heating–cooling cycle describe the residual crack network, including the cracks generated by cooling itself, and are upper bounds on the in-situ response at temperature. Confinement can also reverse the sign: under 5–25 MPa effective normal stress a natural granite fracture loses 20–75% of its hydraulic aperture on heating to 110 °C [110], whereas the large increases reported for granite were measured at 2–5 MPa [108, 109]. The threshold is mineralogical rather than universal, tracking the α–β quartz transition in quartz-rich granite but set by carbonate and sulphide breakdown at 400–500 °C in shale [101], and heating rate shifts it by well over 100 °C [108]. For drilling, which disturbs pre-existing fractures under high effective stress rather than a heat-treated intact matrix, the confined in-situ measurements are the most transferable evidence, though they reach only about 140 °C.

To describe the temperature-dependent permeability variation at high temperatures, Liang et al. [114] derived an exponential model incorporating a threshold temperature parameter based on Duhamel-Neumann thermal stress theory. The model indicates that below the critical thermal fracturing threshold, permeability increases slowly with temperature. Once the threshold is exceeded, thermal stress-induced fracture propagation dominates flow, causing permeability to rise exponentially:

$$k = ae^{b(T-c)} \tag{2}$$

where a and b are fitting constants related to rock properties, c is the critical threshold temperature at which permeability undergoes abrupt change, and T is the rock temperature. Calibration of the parameters generally requires measured permeability data at several temperature points on both sides of the threshold. This model is applicable to the high-temperature stage dominated by thermal-crack propagation and does not cover the low-temperature pore-compaction stage described by Eq. (1). In addition, the original equation was fitted from data measured without confining pressure, and its critical threshold temperature is precisely the confinement-dependent permeability-transition threshold discussed above, which will shift toward higher temperatures under high in-situ effective stress. For deep applications, therefore, the T_0 calibrated from low-confinement experiments cannot be adopted directly, and the model parameters must be recalibrated against the in-situ stress state. Chen et al. [108] used acoustic emission to monitor two key temperature thresholds, namely micro-crack initiation at 300 °C and the quartz phase transition at 573 °C, and pointed out that the intragranular cracks induced by high temperature markedly enhance the connectivity of the fracture network. Deng et al. [109] CT scan evidence shows that above 600 °C, rock transitions from a pore-dominated medium to a fracture-pore hybrid medium, accompanied by orders-of-magnitude jumps in permeability. To quantitatively characterize the irreversible damage driven by the conversion of thermal energy into fracture surface energy, this study proposed a temperature-permeability model for high-temperature conditions based on energy dissipation principles and fractal theory:

$$k = C_d \left[1 - \left(\frac{\epsilon_{min}}{L} \right)^{\frac{C_s \alpha_L{}^2}{4\gamma_s H N_0 l_c}(\Delta T)^2 - \frac{C_p M}{2\gamma_s H N_0 l_c}\Delta T} \right]^{n+1} \tag{3}$$

where C_d is a geometric structural constant obtained by empirical fitting, $C_d = \beta A/b$, where β is the empirical equivalent coefficient, A is the rock cross-sectional area, and b is a tortuosity-related parameter; ϵ_{min} is the minimum resolution scale, limited by CT/SEM imaging resolution; C_s is the elastic tensor parameter; α is the linear thermal expansion coefficient, generally (6–9)×10^{-6} K^{-1} for granite; L is the characteristic scale or cross-sectional diameter of the rock sample, measured directly by geometry; n is the tortuosity index; C_p is the specific heat capacity of the rock, generally 700–900 $J \cdot kg^{-1} \cdot K^{-1}$ for granite; M is the rock mass; and γ_s is the specific surface energy of the rock; H is the layer height of the computational model; N_0 is the material constant of the damage distribution, inverted from the damage density; and l_c is the maximum damage size with self-similar characteristics. The validity of the model relies on the following key assumptions: (1) the spatial distribution of thermal damage is self-similar and fractal; (2) the dominant damage mechanisms are mineral thermal-expansion mismatch and the α/β quartz transition; and (3) the confining-pressure effect is not given explicitly but is absorbed into the lumped constants. The model is best suited to crystalline dense rocks such as granite over 200–800 °C; below 200 °C plastic thermal damage is not fully developed and predictions may deviate from measurements, while above 800 °C mineral melting or significant plastic flow may exceed the model's basic assumptions. This model reveals the physical mechanism of quadratic evolution of fractal dimension with temperature, correcting deviations in traditional thermoelastic models when describing the plastic damage stage. Here, the exponential term in Eq. (3) is derived from thermodynamic energy conservation; it is precisely through this exponent that the thermo-mechanical coupling enters the model, and fractal geometry then converts it into permeability, with the full derivation and parameter calibration given in Appendix A2. In complex metamorphic rocks present in geothermal reservoirs, dehydration, decomposition, or phase transformation of volatile-bearing minerals under high temperatures are key drivers of macroscopic fracture surface formation and sharp increases in volumetric porosity, thereby dominating permeability enhancement [101, 115]. In addition, the full-scale characteristic model proposed by Li et al. [116] further quantifies the relationship between the thermal-damage-induced change in tortuosity and porosity, confirming that the contribution of large-scale fractures to permeability at high temperature far exceeds that of matrix pores. This permeability evolution also exhibits pronounced anisotropy and transient features [102, 117]. THM coupling simulations of geothermal reservoirs by Ma et al. [118] show that fractures parallel to the minimum principal stress are more prone to shear slip and dilation under thermal stress, and that as the thermal front advances and local thermal stress dissipates some fractures may re-close at later stages, causing permeability to undergo a dynamic rise-then-fall process. Therefore, permeability models for deep geothermal reservoirs must simultaneously account for the permeability-enhancing effect of thermal fracturing and the closure-suppressing effect of in-situ stress.

As thermal fracturing and cooling shocks complicate fracture networks, fluid flow in rough fractures increasingly deviates from the linear Darcy's law, transitioning to the nonlinear Forchheimer regime [119-121]. By solving the Navier-Stokes equations, Liu et al. [122] pointed out that there exists a critical hydraulic gradient above which eddies appear in the streamlines and inertial effects become non-negligible. Based on a non-Darcy criterion, Tan et al. [123] further confirmed that this causes the critical hydraulic gradient to decrease as temperature rises, so that the fluid can enter the non-Darcy regime at a lower hydraulic gradient. High-temperature conditions in deep formations promote the onset of this nonlinear flow [124, 125]. Rock temperature influences flow behavior through dual mechanisms. On one hand, elevated temperatures reduce fluid viscosity, thereby decreasing flow resistance [126, 127]. For example, the numerical simulation study by Li and Ye [128] shows that a high-temperature environment significantly reduces fluid viscosity, thereby changing the flow regime and making the fluid flow paths within fractures more complex. On the other hand, thermal expansion-induced fracture closure not only reduces effective hydraulic aperture but also substantially amplifies inertial effects [129, 130]. Additionally, fracture surface roughness influences flow mechanisms: large-scale undulations govern pressure distribution and overall flow direction, while small-scale irregularities create boundary layers across the domain and induce local nonlinear dynamic eddies, significantly reducing effective convective aperture and enhancing flow nonlinearity [131].

At the level of quantitative criteria, the critical Reynolds number (Re_c) of rough fractures is the core parameter distinguishing the Darcy and Forchheimer regimes. Experiments show that the Re_c of rough rock fractures is mostly on the order of single to tens of units [132], far below the turbulent-transition threshold of pipe flow, and is highly sensitive to fracture-surface morphology: a threefold increase in relative roughness can lower Re_c by about one order of magnitude [133]. This means that once drilling disturbance alters the near-wellbore fracture surfaces, the fluid may enter the nonlinear regime even at low flow rates. The extreme temperature–pressure environment of deep geothermal reservoirs further dynamically affects Re_c: fracture closure under high in-situ stress and shear disturbance from drilling unloading can cause Re_c to vary by up to four orders of magnitude, and under high confining pressure Re_c is usually well below 1 [134, 135]. Thermally induced roughening and matrix thermal damage in high-temperature formations further lower the critical threshold for nonlinear flow [125]. Taken together, the high-temperature thermal damage, high-stress shear, and rough fractures characteristic of deep geothermal reservoirs greatly weaken the applicability of the classical linear Darcy law, so that even slight drilling-fluid loss readily enters the nonlinear Forchheimer dissipation regime.

To accurately describe flow in such complex conditions, Wang et al. [135] modified the Forchheimer equation by incorporating contact area ratio, quantitatively capturing the coupled effects of high temperature, high pressure, and roughness on nonlinear seepage. The expression is:

$$-\nabla P = \frac{12\mu_f}{we_h^3\eta^3}Q + \frac{\beta\rho(1+\omega)^{4/3}}{w^2 JRC^5(1-\omega)^{4/3}}Q^2 \tag{4}$$

where $-\nabla P$ is the pressure gradient, Q is the volumetric flow rate, μ_f and ρ are the dynamic viscosity and density of the fluid, respectively, e_h and w are the hydraulic aperture and fracture width, η is the rock thermal expansion coefficient ratio (used to correct aperture changes due to temperature), ω is the contact area ratio (reflecting mechanical closure under high pressure), JRC is the joint roughness coefficient, and β is the nonlinear term fitting coefficient. This model is applicable to the case of a single rough fracture under high confining pressure where the hydraulic gradient exceeds the Darcy–Forchheimer transition threshold, and is not applicable to porous-matrix flow or to fracture networks that have not undergone upscaling. Fracture surface roughness alters fluid flow characteristics, thereby affecting convective heat transfer efficiency and further highlighting the close interplay between hydraulic and thermal properties.

The hydraulic characteristics of deep geothermal reservoirs exhibit highly complex nonlinear responses. Unlike conventional formation drilling, deep geothermal drilling encounters coupled ultra-high in-situ stress and high-temperature environments, so that fracture permeability evolution can no longer be described by the simple linear Darcy's law. In geothermal drilling engineering, high in-situ stress compresses reservoir fractures to micron or even sub-micron scales, shifting fluid flow to low-velocity nonlinear regimes. This greatly complicates predictions of drilling fluid invasion depth and assessments of lost circulation risk. Simultaneously, the cooling effect of drilling fluids induces thermal stresses that alter fracture apertures, creating dynamic permeability feedback loops that directly impact heat exchange efficiency between the wellbore and formation. Therefore, in deep geothermal drilling design, conventional static permeability models are inadequate for engineering needs. Flow equations incorporating THM coupling and nonlinear dissipation corrections are required instead.

3.3 Evolution of thermal properties

Under the coupled high-temperature and high-pressure conditions in deep geothermal reservoirs, the effective thermal conductivity of rocks exhibits complex nonlinear evolution. It is no longer a constant but is jointly controlled by temperature, pressure, mineral composition, and pore structure [136, 137]. To intuitively reveal the intrinsic connections among these physical variables and the extent of their influence on heat transfer, a parameter-correlation network of geothermal-environment rock under multi-field coupling is presented in Fig. 7. In addition to basic environmental parameters such as temperature and pressure, the microstructural changes induced by thermal damage (e.g., damage degree and hydraulic-channel width) and the nonlinear dissipation in fluid seepage (the viscous and inertial dissipation coefficients in Forchheimer's law) all exhibit a high correlation with thermal conduction and heat-transfer performance. This strong interaction among multiple variables indicates that assessing the thermal response of a formation must comprehensively account for the real-time feedback between pore-structure evolution and fluid-dynamic characteristics.

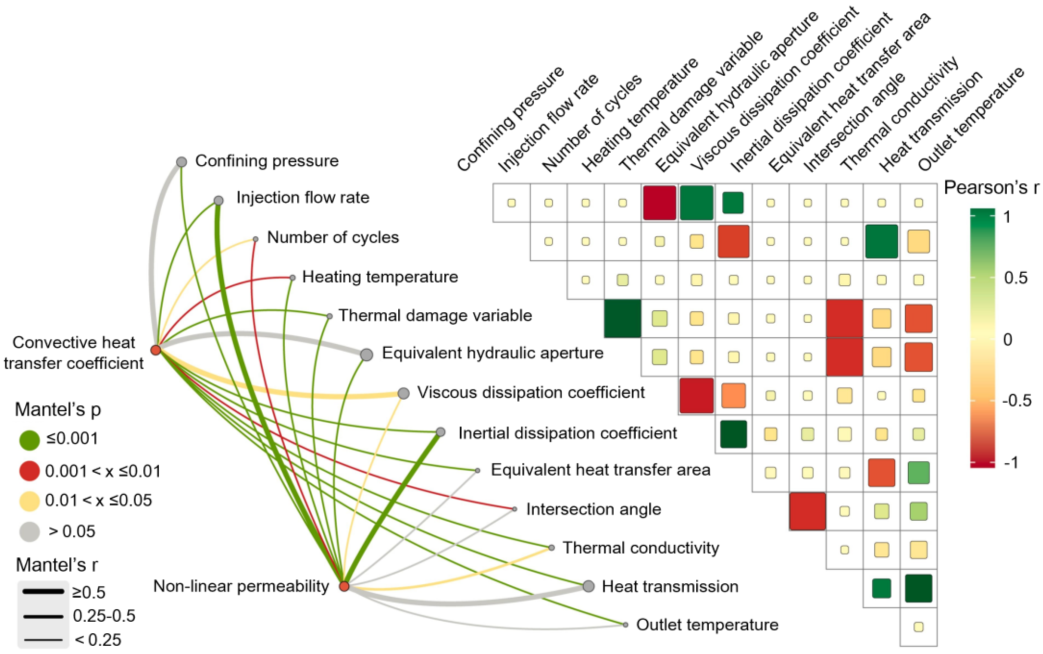

Fig. 7. Correlations between heat-transfer performance, nonlinear permeability, and influencing factors in geothermal environments (the shade of each cell indicates the sign and strength of the Pearson linear correlation between variables, and the thickness of the connecting lines at the bottom represents the combined contribution weight of each environmental factor to nonlinear permeability and the convective heat-transfer coefficient based on the Mantel test) [124].

Temperature is a key parameter controlling rock heat transport properties. Within a certain range, rock thermal conductivity exhibits a strong declining trend with increasing temperature [138, 139]. The microscopic physical mechanism is based on phonon gas kinetic theory, where lattice thermal diffusivity is proportional to the mean free path of phonons. As temperature rises, phonon-phonon interactions related to lattice potential anharmonicity intensify significantly, with strong temperature dependence. This markedly shortens the phonon mean free path, directly reducing macroscopic thermal diffusivity [140]. Sun et al. [141] in heating experiments on granite, found that the thermal conductivity decreased from 2.226 to 1.352 W/(m·K) as temperature rose from 25 to 900 °C. Chen et al. [142] further classified this decay by initial thermal conductivity, noting that rocks with high room-temperature conductivity such as carbonates show a strongly concave-downward decline with temperature, whereas low-conductivity rocks are insensitive to temperature.

Confining pressure has a significant enhancing effect on thermal conductivity, opposite to the influence of temperature [143, 144]. Pashuk et al. [145] in high-pressure tests on sandstone, showed that as pressure increases the rock skeleton is compacted, grain-contact thermal resistance decreases, and thermal conductivity grows linearly, with closed pores being 15%–20% more pressure-sensitive than open pores. Emirov et al. [146] revealed that pressure changes the temperature-dependence exponent of thermal conductivity, because the increased atomic vibration frequency and elevated Debye temperature under high pressure partly offset the decline in thermal diffusivity. However, under in-situ conditions, the weakening effect of temperature on thermal conductivity generally outweighs the enhancing effect of pressure, resulting in an overall declining trend with increasing depth [147].

In addition, beyond the dominant roles of temperature and pressure, pore fluid saturation and microstructural anisotropy in rocks are also key variables determining effective thermal conductivity in deep reservoirs. Neglecting these factors can lead to misjudgments of formation thermal responses. Through experimental studies on rock samples from the Datong Basin, Ji et al. [148] found that water filling the pores acts as a bridging medium, forming liquid bridges at mineral grain contacts and significantly enhancing rock thermal conductivity. In clastic rocks with higher porosity, saturated conditions can increase thermal conductivity by up to 35% compared to dry states. For foliated rocks common in deep formations, thermal diffusion anisotropy remains pronounced, with the highest heat conduction efficiency parallel to lineation and the lowest perpendicular to foliation planes [140]. At the grain scale, Liu et al. [149] further showed, through multi-mineral polydisperse discrete-element (DEM) simulations, that the more uniform the distribution of grain volume fractions, the larger the effective thermal conductivity and the weaker its anisotropy, whereas grain-contact rearrangement induced by temperature differences and confining pressure alters the force-chain network and thereby modulates the anisotropic evolution of effective thermal conductivity. This implies that in directional geothermal drilling design, the relative angle between the well trajectory and formation bedding directly affects heat exchange efficiency and thermal stress distribution in the surrounding wellbore rock. Furthermore, under deep hydrostatic confinement the pore fluid mostly exists as single-phase compressed liquid water, but local depressurization induced by drilling-fluid loss or drilling unloading can drive the pore fluid across the saturated-vapor-pressure curve into a water–vapor phase change, and the evolution of the pore phase has a non-negligible influence on the effective thermal conductivity. In liquid–gas substitution experiments, the thermal conductivity of water is far higher than that of air, which is the physical basis for pore saturation strongly altering the equivalent thermal conductivity of rock [150]. Systematic measurements of 101 samples from the Songliao, Gonghe, and Ordos geothermal basins in China by Yu et al. [151] showed that thermal conductivity can increase by up to 50% as rock changes from unsaturated to saturated, and an improved predictive model coupling saturation and porosity was proposed accordingly. Based on KTB deep-borehole measurements over 25–300 °C, Pribnow et al. [152] found that the thermal conductivity of water-saturated samples declines with temperature much more slowly than that of dry samples, because the thermally induced micro-cracks generated in dry samples during heating are occupied by low-conductivity air, amplifying the temperature coefficient. This implies that extrapolating in-situ conditions from dry samples overestimates the decline of deep thermal conductivity, and in-situ correction should be based on saturated-sample measurements. Therefore, for near-wellbore conditions where local two-phase flow may occur during drilling, downhole THM-response prediction should incorporate the pore phase state and its saturation as key state variables in the coupled simulation framework.

In contrast to the declining trend of thermal conductivity with rising temperature, rock specific heat capacity typically increases with temperature [153]. This directly governs the temperature response rate of near-wellbore rock under drilling-induced thermal disturbances. Sun et al. [154] conducted thermal property tests on sandstone, revealing that the specific heat capacity exhibits four distinct evolutionary stages across the temperature range of 25 °C to 900 °C: rapid increase in the low-temperature range (25 °C-200 °C), relative stability between 200 °C and 600 °C, and significant decline above 600 °C due to mineral melting or lattice destruction. For typical geothermal deep-well temperatures and common crystalline rocks such as granite, specific heat capacity increases monotonically with temperature [155]. However, during drilling, circulating drilling fluids subject wellbore rocks to repeated cooling cycles. Becattini et al. [156] studying six rock types (including granite and limestone) under thermal cycling between 100 °C and 600 °C, found that such cycles induce irreversible physicochemical changes, leading to reduced specific heat capacity. Specifically, in rocks rich in hydrous minerals, high-temperature cycling triggers dehydration reactions; in carbonates, decarbonation occurs. These reactions cause mass loss and structural damage, ultimately resulting in substantial post-cycle declines in specific heat capacity. This thermal fatigue effect induced by cycling indicates that in high-temperature formations, the actual heat storage and exchange capacity of rocks may gradually diminish during drilling due to fluid-induced thermal cycles. This represents a critical mechanism that is easily overlooked when considering only single-cycle heating experiments.

Thermal diffusivity (D), a comprehensive indicator of the rate at which temperature equalizes within a rock, is determined by thermal conductivity, density, and specific heat capacity [153, 157]:

$$D = \frac{\lambda}{\rho_r C_p} \tag{5}$$

where λ is thermal conductivity, and ρ_r is rock density. Under conditions of moderate temperature increase, thermal diffusivity is jointly controlled by thermal conductivity and specific heat capacity. Since specific heat capacity increases with rising temperature while thermal conductivity decreases, this differential evolution of thermal properties causes thermal diffusivity to decline at a rate significantly faster than that of thermal conductivity alone [158, 159]. However, the differential evolution of thermal properties induced by high temperatures complicates heat conduction behavior in deep high-temperature formations. Additionally, constrained by the physical limits of phonon population and mean free path in the crystal lattice, thermal diffusivity decreases markedly at high temperatures and approaches a constant value [160, 161]. This characteristic is crucial for predicting the rate at which heat generated by the drill bit dissipates into the formation during deep well drilling, as well as the distribution of thermal stresses along the wellbore wall.

The high-temperature thermal-damage data reviewed in this chapter span mineral phase transitions and differential thermal expansion, microstructural crack evolution, and the temperature dependence of rock strength parameters. Among these, the temperature-dependent strength parameters are an important basis for judging the rock-breaking mode transition in Section 4, while the high-temperature strength and permeability evolution provide the boundary conditions for the wellbore-stability and lost circulation analyses in Sections 5 and 6.

4 Mechanical response and energy efficiency evolution in the drilling rock-breaking process

In deep high-temperature geothermal well drilling, polycrystalline diamond compact (PDC) bits and roller-cone bits are the two primary tools, each with distinct strengths and weaknesses in hot hard-rock environments [31, 162-164]. PDC bits, lacking moving parts, eliminate the risk of bearing and seal failure at high temperatures. They also offer higher ROP and longer service life in homogeneous formations [30, 165]. However, conventional PDC bits are prone to cutter chipping in extremely hard or heterogeneous formations and exhibit insufficient durability under frequent impact loading [166, 167]. Roller-cone bits, relying on their unique crushing and impact rock-breaking mechanisms, have long been the preferred tool for highly abrasive and extremely hard formations [168, 169]. Their primary advantage lies in strong adaptability to complex geological conditions, effectively handling uncertain formations. Nevertheless, roller-cone bits also face failure risks in high-temperature deep wells. On one hand, elevated temperatures reduce tooth retention strength, leading to on-site tooth loss incidents [170, 171]. On the other hand, downhole high temperatures and frictional heat accelerate seal wear and aging, limiting bearing system lifespan [172]. To overcome the limitations of single-bit types, hybrid bits combining the shearing efficiency of PDC cutters with the durability of roller-cone bits have been developed [173]. These aim to balance cutting speed and rock-breaking stability in high-temperature hard-rock environments. Rock-breaking mechanisms with drill bits become extremely complex due to changes in rock properties in deep geothermal reservoir environments. This process no longer follows the simple brittle fracturing patterns observed at room temperature but instead exhibits pronounced THM coupled nonlinear characteristics. It is controlled by multiple factors, including temperature thresholds, cooling shocks, confining pressure, multidimensional impact loading, and complex dynamic rock constitutive relations. To facilitate an intuitive comparison of the engineering characteristics of the three mainstream bit types in deep geothermal drilling, Table S2 provides a systematic comparison in terms of rock-breaking mechanism, operating characteristics, failure modes, temperature ceiling, and applicable formations.

4.1 Rock-breaking in deep geothermal reservoirs

4.1.1 Transition in mechanical behavior of rock-breaking in deep geothermal drilling

The changes in strength, modulus, and wave velocity discussed in Section 3.1 were measured under atmospheric pressure on rock samples that had been heat-treated and then cooled, and they describe the direction in which the rock properties evolve. However, when the same rock is subjected to the coupled condition of high temperature and high confining pressure at the bottom of the hole, the rock-breaking response is governed not by the rock properties alone but by the combined effect of three factors: the rock properties, the restraint of confining pressure on crack propagation, and the efficiency of energy transfer under dynamic loading. The distinctive feature of deep geothermal drilling lies precisely in the fact that the latter two factors change markedly under high temperature and high confining pressure: confining pressure closes the thermally induced micro-cracks, so that brittle crack propagation cannot develop by relying on static strength deterioration; while the plastic flow and grain-boundary sliding activated by temperature absorb the impact energy that should otherwise act on rock breaking. The most direct manifestation of this coupling mechanism is that, once the temperature crosses the brittle-ductile transition threshold, the rock response shifts from instantaneous brittle crushing to continuous plastic flow, the intrusion mechanism of the cutter changes accordingly, and the rock-breaking energy efficiency drops sharply [174, 175]. The experimental results of Dai et al. [176] quantified this mechanism, as shown in Fig. 8. The results indicate that before the brittle-ductile transition at 25–240 °C, the intrusion efficiency increases with temperature, because the initiation of thermally induced micro-cracks enhances the chipping effect under the lateral force of the cutter; within this temperature range, the tensile strength of the rock decreases significantly faster than its compressive strength, the brittleness index keeps rising, and cracks propagate more readily to form effective chipping. However, once the temperature exceeds about 240 °C, the compressive strength of granite drops sharply, the difference between compressive and tensile strength narrows rapidly, the chipping mechanism is suppressed, and the failure mode shifts from fracture-driven to plastic-flow-driven, so that the rock-breaking efficiency plummets and stabilizes at a low level above 360 °C. The experiments of Zhang et al. [177] show that the plastic-flow temperature threshold during sandstone drilling is higher, and only when the temperature exceeds 700 °C does the melting of the cementing material cause the rock-breaking mechanism to shift completely to a flow-dominated regime. This temperature-dependent evolution of efficiency offers the following engineering insights. First, the brittle-ductile critical transition interval of granite under PDC-cutter cutting lies between 240 and 360 °C, which is markedly lower than the rock yield temperature given by conventional uniaxial compression tests, because the stress concentration beneath the cutter tip accelerates the local plasticization process. Second, once the formation temperature exceeds this interval, adjusting cutter parameters such as the back-rake angle alone can hardly restore drilling efficiency, and auxiliary means such as high-frequency impact, thermal-stress-assisted rock breaking, or liquid-nitrogen injection are needed to further break through the drillability bottleneck.

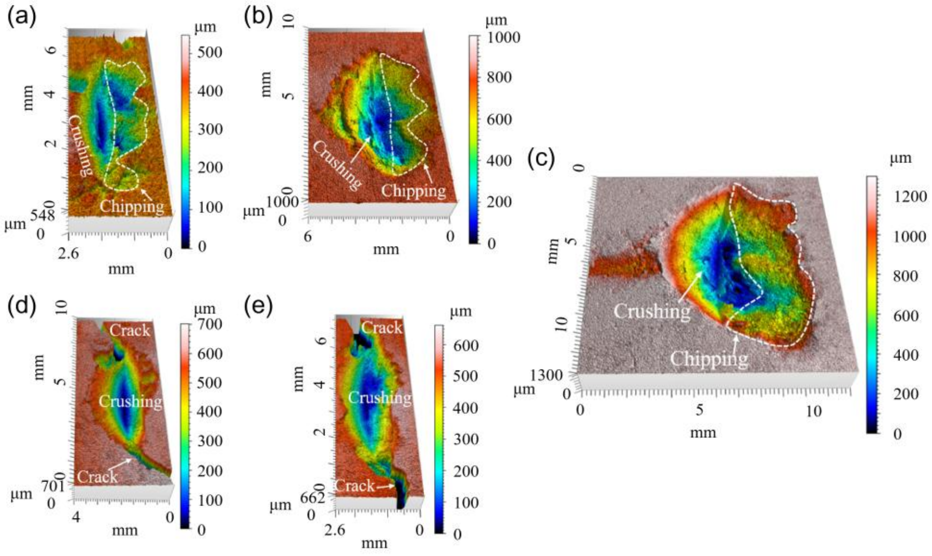

Fig. 8. Rock-breaking performance of PDC bits at different rock temperatures (modified from Dai et al. [176]). (a) 25 °C, (b) 120 °C, (c) 240 °C, (d) 360 °C, (e) 480 °C.

In deep drilling environments, high confining pressure is another key factor limiting rock-breaking efficiency [178, 179]. Its negative effects primarily manifest in two ways: suppressing crack propagation and inducing rock plastic transition. First, confining pressure significantly restrains crack extension under impact loading during drilling. Li et al. [180] found experimentally that confining pressure markedly inhibits lateral crack propagation around impact craters. At 20 MPa the fragmented volume decreases by over 90%, as shown in Fig. 9, at 0 MPa pronounced radial main cracks develop around the impact point and can extend to the edge of the specimen; at 5–10 MPa the extension length and number of radial main cracks decrease simultaneously, transitioning from a "through-going" to a "semi-through-going" pattern; at 15–20 MPa no complete radial cracks are observed, and the damage transforms into a crushed zone centered on the impact point. Second, high confining pressure fundamentally alters rock failure modes [181, 182]. Dai et al. [183] used numerical simulations to further demonstrate the negative effects of confining pressure on drilling. Under high confining pressure in deep formations brittle fracturing characteristics disappear and plastic flow dominates failure. This significantly increases mechanical specific energy (MSE) and suppresses crack propagation during drilling.

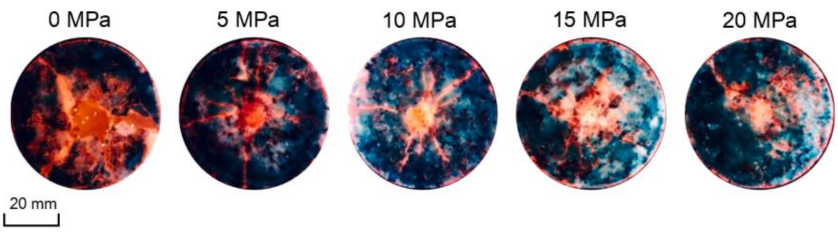

Fig. 9. Crack patterns in rock under single impact at different confining pressures (red indicates cracks marked with a mixture of red fluorescent dye and two-component epoxy resin) (modified from Li et al.

[180]).

Beyond the effects of rock property changes on breaking modes and efficiency, energy transfer during drilling is also a critical factor influencing rock breaking. High-temperature environments alter energy transfer patterns in the process [184]. Zhao et al. [185] conducted high-temperature and high-pressure impact experiments on large granite samples. They found that under 100 MPa confining pressure the net effect of heating remains a marked reduction in specific rock-breaking energy; once the temperature exceeds 150 °C, however, increased micro-cracks and emerging plastic features significantly buffer the impacts, causing the growth of the penetration rate to nearly stagnate over the 150–300 °C range and hindering full utilization of the impact energy. Song et al. [186] examined energy transfer numerically. They noted that although high temperatures lower rock strength, they also weaken elastic modulus, thereby reducing propagation efficiency of impact stress waves within the rock. Simulations showed that as rock temperature rises from 298 K to 873 K, impact energy transfer efficiency decreases by approximately 47.8%. Liu and Huang [187] refined this mechanism using finite-discrete element methods. Although high temperatures exacerbate thermal damage and make rock more susceptible to failure, the high-temperature environment actually suppresses effective absorption of impact energy by the rock. Simulations indicate that as temperature increases, the proportion of energy absorbed by the rock does not rise significantly. Instead, increased frictional dissipation keeps energy transfer efficiency low, with only about 7.5%-12.5% used for actual rock breaking. These two figures are not on a common basis: the 47.8% loss refers to the fraction of impact energy that reaches the rock, whereas the 7.5%–12.5% refers to the fraction ultimately consumed in creating fracture surface, so the second is nested within the first rather than contradicting it. Whether this fraction can represent the true downhole energy efficiency of deep geothermal wells requires further discussion. As noted in Section 3.1.1 and earlier in this section, temperature and confining pressure act on rock breaking in opposite directions. In the high-temperature, high-confining-pressure environment imposed on bottom-hole rock as geothermal wells deepen, the two act simultaneously, and the net rock-breaking efficiency depends on whether the geothermal gradient or the confining-pressure gradient dominates. This mutually constraining relationship, however, currently remains qualitative: the experiments that yield quantitative conclusions are almost all single-variable designs, heating at constant confinement can reduce the specific rock-breaking energy by about 50% [185], whereas at room temperature raising the confining pressure from 0 to 20 MPa reduces the fragmentation volume by more than 90% and raises the specific breaking energy by nearly an order of magnitude [180]. Each type of experiment examines only a single variable, and two-factor temperature–confinement coupling studies have not yet been carried out, so each reflects only one side of the coupling, producing apparently opposite conclusions on rock-breaking efficiency in deep environments. Subject to this limitation, the above 7.5%–12.5% rock-breaking energy fraction likewise requires a statement of its applicable conditions: the value was obtained from unconfined, single-cutter, single-impact numerical simulation, reflects only the temperature side of the coupling, and does not account for the order-of-magnitude suppression exerted by downhole confining pressure. Given that the suppression by confinement is far stronger than the gain from temperature, this value is better regarded as an upper bound on downhole rock-breaking energy efficiency rather than a directly transferable representative value. This further points to a specific research limitation: a calibration of rock-breaking energy partitioning under crossed temperature–confinement conditions within a single experimental system is still lacking, so the critical temperature–pressure conditions under which the coupled net effect becomes more favorable to rock breaking cannot yet be determined. This is precisely the prerequisite for choosing percussive or composite rock-breaking methods in deep geothermal drilling.

Bringing together the temperature-induced plasticity, the confinement of cracks by confining pressure, and the attenuation of energy transfer, the mechanical response of rock under deep geothermal drilling conditions can be divided into four mechanism regimes in the temperature–confining-pressure (T–σ) plane (Fig. 10). When confining pressure is low and the temperature lies below the brittle–ductile transition threshold (Regime 1), micro-cracks induced by thermal perturbations such as heating-induced weakening or cooling shock remain open and propagate effectively, brittle splitting dominates, and thermal weakening translates directly into higher rock-breaking efficiency, which is the physical basis for thermal-stress-assisted and cooling-shock spalling techniques [175, 188]. When the temperature exceeds the transition threshold while confining pressure is still low (Regime 2), thermal plasticity is already active while confining pressure has not yet constrained crack propagation, so the gains from thermal weakening and the losses from ductile dissipation roughly offset each other, with limited engineering benefit. The case of high confining pressure but still-low temperature (Regime 3) is common in deep, non-high-temperature formations: micro-cracks are pressed shut, the thermal pre-damage effect is mechanically shielded, and rock-breaking requires additional impact to re-activate crack propagation [189, 190]. In the high-temperature, high-confining-pressure regime characteristic of deep hot-dry-rock bottom-hole conditions (Regime 4), the two suppression mechanisms superimpose, and the net benefit of thermal weakening is substantially compressed. Within this framework, the static strength degradation documented in Section 3.1 and the in-situ reduction of rock-breaking efficiency discussed here are not contradictory but are different projections of the same set of physical processes onto different regimes of the T–σ space.

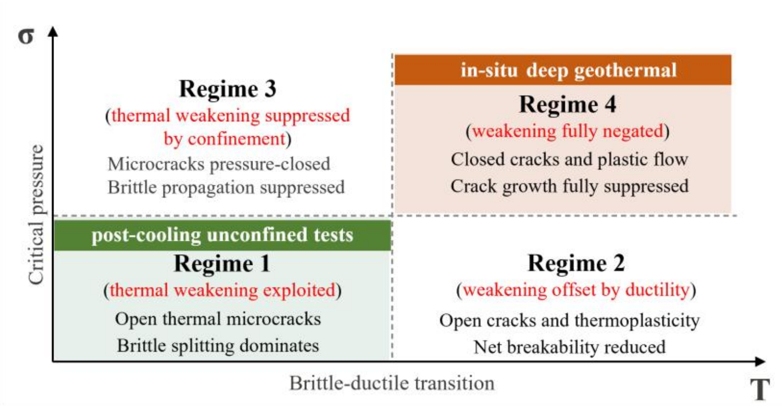

Fig. 10. T–σ mechanism map of thermal pre-damage and in-situ thermo-mechanical coupling behavior in deep geothermal drilling. The regime boundaries are derived from granite data; their positions for other lithologies are expected to shift and have not been validated.

4.1.2 Efficient rock-breaking technologies and methods for deep geothermal drilling

Addressing the core challenges described in Section 4.1.1, including high confining pressure suppressing crack propagation, temperature-induced enhancement of rock plasticity causing penetration difficulties, and low rock-breaking energy transfer efficiency, conventional single-mode mechanical cutting or crushing rock-breaking approaches have encountered performance bottlenecks in ultra-deep geothermal drilling [31, 191]. To overcome the limitations on drilling rate of penetration (ROP) imposed by poor drillability in geothermal reservoirs, rock-breaking techniques have gradually shifted from single mechanical loading to superimposed dynamic loads, multi-field coupling, and directed energy methods. To provide a clear comparison of the physical mechanisms, engineering applicability, and development stages of various rock-breaking technologies in current geothermal drilling, Table 2 summarizes relevant studies on efficient techniques for deep geothermal wells.

Table 2. Summary of research on efficient rock-breaking technologies for deep geothermal wells

Technology category	Physical mechanism for geothermal hard rock	Field implementation complexity	Research and application status	Economic characteristics	References
Composite impact drilling	Uses high-frequency stress waves to create a tensile-failure zone at the bottom hole, overcoming the restraint of high confining pressure on crack propagation	Requires integrating tools such as hydraulic hammers or torsional oscillators	Laboratory studies have systematically verified the potential for improved rock-breaking efficiency; preliminary field application carried out in the high-temperature well Fushenre-1	Good compatibility with existing BHA; in laboratory granite tests, penetration depth and ROP rose by about 170% and 180% respectively over purely axial impact; single-well economic return still needs long-term field validation	[190, 192-194]
Geothermal-specific hybrid bit	Combines PDC and roller-cone characteristics, or uses conical cutters to generate extremely high local stress	No modification of existing equipment required	Engineering-application stage; deployed at scale in high-temperature/hard-rock projects such as Fushenre-1, Salton Sea, and Utah FORGE	At Salton Sea, ROP rose ~35% over roller-cone bits; at Fushenre-1, the three-ridge-tooth PDC raised ROP by 24.5%–27% and footage by 2.36–7.07× over conventional bits; can cut costs 12%–24% (vertical wells) and 18%–26% (directional wells)	[36, 195, 196]

Liquid-nitrogen / cryogenic-fluid assistance	Uses intense thermal–cold cycling to induce intergranular crack propagation, generating tensile thermal stress to offset the clamping effect of high in-situ stress	Involves ultra-low-temperature medium storage and cryogenic insulated tubular-string challenges	Laboratory stage; effects of different cooling media on granite systematically studied; the cutting + LN_2 jet coupling mechanism established	No downhole application record yet; surface LN_2 preparation and storage/piping are highly complex; economics of large-scale deployment remain to be quantified	[91, 197-199]
Hydrothermal jet	Non-contact thermal mechanism using the high-temperature fluid of a hydrothermal flame to rapidly heat the rock surface, inducing extremely high local thermal stress	High complexity; a stable supercritical hydrothermal flame must be maintained in a high-pressure downhole liquid environment	Prototype and demonstration-project stage; model evaluation and experimental validation of thermal-jet drilling established	HSD estimated to cut costs ~15%–20% in hard-rock sections; commercial economics still require field-data validation	[200-202]
Directed energy	Uses high-power, high-frequency millimeter-wave energy from a gyrotron to directly melt and vaporize rock	High complexity; requires a megawatt-class power source and metal waveguides for directional energy transmission	Entered field-demonstration stage from 2025: in Texas, 48 kW millimeter-wave drilling of granite/basalt reached ROP of 2 cm/min	Megawatt gyrotron and waveguide give extremely high single-well initial investment; current feasibility not yet quantified; with scale-up, ultra-deep ultra-hot section costs may become comparable	[203-206]

2

To address the challenge of high confining pressure suppressing crack propagation in geothermal reservoirs, introducing high-frequency dynamic impact loading has become a key approach for enhancing rock-breaking efficiency [189, 207]. Li et al. [192] proposed using the high-frequency impact force generated by a down-the-hole hammer to create a micro-fracture network around the wellbore. Their laboratory tests, conducted on granite at room temperature and pressure, used a hydraulic down-the-hole hammer (hole diameter 95 mm, impact energy 185 J, impact frequency 13 Hz) for percussive rock breaking and compared it with diamond rotary drilling under the same drilling parameters; the results showed that the near-wellbore rock damage volume produced by percussive rotary drilling was about 5–7 times that of diamond rotary drilling, and the breakdown pressure of subsequent hydraulic fracturing was reduced by nearly 50%. Huang et al. [208] similarly advocated high-frequency impact loading to overcome confining pressure constraints by generating instantaneous high-energy stress waves that create tensile failure zones inside the rock, enabling efficient breaking. Building on this, axial-torsional coupled composite impact shows even greater advantages. Xi et al. [190] found that compared to conventional drilling, introducing high-frequency coupled axial and torsional impacts shifts rock failure modes from simple shear or compression to combined tensile-shear failure, with tensile damage becoming dominant. Numerical simulations and experimental data indicate that axial-torsional coupled impact drilling can increase mechanical ROP by over 30%. Optimal phase differences and frequencies maximize volumetric breaking efficiency while effectively suppressing stick-slip vibrations, resulting in smoother cutting. Rossi et al. [209] divided the rock-breaking process into three stages: wear-dominated, compressive crushing, and retraction. Coupled impact technology aims to keep the bit operating in the efficient compressive crushing stage. Wang et al. [210] proposed a composite impact rock-breaking concept. Their numerical simulations confirmed that, compared to steady-state cutting, introducing axial-torsional coupled impact loads effectively shifts rock failure from plastic to brittle fracturing, increasing fragmented volume by 7.5% and reducing MSE by 12.3%. In field practice, pneumatic down-the-hole hammers (air hammers) drive the impactor and carry cuttings with compressed air, which avoids the high-temperature deterioration of drilling-fluid performance and removes drilling-fluid losses altogether, and they are widely applied in geothermal hard-rock drilling. Their operating envelope, however, is set outside rock mechanics: without a hydrostatic column the well is drilled underbalanced, so wellbore-stability and well-control margins are narrower; impact performance falls sharply once formation water influx becomes significant; and the practical depth and temperature limits are governed by the thermal tolerance of impactor lubrication and seals and by cuttings transport and bit cooling rather than by the rock-breaking mechanism itself [162]. Quantitative envelopes for these limits under deep geothermal conditions have not been published.

Beyond optimizing load application, bit geometry offers another critical pathway to counter high-temperature rock plastic hardening [211, 212]. Addressing penetration difficulties due to enhanced plasticity at high temperatures, Dai et al. [176] found that cutter back-rake angle significantly affects breaking efficiency. Under high-temperature plastic conditions, smaller back-rake angles cause primarily elastic deformation, whereas appropriately larger angles generate horizontal components that promote crack propagation. In bit design strategies, novel non-planar cutters differ from traditional flat-contact modes by leveraging point-loading effects to overcome drillability bottlenecks in hard rock [213]. These designs convert surface contact to highly concentrated point contact, generating local loads far exceeding rock yield strength to force volumetric fracturing even under extreme temperature-pressure conditions. In Tauhara geothermal field applications, non-planar cutter designs achieved 20%-50% drilling performance improvements, substantially reducing costs [166]. For ultra-deep high-temperature granite reservoirs, hybrid PDC bits further optimize energy transfer efficiency through coupled cutting-crushing mechanisms [214]. In China's first ultra-deep high-temperature geothermal well, Fushenre-1, this technology successfully handled hard-rock formations above 150 °C, reducing average tangential forces by 21.22%-24.27% and markedly suppressing torsional vibrations and stick-slip caused by enhanced rock plasticity during deep drilling. Although intensified friction from point contact poses severe challenges to cutter thermal stability, optimizing parameters such as cutter spacing and height differences maintains high rock-breaking specific energy while significantly improving bit surface cooling and cuttings removal. This ensures extended bit life in high-temperature environments [195].

To fundamentally overcome the bottleneck of impeded energy transfer, combined rock-breaking mechanisms that exploit temperature-difference-induced thermal stresses have become a research hotspot. Heat conduction between fluid and high-temperature rock creates significant temperature gradients in the rock surface layer, thereby inducing tensile thermal stresses. These tensile stresses effectively counteract the clamping effect of bottom-hole pressure, forming tensile zones inside the rock and promoting crack initiation and propagation [215]. Compared with purely mechanical rock breaking, incorporating thermal stress assistance significantly increases cutting depth and fragmented volume, fundamentally improving drillability in high-temperature hard rock [216, 217]. Fig. 11 shows the tensile failure of rock after liquid-nitrogen treatment. The fracture-surface relief of naturally cooled samples remains roughly stable over the 25–300 °C preheating range, whereas that of liquid-nitrogen-cooled samples increases from about 0.3 mm to about 0.7 mm as the preheating temperature rises, indicating that liquid-nitrogen treatment induces more intense tensile damage. Based on thermal damage theory, Dai et al. [198] proposed a new approach of liquid-nitrogen-jet-assisted cutting, confirming that the liquid-nitrogen jet, owing to its low-temperature characteristics and relatively low heat-transfer efficiency, can induce an extremely large temperature gradient and irreversible tensile damage on the rock surface, and that this pre-damage mechanism significantly reduces the resistance of the subsequent mechanical cutting. However, the deep-depth feasibility of these non-contact thermal methods remains largely unquantified. For LN_2-assisted breaking, the main constraint lies in field supply: liquid nitrogen must be produced, stored, and resupplied at about −196 °C and conveyed through vacuum-insulated tubulars to kilometre-scale depths to suppress in-string boil-off; otherwise the thermal-shock potential is dissipated before the fluid reaches the bit. As for large-scale deployment, no cost data for downhole application have yet been reported, and only a qualitative judgment can be made based on process characteristics.

The cost of liquid-nitrogen assistance arises mainly from surface production or procurement, cryogenic storage and vaporization losses, and the provision and maintenance of ultra-low-temperature vacuum-insulated tubing; among these, the along-hole vaporization and heat leakage during deep-well delivery determine the nitrogen consumption per well, and the cost rises nonlinearly with well depth and geothermal gradient. Its economic viability is therefore difficult to realize in shallow or medium-depth wells and is more likely to appear in ultra-deep, ultra-high-temperature hard-rock intervals where the service life of conventional PDC bits and the ROP are severely constrained. In such intervals the non-productive time is itself a major cost, and if cold-shock pre-damage can markedly increase the ROP and extend the footage per run, the additional investment in the liquid-nitrogen system may be offset by shortening the drilling cycle. Limited by the complexity of direct downhole application, its engineering implementation is more likely to proceed in stages: in the near term, mainly intermittent near-wellbore cold-shock pre-damage during tripping intervals, avoiding the insulation difficulties of continuous downhole delivery; in the medium term, the development of integrated liquid-nitrogen-jet and mechanical-cutting tools; and in the long term, dependent on the maturation of supporting technologies such as vacuum-insulated tubing, downhole phase-state monitoring, and closed-loop nitrogen recovery. Overall, liquid-nitrogen-assisted rock breaking is still in transition from mechanistic study to engineering validation and is better regarded as a supplement to, rather than a replacement for, specific hard-to-drill intervals. As another non-contact thermal technique, directed energy has already entered field testing, but its megawatt-class gyrotrons and waveguides entail very high initial per-well investment, and its cost can become competitive only through economies of scale and application in ultra-deep, ultra-hot intervals where conventional bit life is severely constrained.

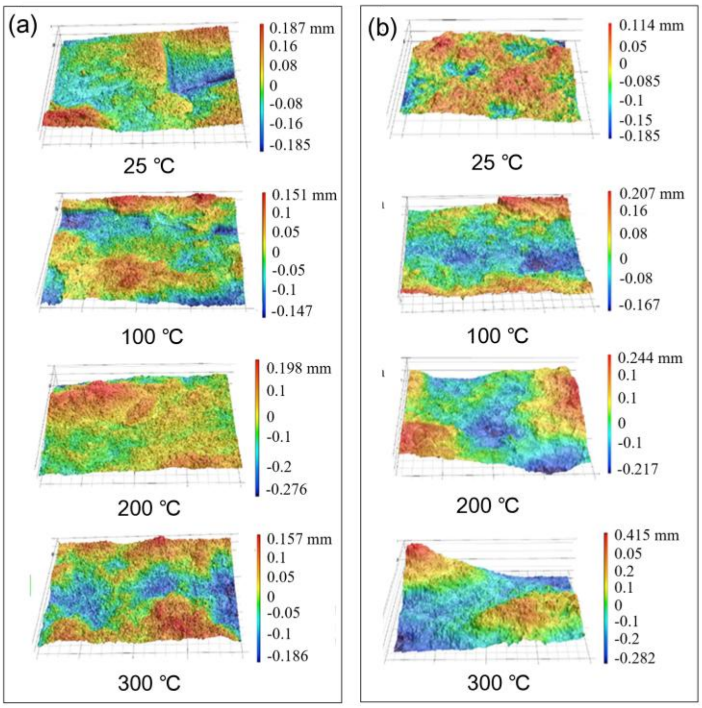

Fig. 11. Tensile fracture morphology of rock after natural cooling and liquid-nitrogen treatment at different temperatures: (a) natural cooling; (b) liquid-nitrogen treatment [218].

In summary, rock-breaking technologies for deep geothermal reservoirs have gradually evolved from traditional single mechanical loading to multi-energy field coupling and multi-mode integration. Current research can, to a considerable extent, mitigate crack suppression due to high confining pressure and rock plasticity enhancement induced by high temperatures, thereby significantly increasing ROP and suppressing stick-slip vibrations in ultra-deep high-temperature hard-rock formations. Successful field applications of specialized bits for geothermal wells fully validate the feasibility of reducing tangential forces and improving drilling economics through optimized cutting structures. Future developments in efficient deep geothermal rock-breaking technologies can target intense temperature rises from point-contact cutting in ultra-deep formations, further enhancing thermal stability and impact toughness of PDC cutters to ensure bit service life. Thermal stress assistance and cryogenic fluid pre-damage technologies are in transition from mechanistic studies to engineering validation; their potential to fundamentally reduce hard-rock drillability by artificially reshaping the bottom-hole thermal damage field is expected to be realized first in ultra-deep, ultra-high-temperature intervals where the life and penetration rate of conventional PDC bits are severely constrained.

4.2 Energy efficiency evaluation models for rock breaking under multi-field coupling

Because of the complex multi-physical-field coupling in geothermal well drilling, conventional rock-breaking models developed for standard formations often fail in high-temperature hard-rock drilling. Current research focuses on rock-breaking models based on damage constitutive relations and temperature fields, as well as multi-feature nonlinear prediction models.

Although significant progress has been made in understanding dynamic responses and meso-scale damage evolution in deep hard rocks, quantifying rock-breaking efficiency from the perspective of energy transfer and conversion remains a critical challenge in practical engineering applications [219, 220]. Particularly under the extreme high-temperature and high-pressure conditions and complex loading scenarios such as combined impacts in deep geothermal development, single mechanical failure criteria often fail to fully capture the overall performance of the drilling system [221]. Therefore, developing energy efficiency evaluation models that adapt to complex rock-breaking modes in geothermal wells and accurately characterize energy utilization in geothermal reservoir environments is essential for practical engineering. Such models are also key to achieving intelligent decision-making for drilling parameters and maximizing rock-breaking efficiency [210, 222]. For combined impact drilling in deep HDR development, Huang et al. [208] proposed a MSE equation based on the classic Teale theory [223, 224]:

$$MSE = \sum_{i=1}^{n} \left[\frac{dF_i + F_v}{A_b} + \frac{120 \cdot \pi \cdot RPM \cdot (dT_i + T_b)}{D_b \cdot V_{ROP}} \right] \tag{6}$$

where dF_i is the average weight on bit per unit time, F_v is the axial impact force, dT_i is the average torque per unit time, T_b is the impact torque, A_b is the bit cutting area, D_b is the bit diameter, and V_{ROP} is the drilling ROP. Subsequent numerical simulations employed the Drucker-Prager constitutive model and equivalent plastic strain failure criterion. They revealed that under combined impact modes, rock failure exhibits a tensile-shear mixed mechanism, with residual plastic deformation reduced by approximately 4.28% compared to conventional drilling. This model provides a direct tool for quantifying drilling efficiency in high-temperature hard rocks from an energy perspective. To more accurately describe the dynamic interaction between the bit and high-temperature hard rock, Ji et al. [225] proposed the improved drifting oscillator model. The model first introduces fractional derivatives to describe the nonlinear rheological properties of high-temperature rock, with the constitutive equation:

$$\sigma(t) = \mu \frac{d^p \epsilon(t)}{dt^p} \quad (0 < p < 1) \tag{7}$$

where μ is the viscosity coefficient and p is the fractional order. The fractional order p is a continuous transition parameter between purely elastic and purely viscous behavior, allowing the viscoelastic composite response of high-temperature rock to be described quantitatively with a single parameter. The closer p is to 0, the more the rock recovers elastically and the more efficiently impact energy is transmitted as stress waves to initiate cracking and chipping. The closer p is to 1, the more viscoplastic the response, with impact energy absorbed and dissipated by plastic flow and effective rock-breaking efficiency dropping markedly. Thus p is a key model parameter for quantifying the rock-breaking mode of high-temperature hard rock, and its value directly determines the degree of rock-breaking-efficiency attenuation in deep high-temperature formations. Incorporating temperature-dependent Young's modulus $E(T)$ and viscosity $\eta(T)$, the model further establishes a differential equation for rock surface motion including temperature effects:

$$\left(m_1 + \frac{\rho_r AL}{3}\right)\ddot{x}_t + \frac{A\eta(T)}{L}\dot{x}_t + \frac{AE(T)}{L}x_t + \frac{A\mu}{L}\frac{d^p x_t}{dt^p} = F(t) \tag{8}$$

where m_1 is the bit mass, A is the cross-sectional area of rock affected by impact, L is the depth of rock affected by impact, $\rho_r AL/3$ is the equivalent spring mass of the rock, x_t is the displacement of the rock surface, $\dot{x}_t$ and $\ddot{x}_t$ are the velocity and acceleration of the rock surface, respectively, and $F(t)$ is the impact load applied to the bit. Within this dynamic framework, the criterion for bit penetration into the rock is defined as the instantaneous contact force (F_c) exceeding the critical rock resistance (F_r):

$$F_c = \frac{A}{L}\left[\eta(T)\frac{d(x_t - x_b)}{dt} + \mu\frac{d^p(x_t - x_b)}{dt^p} + E(T)(x_t - x_b)\right] > F_r \tag{9}$$

where x_b represents the bit penetration depth into the rock. This model accounts for deformation evolution and energy dissipation characteristics of rock in high-temperature environments. It demonstrates at the dynamic equation level that high-frequency impacts can effectively overcome high viscous resistance induced by elevated temperatures. However, current research on rock-breaking equations incorporating thermodynamic factors primarily focuses on non-contact drilling techniques that rely on thermal stress fracturing. Traditional mechanical models struggle to describe the rock fracturing patterns induced by thermal stresses. Rauenzahn and Tester [226] based on Weibull statistical failure theory [227, 228], combined heat flux density, rock properties, and drilling rate to develop an analytical model for drilling ROP:

$$\frac{\sigma_t}{\sigma_0} = \left[\frac{2\,ln\big(1/(1-P)\big)}{\pi C_L^2}\left(\frac{mV_{ROP}}{D}\right)^3\right]^{1/m} \tag{10}$$

where σ_t is the thermal stress on the rock surface, σ_0 is the characteristic strength parameter of the Weibull distribution, P is the rock failure probability, C_L is the aspect ratio of spalled chips, and m is the Weibull homogeneity parameter. Walsh et al. [229] first highlighted the limitation in traditional models of assuming constant chip shape. They proposed that the aspect ratio of spalled chips should be a function of depth from the surface. By modifying the energy balance equation, they developed a heat flux equation accounting for size dependence:

$$Q_t = \rho_r C_p V_{ROP}\frac{(1-\nu)\sigma_0}{\beta_t E}\left[\frac{4\,log(0.5)}{\pi\int_0^\infty C_L(x)^2 x^2\,exp(-\xi x)\,dx}\right]^{1/m} \tag{11}$$

where $\xi = V_{ROP}m/\alpha$ is the thermal diffusion-related term. This model demonstrated that neglecting nonuniform changes in chip morphology with size can lead to approximately 15% error in predicting required heat flux. Building on this, for the more complex hydrothermal jet drilling, Hu et al. [230] developed an analytical model incorporating high-velocity jet impact-assisted rock breaking. The model introduced a jet impact coefficient W to modify the rock failure stress σ_r:

$$\sigma_r = W\sigma \quad (0 < W \leq 1) \tag{12}$$

where σ is the UCS of the rock. Based on this correction criterion, they derived a predictive equation for the critical rock surface temperature (T_s) and ROP incorporating jet impact effects:

$$T_s = T_0 + W\sigma\left(\frac{1-\nu}{\beta_t E}\right)\left(\frac{2\times 0.693}{\pi C_L^2}\right)^{1/m}\left(\frac{mV_{ROP}}{D}\right)^{3/m} \tag{13}$$

where T_0 is the initial rock temperature. They further obtained the heat flux density required to maintain a specific ROP:

$$Q_s = \left(\rho C_p V_{ROP}\right)^{\frac{m+3}{m}} W\sigma\left(\frac{1-\nu}{\beta_t E}\right)\left(\frac{2\times 0.693}{\pi C_L^2}\right)^{1/m}\left(\frac{m}{T_0}\right)^{3/m} \tag{14}$$

These equations quantify the coupling mechanism between jet impact energy and thermal energy. They indicate that enhancing jet impact can significantly reduce the heat flux density and surface temperature required to fracture the rock, thereby optimizing energy efficiency in hard-rock drilling.

Although the aforementioned theoretical models have improved the applicability of conventional rock-breaking mechanisms to geothermal reservoirs from energy transfer and dynamics perspectives, predictions of ROP and specific energy remain typical nonlinear multivariate problems. Solving them still faces challenges such as overly complex multi-field coupling equations and difficulties in accurately calibrating parameters under high temperature and high in-situ stress [231, 232]. Consequently, research approaches are shifting from traditional mechanism-driven regression to intelligent inversion based on field data [222, 233]. For typical nonlinear multivariate predictions such as ROP, Yazitova and Yagiz [234] employed multivariate nonlinear regression to reveal the mechanisms involving rock brittleness and drilling parameters. This study used core input variables such as brittleness index, UCS, and density, combined with drilling parameters like bit diameter and rotary speed, to establish a power-law prediction equation for ROP. However, engineering applications of the model remain constrained by inherent limitations of downhole sensor data. Key rock parameters like brittleness index rely on core experiments or log interpretation, introducing significant time lags and hindering dynamic feedback during drilling. In engineering applications and intelligent prediction, machine learning models demonstrate superior potential. Addressing strong noise and nonlinearity in deep geothermal well data, Yehia et al. [235] compared ten machine learning algorithms using U.S. FORGE field data. Ensemble learning-based algorithms showed greater stability in handling complex nonlinear relationships compared to artificial neural networks. Zhai et al. [236] further validated the advantages of machine learning in geothermal drilling data, noting that optimized random forest models are over 90% faster computationally than back-propagation neural networks while achieving significantly higher prediction accuracy. Additionally, Mantegazini et al. [237] introduced response surface methodology and multi-objective optimization strategies, achieving simultaneous maximization of drilling ROP and minimization of MSE. They confirmed the feasibility of multi-objective optimization in geothermal well drilling predictions.

The apparent disagreement among these comparisons reflects what each study was able to test rather than an intrinsic ranking of algorithms. Ensemble methods outperform neural networks mainly where the training set is small and noisy, which is the normal condition for geothermal wells, so the reported advantage is a property of the data rather than of the method. More critically, all of these comparisons validate on random splits within the same wells, and none reports blind-well extrapolation, so the accuracies quoted measure interpolation within a known field and not the transfer to a new formation that ROP prediction actually requires during drilling. Nor do the input sets include temperature explicitly, which is the variable that most distinguishes geothermal from conventional drilling. For deep geothermal application the physics-based and hybrid formulations therefore remain the more defensible basis, not because they predict more accurately on existing datasets, but because their parameters retain meaning outside the interval on which they were calibrated.

Accurate acquisition of rock mechanical parameters under high-temperature and high-pressure conditions is a prerequisite for drillability evaluation. Auriol et al. [238] proposed an intelligent sensing and inversion framework based on surface top-drive data. Using the nonlinear mapping capability of multilayer perceptron neural networks, they took recorded top-drive drilling parameters as inputs to establish an implicit mapping between drilling dynamics and intrinsic specific energy at the bit, without requiring downhole measurement-while-drilling tools. This approach enables near-real-time inversion of formation drillability and effectively addresses the engineering challenge of downhole electronic sensor failure in deep high-temperature wells. Kong et al. [239] experimentally verified strength damage and plastic yield characteristics of rock under high-temperature and high-pressure conditions. These lead to significant quadratic nonlinear correlations between static mechanical parameters and logging parameters, rather than simple linear relationships. They further corrected traditional log interpretation models, providing an important physical basis for lithology parameter calibration in deep geothermal well drilling ROP prediction models. In summary, rock-breaking models for deep geothermal reservoirs have evolved from early single mechanical criteria to multidimensional evaluation systems incorporating thermo-mechanical coupling, multiple rock-breaking mode impacts, and big data-driven approaches. Different models emphasize varying aspects of physical mechanism description, computational complexity, and field adaptability. To provide a clear comparison of major existing rock-breaking models, their theoretical adaptability to geothermal drilling, and application potential, Table 3 summarizes the core features, feasibility analysis for geothermal drilling, and limitations of each model type.

Table 3. Summary of rock-breaking model research

Model name	Model category	Key features	Application feasibility for geothermal drilling	Limitations
Teale mechanical specific energy model [223]	Physics-based model	Inputs WOB, torque, RPM, etc., to define the minimum energy required for rock breaking.	Serves as a fundamental physical criterion for evaluating hard-rock breaking efficiency.	Assumes ideal cutting, neglecting drill string friction, hydraulic energy, and wear; calculated values are overestimated in heterogeneous formations.
MSE monitoring and adjustment model [240]	Physics-based model	Introduces a mechanical efficiency factor to modify the Teale equation.	Addresses issues of PDC bit chipping and vibration during drilling.	Heavily influenced by drill string frictional torque interference when relying on surface data; serves only as a trend analysis tool; the efficiency factor is empirical.
Compound impact MSE model [208]	Physics-based model	Introduces axial impact force and impact torque to modify the MSE equation, combined with the Drucker-Prager criterion.	Specifically targeted at compound impact drilling technologies used in geothermal hard rocks.	Difficult to fully reflect the strong non-linear characteristics of deep formations when high-temperature and high-pressure parameters are hard to accurately calibrate.
Improved drifting oscillator model [225]	Dynamic numerical model	Introduces fractional derivatives and considers rock modulus evolution with temperature.	Accounts for the impact of high temperature on rock rheology.	Dynamic equations are extremely complex and highly dependent on experimentally determined rock constitutive parameters, making them difficult to solve.
Weibull Thermal Spallation Model [226]	Physics-based model	Based on Weibull failure theory; establishes analytical relationships between heat flux, characteristic strength, and ROP.	Suitable for quantifying links between thermal gradients, ROP, and cuttings size distribution in non-contact drilling of hard rocks.	Assumes a constant aspect ratio for cuttings, ignoring morphological changes with size, which leads to prediction errors.

Size-dependent correction model [229]	Physics-based model	Introduces a thickness-dependent cuttings aspect ratio function to modify the Weibull probability distribution and energy balance equation.	Corrects geometric flaws in the original thermal spallation models.	Introduces complex integration terms, increasing mathematical complexity; requires precise experimental parameters like high-temperature thermal diffusivity.
Hydrothermal jet assisted model [230]	Physical analytical model	Introduces a jet impact coefficient to modify failure stress; establishes critical temperature prediction equations.	Suitable for coupled jet energy and thermal energy rock breaking to improve ROP in ultra-deep hard rocks.	Real-time acquisition of model parameters in complex downhole dynamic environments remains challenging.
Intelligent ROP prediction model [235]	Machine learning model	Compares various machine learning algorithms based on FORGE field data.	Specifically targeted for modeling the geothermal well drilling process.	Prediction performance is highly dependent on data cleaning; model transferability is limited by geological differences.
Machine learning optimization model [236]	Machine learning model	Employs BP neural networks and random forests; utilizes hyperparameter optimization to improve model generalization.	More efficiently processes large-scale real-time drilling data from deep geothermal wells.	Functions as a "black box" model, lacking physical intuitive explanations for the multi-field coupled rock-breaking mechanisms.
Deep learning mechanical parameter inversion model [241]	Hybrid model	Utilizes MLP neural networks combined with the Cuckoo algorithm to invert mechanical parameters from MSE.	Provides real-time critical rock parameters like UCS in intervals lacking logging data to assist in dynamic adjustment of drilling parameters.	Heavily dependent on the accuracy of MSE data; computational load increases significantly with parameter dimensionality.
Multi-objective response surface optimization model [237]	Statistical optimization model	Employs RSM and multi-objective optimization to balance ROP maximization and MSE minimization.	Addresses the trade-off between ROP and MSE during the geothermal drilling process.	Classified as an empirical statistical method; results are only valid within specific parameter windows and equipment specifications.

In summary, the transition of granite from brittle-fracture-dominated to plastic-failure-dominated behavior at high temperature is the direct mechanical cause of the sharp decline in penetration rate in deep geothermal hard rock, while high confining pressure further suppresses crack propagation and energy transfer. Auxiliary techniques such as thermal-stress assistance, high-frequency percussion, and liquid-nitrogen jetting essentially aim to restore or reconstruct the brittle rock-breaking mode under high-temperature, high-confining-pressure conditions, and their design must be guided holistically by the high-temperature rock-breaking modes reviewed in this section.

Although existing research has made significant progress in understanding rock-breaking mechanisms and ROP prediction for deep geothermal hard-rock drilling, limitations persist when confronting the extreme ultra-high-temperature and high in-situ stress environments of geothermal reservoirs. Future research on geothermal drilling rock-breaking and prediction models could further develop machine learning approaches that integrate physical mechanisms with data-driven methods. Overall, the three classes of prediction methods, namely physics-based models, purely data-driven models, and physics-informed neural network (PINN), differ fundamentally in interpretability, physical consistency, and extrapolation capability: purely data-driven models depend on training data and are limited in generalizability and interpretability; PINN are expected to bridge this gap by embedding physical constraints, but have seen limited application in geothermal drilling. A systematic comparison of the three classes of methods, their limitations, and the validation requirements specific to geothermal environments is given in Appendix A3. On this basis, future research may construct PINN in which the energy-conservation equation and rock-damage-evolution criteria are embedded as regularization terms in the loss function. This is expected to balance predictive accuracy and physical consistency under limited field data, and to alleviate the insufficient generalization of purely data-driven models under unseen operating conditions. However, their training stability and computational cost in fully coupled multi-field problems remain key bottlenecks constraining their engineering implementation. In addition, current ROP prediction models are mostly based on static rock-parameter inputs and neglect the influence of transient changes in the temperature and stress fields during drilling on rock drillability. It is necessary to establish a multi-field-coupled constitutive correction model for rock, using in-situ field measurements to invert in real time the true mechanical parameters of bottomhole rock under the current temperature and confining pressure, thereby replacing the lagging core-experiment data and achieving real-time inversion of rock drillability in ultra-high-temperature and high-pressure environments. Finally, with the application of new technologies such as composite impact and hydrothermal-jet-assisted rock breaking, a single mechanical rock-breaking criterion can no longer comprehensively evaluate the system energy efficiency. Although existing multi-objective optimization studies have addressed the coordination of ROP and MSE, they are mostly confined to steady-state prediction. The future direction should shift toward intelligent dynamic decision-making of drilling parameters. Based on digital-twin technology, a comprehensive dynamic model incorporating bit-rock interaction, multiphase fluid circulation in the wellbore, and heat-transfer processes can be constructed to achieve real-time optimization of weight on bit, rotary speed, and hydraulic parameters while ensuring wellbore stability and drill-tool service life, so as to cope with complex conditions such as abrupt formation changes in deep geothermal drilling.

5 Drilling fluid thermal evolution and lost circulation control

In deep geothermal drilling, the wellbore is not merely a mechanical excavation boundary. It serves as a dynamic interface of multi-physical field co-evolution driven by drilling fluid invasion, heat exchange, and chemical interactions once the in-situ geomechanical equilibrium of the formation is disrupted. Wellbore instability is not an isolated mechanical event. It develops along a causal chain consisting of two driving links and one response. First, the cooling cycles of the drilling fluid and its high-temperature rheological evolution shape the wellbore temperature field. This field sets the magnitude and distribution of the transient thermal stress. Second, the evolution of the seepage field and the occurrence of lost circulation alter the near-wellbore pore pressure and the effective stress state. Together these two links constitute the driving conditions of instability. Through the failure criteria, they are ultimately expressed as tensile fracturing, shear collapse, or time-dependent deformation. The two driving links are governed mainly by the thermal and hydraulic behavior of the drilling fluid rather than by the mechanical response of the rock mass, and they are therefore treated in this section as a self-contained topic. This section reviews the evolution of the wellbore temperature field (Section 5.1), the seepage field and lost circulation mechanisms (Section 5.2), and lost circulation control strategies under complex multi-field environments (Section 5.3). The temperature and pore-pressure fields established here provide the boundary conditions for the failure criteria and instability-evolution mechanisms analyzed in Section 6.

5.1 Nonlinear evolution of the wellbore temperature field

In deep geothermal well drilling, the high-temperature and high-pressure environment of geothermal reservoirs induces complex rheological changes and nonlinear evolution of the thermal properties of drilling fluids. These changes form the physical basis for wellbore temperature distribution and subsequent seepage behavior [242]. For water-based drilling fluids, although high pressure slightly increases viscosity through liquid-phase compression, temperature-induced thermal degradation and microstructural changes remain the dominant mechanisms driving property evolution [243]. High-temperature geothermal reservoir environments disrupt the equilibrium of drilling fluid colloidal systems, causing drastic fluctuations in rheological parameters. Fluids typically first exhibit significant reductions in apparent and plastic viscosity. Subsequently, high-temperature flocculation of clay particles or thermal degradation and crosslinking of polymer molecules may lead to abnormal thickening or even solidification [244, 245]. Fig. 12 systematically illustrates the microstructural evolution paths of typical additives (clay particles and functional polymers) in water-based drilling fluids under high-temperature geothermal conditions.

In terms of specific additive systems, current high-temperature-resistant drilling-fluid systems have developed a variety of targeted additives. Among temperature-resistant viscosifiers, fibrous clays such as sepiolite can replace bentonite to provide viscosity and suspension in high-salinity, high-temperature environments; although their crystal structure evolves slightly, they remain stable overall up to 260 °C [246]. Introducing acrylamide (AM)-based synthetic copolymers is an effective way to improve the filtration control of drilling fluids at extreme high temperatures. For example, AM copolymers incorporating temperature-resistant sulfonate monomers can maintain good filtration control under 240 °C high-temperature, high-salinity conditions [247]. Organosilane-modified AM quaternary copolymer microspheres, owing to their rigid cross-linked core and hydrophilic shell, still maintain good filtration control at 200 °C [248]. In the development of systems dedicated to geothermal drilling, a sodium-rectorite formulation modified with organo-lithium-saponite, owing to its structural stability at high temperature, shows practical application potential in deep geothermal drilling [249]. When the formation temperature approaches or exceeds 260 °C, existing water-based polymer systems generally approach the upper limit of their thermal-stability window, and this range remains a future research direction. Particle-stabilized foams, colloidal gas aphrons, and polymer–inorganic nanocomposite systems are important development directions for ultra-high-temperature drilling fluids.

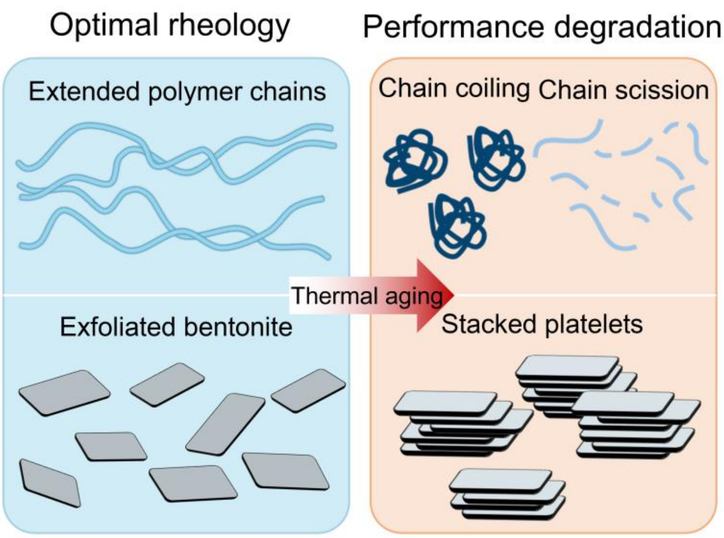

Fig. 12. Schematic of microstructural evolution of drilling fluid additives under high-temperature conditions

These rheological fluctuations affect heat transfer efficiency at the wellbore. Treating the drilling fluid as Newtonian and ignoring viscosity variations overestimates the convective heat-transfer coefficient and leads to misjudged wellbore cooling rates [250]. Mao and Zhang [251] developed a transient temperature model for horizontal wells. This model confirms that changes in drilling fluid viscosity and density alter flow regimes, directly influencing wellbore temperature distribution. Lost circulation of drilling fluid also modifies temperature and pressure fields in the wellbore and near-wellbore region, creating complex dynamic feedback mechanisms. Fomin et al. [252] developed a model showing that lost circulation through discrete fractures removes substantial heat, significantly lowering temperatures in the wellbore and surrounding formation. Zhang et al. [253] conducted numerical simulations of bottom-hole two-dimensional lost circulation to further quantify this cooling effect. Compared to no-loss scenarios, one-dimensional and two-dimensional regional losses reduced bottom-hole temperatures by 9.9 °C and 5.8 °C, respectively. This intense temperature disturbance from lost circulation further influences fracture aperture through thermal expansion and contraction, forming a cycle of lost circulation leading to cooling, which promotes fracture development and intensifies further lost circulation.

To address prediction challenges arising from evolving fluid thermal properties, pure theoretical analysis no longer suffices for accuracy. Coupled models incorporating dynamic parameters are required. Mao et al. [254] developed a transient wellbore heat transfer model accounting for temperature-dependent dynamic changes in drilling fluid thermal properties. They pointed out that ignoring nonlinear effects of density and temperature on thermal conductivity and specific heat capacity causes significant errors in bottom-hole temperature predictions, leading to misjudgments of thermal stress states. Zhang et al. [255] used a transient heat transfer model to reveal unique temperature distribution characteristics in horizontal wells: the highest temperature in drill-string fluid occurs at the bottom hole, whereas in annular fluid it often appears at some distance from the bottom hole. Sensitivity analysis shows that inlet temperature dominantly influences outlet temperature, while vertical depth and geothermal gradient are key factors controlling bottom-hole temperature.

For predicting wellbore temperature fields under thermo-fluid coupling in deep geothermal drilling, current research indicates that physics-informed machine learning methods offer superior generalization and physical robustness compared to purely data-driven approaches. Yuan et al. [256] compared traditional finite difference methods, purely data-driven machine learning, and PINN. By embedding momentum conservation equations (including gravity and friction terms) and energy conservation equations (accounting for formation heat exchange) as physical constraints in the loss function, PINN demonstrated greater robustness under data-scarce complex geological conditions. They also ensured physical consistency in predictions, achieving average relative errors of only 0.20% for pressure and 0.75% for temperature under extreme conditions. Xie et al. [257] integrated PINN with heat transfer models to enable real-time prediction of transient wellbore temperatures. Their study specifically quantified operational effects on temperature: extending circulation stoppage by 10 hours reduces deep-well temperatures by 7.43 °C through enhanced convective heat exchange, while increasing rotary speed from 60 rpm to 100 rpm raises bottom-hole temperature by 2.1 °C due to frictional heat.

5.2 Evolution of wellbore seepage field and lost circulation mechanisms

Deep geothermal reservoirs typically feature coexisting dense matrix and well-developed natural fractures. Although these fractures serve as primary pathways for geothermal fluid migration and heat exchange, they also provide conduits for drilling fluid loss. This results in substantial fluid losses, significantly increasing operational costs and non-productive time while potentially inducing wellbore instability and reservoir damage [258, 259]. Moreover, when loss pathways connect to critically stressed faults, the pore-pressure perturbation induced by the losses may also trigger micro-seismicity [260]. Consequently, drilling fluid lost circulation has become one of the key factors hindering efficient drilling in deep fractured geothermal reservoirs and limiting productivity from geothermal wells [261, 262].

The nonlinear evolution of drilling fluid properties induced by deep geothermal reservoir environments governs the dynamics of fluid seepage. Drilling fluid loss occurs through four main pathways: matrix pores, natural fractures, drilling-induced fractures, and vugs or cavernous formations (Fig. 13). Matrix pore seepage represents the most basic form of loss in permeable formations. In geothermal reservoirs, both the frequency and scale of fracture-related losses are significantly higher than in conventional oil and gas reservoirs [34, 263-265]. Although extensive studies have explored lost circulation mechanisms in fractured formations, failure mechanisms in geothermal deep wells under complex conditions remain highly uncertain. From an engineering-quantification perspective, the four types of loss pathways above differ by orders of magnitude in permeability and aperture scale. The matrix permeability of deep crystalline-basement geothermal reservoirs is extremely low, generally on the order of nano-darcy to micro-darcy, and it decreases further as the effective confining pressure increases [38]. At this magnitude, matrix seepage generally does not constitute significant loss, and the main loss risk of geothermal reservoirs comes from fracture pathways. The geometric aperture of natural fracture pathways in geothermal reservoirs spans several orders of magnitude. For example, in the deep granitic geothermal reservoir at Rittershoffen, France, the apparent aperture of the main permeable fractures ranges from tens of micrometers to tens of centimeters. Some of these large-aperture fractures can correspond to drilling-fluid losses on the order of cubic meters per hour during drilling [266]. For natural fractures in granite at the Grimsel test site in Switzerland, under effective normal stresses ranging from a few megapascals to tens of megapascals, the measured hydraulic aperture is on the order of tens of micrometers and exhibits clear hysteretic evolution with temperature and stress cycling [110]. The equivalent permeability of fractures with sub-millimeter apertures can be several orders of magnitude higher than that of the dense crystalline-rock matrix; therefore, even if the matrix is dense, a formation containing open fractures may still induce significant loss. The aperture range of drilling-induced fractures is generally about one order of magnitude narrower than that of natural fractures, and their actual aperture is highly sensitive to the local stress state and the magnitude of the temperature drop [267]. The key difference from natural fractures is that the aperture of induced fractures is not fixed by geological factors but evolves dynamically with the cyclic operating conditions. This is the fundamental reason why they are difficult to seal effectively by static plugging schemes. The formation mechanism of induced fractures and their THM-coupled propagation behavior are discussed later in this section. Vugs or cavernous formations are the largest in scale and the most difficult to deal with among the four types, with characteristic dimensions spanning the flow resistance and irregular geometry, conventional loss models based on Darcy's law can hardly predict the loss volume quantitatively. The sealing success rate of conventional lost circulation materials and wellbore-strengthening methods is also markedly lower than that for fracture-type loss millimeter to meter range. When well connected, they can create a total-loss scenario at the instant of penetration. Because such pathways have extremely low [265]. In engineering practice, loss in vugs or cavernous formations is often coupled with wellbore collapse to form a compound loss scenario. The continuous loss of returns disturbs the near-wellbore stress balance and erodes weak interlayers, further inducing wellbore instability. The cuttings produced by collapse in turn change the effective aperture and connectivity of the pathway, making it difficult for conventional plugging materials to establish a stable sealing layer.

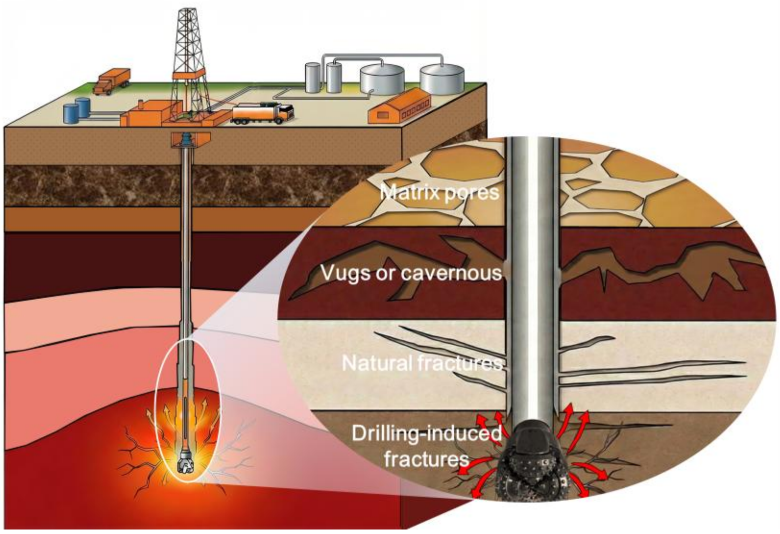

Fig. 13. Schematic of drilling fluid loss pathways

For matrix pore loss mechanisms, Zhang et al. [268] revealed dynamic characteristics where matrix seepage velocity peaks at the wellbore wall and decays exponentially with radial distance. Therefore, accurately describing fluid properties and heat transfer efficiency at high temperatures is a prerequisite for predicting matrix seepage and wellbore stability. For loss in fractured formations, Liu et al. [267] used discrete-fracture-network simulations and showed that the number and location of fracture-wellbore intersections dominate drilling-induced fracture loss more than fracture density alone. This study identified a pressure threshold range for drilling fluid at the wellbore wall. Within this range, increasing fluid pressure helps suppress shear failure and reduces the risk of drilling-induced fracture loss. However, exceeding this range causes fracture connectivity to lead to abnormal pore pressure buildup in the near-wellbore region. This significantly increases radial and hoop stresses, inducing tensile failure and exacerbating loss.

Beyond pressure-difference-driven drilling fluid loss, thermal stresses induced by large temperature differences in geothermal drilling represent a key mechanical mechanism for fracture initiation and exacerbation of fracture-related lost circulation [79, 269]. As discussed in Section 3.3, sharp temperature-dependent changes in rock specific heat capacity and thermal conductivity significantly affect transient heat conduction processes but have relatively limited impact on heat conduction velocity itself. However, in wellbore stability analysis for geothermal reservoirs, the thermal expansion coefficient dominantly controls peak thermal stress, far exceeding the influence of thermal conductivity and elastic modulus [270, 271]. Wu et al. [272] developed a transient analytical model that further shows cold fluid circulation rapidly lowers bottom-hole temperature. This transient cooling effect significantly weakens compressive stress in the near-wellbore region. When hoop stress decreases enough to overcome rock tensile strength, it induces tensile fracturing and consequent lost circulation. Suo et al. [273] quantified this effect through numerical simulations and experiments on HDR granite. Their study shows that under high-temperature conditions with cold fluid invasion, hoop stress around the wellbore decreases much faster than radial stress. This lowers formation breakdown pressure, exacerbates micro-fracture propagation, and causes thermally induced fracture loss. Fig. 14 shows simulated wellbore hoop and radial stress distributions after invasion by different cooling fluids. Zhu et al. [270] calculated that in deep HDR drilling, stress intensity factors at crack tips can reach 200 MPa·m$^{0.5}$, far exceeding granite fracture toughness. This implies that thermally induced cracking and propagation around the wellbore are nearly inevitable, with crack opening widths exceeding 1 mm, providing direct pathways for drilling fluid loss.

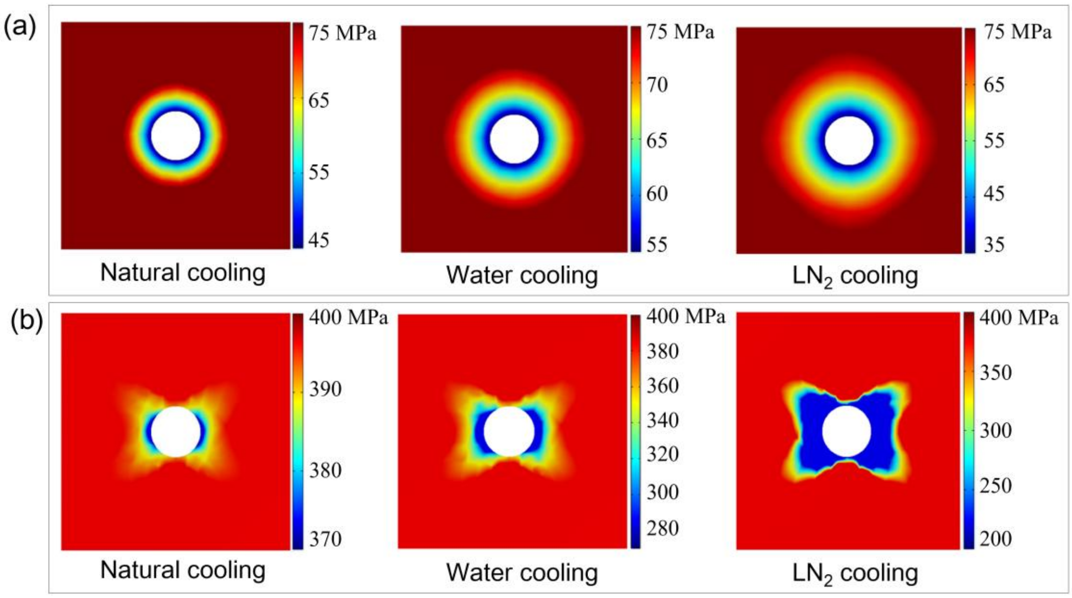

Fig. 14. Wellbore stress distribution 500 seconds after different cooling methods: (a) Radial stress; (b) Hoop stress [273]

Chemical coupling mechanisms also influence drilling fluid loss. Under combined chemical potential and temperature gradients, flow between the wellbore and formation involves not only pressure-difference seepage but also chemico-osmotic and thermo-osmotic effects [274, 275]. When drilling fluid solute concentration exceeds that of formation fluid, chemical potential difference drives pore water expulsion, reducing pore pressure and increasing effective stress to suppress fracture development.

However, when this chemical shrinkage superimposes on cooling-induced shrinkage, under deep formation conditions with high chemical potential and strong cooling, matrix contraction significantly induces tensile stress concentration at the wellbore wall, leading to tensile failure and heightened loss risk [276, 277]. Additionally, the temperature field nonlinearly regulates solute diffusion rates: heating accelerates diffusion, while cooling slows it. Under large concentration differences, this thermo-chemical coupling produces more pronounced nonlinear stress responses [278]. Tang et al. [279] incorporated thermo-chemical coupling into their analysis. They pointed out that differences in solute concentration between drilling fluid and formation fluid generate chemical potential gradients. Although lowering drilling fluid temperature helps reduce pore pressure, changes in solute concentration alter radial and hoop effective stresses. Particularly when drilling fluid solute concentration is lower than that of formation fluid, this may exacerbate wellbore damage and instability in early stages.

5.3 Lost circulation control strategies under complex multi-field environments

The above analysis demonstrates that lost circulation is a dynamic process driven by multi-field coupling. Temperature field evolution alters fluid properties, while seepage field redistribution induces fracture propagation. These two factors continuously reinforce one another through a positive feedback loop of “lost circulation-cooling-fracture initiation.” Methods relying solely on physical plugging or single-parameter adjustment cannot fully interrupt this feedback loop. For example, conventional lost circulation materials degrade in performance under high temperatures and cannot adapt to dynamic fracture opening and closing caused by pressure fluctuations. Therefore, coordinated strategies are required at two levels: microscopic material reinforcement and macroscopic tool control. These aim to enhance the adaptability of plugging zones to multi-field disturbances and to weaken the thermal-pressure gradients that drive lost circulation.

First, at the microscopic material level, enhancing mechanical stability of plugging zones requires optimizing particle contact networks. Through photoelastic experiments, Yan et al. [280] examined energy dissipation in strong force chains and revealed the failure mechanisms of particle plugging zones under wellbore pressure fluctuations. The study found that force chain networks inside plugging zones dissipate energy under external loads. When input energy exceeds storage limits, force chains break and reorganize, causing macroscopic plugging failure. Plugging layers formed by uniform-sized spherical particles exhibit particularly high energy dissipation rates and poor stability. In contrast, using multi-sized mixtures, non-spherical particles, and fiber additives significantly reduces force chain energy dissipation, maintaining structural integrity under high-frequency pressure fluctuations. Sonmez et al. [281] offered a comprehensive solution perspective, emphasizing the critical role of drilling fluid design in addressing torque and lost circulation issues. The study highlighted that under high-temperature and high-pressure conditions, using $CaCO_3$ with specific particle size distributions as bridging material is crucial. Based on Abrams' rule, experiments demonstrated that adding 30-50 lb/bbl of specific-sized $CaCO_3$ forms optimal plugging layers on 20-120 μm ceramic disks. Additionally, to reduce high torque in extended-reach and horizontal wells, the study recommended adding 1-3% environmentally friendly lubricants to water-based drilling fluids. This reduces friction coefficients by over 90% and indirectly maintains wellbore mechanical stability by minimizing frictional vibrations between tools and the wall.

Second, at the macroscopic tool level, using downhole tools for thermal stress control effectively mitigates lost circulation and instability. Xiao et al. [282] proposed a wellbore cooling method based on insulated drill pipes. Analysis showed that, compared to adjusting circulation rate or rotary speed, reducing drill pipe thermal conductivity is the most sensitive and effective measure for lowering bottom-hole temperature. Double-wall insulated drill pipes substantially lower deep formation temperatures, significantly alleviating high-temperature-induced wellbore surrounding rock fracturing and enabling potential on-drilling geothermal energy extraction.

6 Wellbore instability characteristics and evolution laws under multi-field coupling

The wellbore temperature field, seepage field, and lost circulation behavior reviewed in Section 5 define the thermal and hydraulic loading acting on the wellbore; this section analyses the resulting geomechanical response. Drilling fluid lost circulation and wellbore instability in deep geothermal drilling are not independent engineering issues. Instead, they mutually induce and reinforce each other through complex THM coupling mechanisms [283, 284]. As described earlier, lost circulation not only causes working fluid loss but, more critically, induces fluctuations in wellbore hydrostatic pressure and redistribution of near-wellbore pore pressure, disrupting the originally fragile mechanical balance around the wellbore. When effective support from loss decreases or hoop thermal stress concentration from cooling exceeds rock shear strength, wellbore failure modes shift from tensile fracturing dominated by crack opening to shear failure dominated by rock collapse [79, 285]. Particularly in the high-temperature and high-pressure environments of deep geothermal wells, nonlinear evolution of rock mechanical properties combined with intense cooling-cycle shock effects makes wellbore stability prediction and control far more complex than in conventional oil and gas wells. Therefore, following discussions on lost circulation, wellbore shear instability mechanisms and evolution must be further analyzed from a multi-field coupling perspective.

6.1 Failure criteria under multi-field response

Single-mechanism mechanical models no longer meet the accuracy requirements for assessing wellbore-instability risk in deep geothermal wells. Appropriate failure criteria must be selected from a multi-field coupling perspective. Table 4 summarizes simulation methods, failure criteria, and involved multi-field coupling mechanisms used in wellbore stability studies for different formation characteristics and drilling conditions. As the table shows, current studies mainly adopt the Mohr-Coulomb or Drucker-Prager criterion for granitic formations, and only in shale studies involving chemical-coupling processes have multiple criteria accounting for the intermediate principal stress been systematically compared

Table 4. Summary of wellbore stability research in geothermal drilling

Reference	Simulation software/ method	Failure criterion	Lithology	Drilling condition	Coupling Mechanism
[286]	MATLAB	Mohr-Coulomb, Tensile Failure	Volcanic rock	Drilling fluid seepage, temperature difference	THM coupling; comprehensive evolution of wellbore instability pressure under the superposition of pore pressure and thermal stress after fluid infiltration.
[287]	COMSOL	Mohr-Coulomb	Heterogeneous granite	Drilling fluid circulation cooling	THM coupling in micro-heterogeneous formations; cooling induces micro-thermal stress concentration and micro-cracks at grain boundaries due to differences in mineral thermal expansion coefficients, leading to wellbore instability.
[288]	DEM-FEM	Mohr-Coulomb, Max Tensile	Fractured granite	High-pressure fluid invasion into fractures	Integration of THM coupling and discrete fracture network, revealing a tolerance interval for wellbore stability under high mud pressure.
[289]	GOLEM (MOOSE framework)	Drucker-Prager, Mohr-Coulomb	Fractured formation	Drilling fluid cooling effect	THM coupling; risks of matrix plastic yield and specific fracture slip in fractured rock masses induced by the cooling effect of drilling fluids.
[79]	Analytical	Mohr-Coulomb	High-temperature formation	Drilling fluid circulation heat exchange	Thermo-poroelastic theory; provides analytical solutions considering cooling effects to rapidly predict periwelling stress and temperature distribution.
[290]	Abaqus	Drucker-Prager	HDR	Dynamic drill-string impact, rotary drilling	Dynamic and thermodynamic damage; incorporates drill-string dynamics to simulate mechanical impact from random collisions and its effect on crack propagation in thermally damaged zones.
[291]	COMSOL	Mohr-Coulomb, Tension Cut-off	HDR	Wellbore instability in extreme high-temperature environments	Abrupt thermal changes in material properties; simulates shifts in wellbore failure modes caused by the brittle-to-ductile transition above threshold temperatures.

[270]	Analytical	Max Tensile Stress	HDR	Drilling fluid circulation cooling	Transient heat conduction; analyzes the impact of nonlinear thermal property evolution with temperature on cooling rates and thermal stresses.
[35]	FEM	Drucker-Prager, Maximum Tensile	HDR	Excavation unloading under 3D in-situ stress	3D in-situ stress-THM coupling; how in-situ stress mechanisms dominate stress concentration patterns around the wellbore, determining the final failure morphology.
[292]	Analytical	Mohr-Coulomb, Mogi-Coulomb, etc.	Shale	Chemical potential difference	THMC coupling; introduces chemical potential gradients and evaluates six failure criteria, including the Mogi-Coulomb criterion which considers intermediate principal stress.

Aslannezhad et al. [292] evaluated six failure criteria under thermo-hydro-mechanical-chemical (THMC) multi-field coupling conditions. They found that the Mohr-Coulomb criterion tends to overestimate wellbore failure risk, resulting in overly conservative predictions of critical mud density [293]. In contrast, the Mogi-Coulomb, Modified Lade, and 3D Hoek-Brown criteria, which account for intermediate principal stress effects, provide predictions more consistent with field observations. For complex stress states, Li et al. [294] emphasized the importance of elastoplastic strain-softening models. They noted that mud cake formation effectively blocks fluid seepage, mitigating reductions in effective stress from pore pressure changes and suppressing shear failure propagation.

In the wellbore-stability assessment of deep geothermal wells, the proper selection of failure criteria directly affects the prediction of the critical mud density and the determination of wellbore-instability risk. The applicability of a criterion in geothermal hard rock is jointly determined by the following four engineering factors. (1) Intermediate principal stress effect. Around a deep geothermal wellbore, the three principal stresses are generally unequal. At the Soultz-sous-Forêts site, for example, in-situ stress measurements over the 1.5–5 km depth interval satisfy $\sigma_1 \approx \sigma_2 > \sigma_3$ [295]. Under such a stress state, in which σ_2 markedly exceeds σ_3, the intermediate principal stress exerts a significant strengthening effect on rock strength [293, 296, 297]. Comparisons of true-triaxial and high-temperature triaxial tests on a range of geothermal-related rocks likewise show that failure criteria accounting for the intermediate principal stress are, overall, superior to those neglecting σ_2, although the degree of improvement varies with lithology [298, 299]. Consequently, criteria relying solely on σ_1 and σ_3 tend to overestimate the instability risk in geothermal wellbore-stability prediction, whereas σ_2-incorporating criteria such as Mogi-Coulomb, Modified Lade, and 3D Hoek–Brown more accurately reflect failure strength under complex stress states. (2) Nonlinear strength growth under confining pressure: rock strength grows nonlinearly with confining pressure [300, 301], and the failure envelope flattens near the brittle–ductile transition, so linear criteria systematically overestimate strength under deep high-confinement conditions, while nonlinear criteria such as generalized Hoek–Brown and Modified Lade can capture this curvature [302, 303]. (3) Tensile-failure treatment: as discussed in Section 3.1, intense heat exchange between cold drilling fluid and hot surrounding rock induces strong cooling tensile thermal stresses that may push the hoop stress into the tensile range. The criterion must therefore include a tensile cut-off (as in Mohr-Coulomb and Mogi-Coulomb) or describe tensile failure through a curved envelope (as in Hoek-Brown). By contrast, an uncorrected Drucker-Prager criterion shows significant deviation in the tensile region [299]. (4) Temperature dependence of strength parameters: the high temperatures and thermal cycling experienced by the wellbore require that strength parameters evolve with temperature; Mohr-Coulomb, Mogi-Coulomb, and Modified Lade can be calibrated through temperature-dependent c and φ, while Hoek-Brown further requires a temperature-dependent GSI mapping. Together these four aspects determine the engineering applicability of a criterion, and the practical choice reflects a trade-off among accuracy, parameter availability, and computational complexity. For the typical conditions of deep geothermal wellbores, the four factors above point collectively toward the same tendency. The Mogi-

Coulomb (or Modified Lade) criterion best fits the design requirements. The Mohr-Coulomb criterion should be used only as a lower bound for conservative screening because it systematically overestimates instability risk. The unmodified Drucker-Prager criterion should be avoided under cooling-dominated conditions.

This judgment of cooling-induced tensile failure can be further quantified by a specific example. Through experiments and numerical simulation, Suo et al. [273] showed that after liquid nitrogen acts on a high-temperature granite wellbore for 500 s the wellbore temperature can drop by about 700 °C. The resulting transient thermal stress lowers the hoop stress around the wellbore by about 180 MPa while the radial stress falls by only about 35 MPa. The hoop reduction far exceeds the radial reduction, shifting the Mohr circle strongly leftward and shrinking its radius, while cold-fluid invasion superimposes additional tensile stress near the wellbore, driving the effective hoop stress into the tensile range and inducing radial tensile cracks along the minimum-horizontal-stress azimuth. Liu et al. [267] in a THM numerical model of fractured granite, further gave the operating boundary for wellbore stability: the wellbore remains stable when the temperature difference is kept within 250 °C and the drilling-fluid pressure exceeds the original pore pressure by about 10 MPa. These bounds come from a THM simulation of one fractured-granite case and have not been checked against field data, so they indicate the order of magnitude at which the two failure modes are jointly suppressed rather than a value that transfers to other stress states and geometries. The upper limit of this pressure window is further constrained by the risk of induced seismicity: beyond reservoir hydraulic stimulation, wellbore-pressure perturbations during drilling can themselves induce earthquakes. At the St. Gallen well in Switzerland, after a gas kick occurred in the late stage of drilling, about 700 m^3 of drilling fluid was pumped into the well to suppress the wellhead pressure. This subsequently induced, on a nearby fault, an earthquake sequence that included a felt Mw 3.3 event [260]. During the drilling of the Rittershoffen doublet in France, drilling-fluid losses in the Muschelkalk formation likewise induced tens to hundreds of micro-seismic events around the wells [304]. Although the underlying mechanism likewise originates from a reduction of the effective stress on the fault plane, the failure mode differs from the near-wellbore cooling-induced tensile fracturing discussed above. The latter is tensile opening near the wellbore wall, whereas fault reactivation is shear slip on a pre-existing fault plane, triggered once the ratio of shear stress to effective normal stress reaches the Mohr-Coulomb slip condition. In terms of triggering paths, pore-pressure diffusion is a seismicity-inducing mechanism shared by conventional oil-and-gas drilling and geothermal drilling, arising from drilling-fluid overpressure or losses that diffuse pore pressure along connected fractures toward nearby faults and reduce the effective normal stress on the fault plane. What is specific to geothermal drilling is that the strong temperature contrast between the wellbore wall and the surrounding rock, under prolonged cold-fluid circulation, advances a cooling front into the formation. The resulting thermo-elastic stress perturbation can likewise alter the normal-stress state on nearby fault planes. Induced-seismicity risk assessment for geothermal drilling should therefore consider both the hydraulic and the thermal paths.

The drilling-fluid pressure window is thus bounded in both directions: the lower limit is controlled by cooling-induced tensile fracturing and losses, while the upper limit is jointly defined by wellbore shear failure and fault-induced seismicity. The two do not always control simultaneously. In intervals far from critically stressed faults the upper limit is governed mainly by wellbore shear failure, whereas in intervals approaching critically stressed faults the maximum bottom-hole pressure allowed to avoid fault reactivation may be lower than the mechanical-stability limit, in which case induced seismicity becomes the controlling constraint. The upper limit of the pressure window should therefore be taken as the smaller of the two and adjusted dynamically with well trajectory and distance to faults. Given that fault locations and critical stress states are often difficult to determine precisely in advance, drilling-fluid pressure design for deep geothermal drilling should not only maintain wellbore mechanical stability but also incorporate induced-seismicity risk into the pressure window in combination with the regional stress state and the mapped fault distribution, supported by lost circulation monitoring and real-time micro-seismic monitoring to avoid fault reactivation.

Drawing together the mechanisms reviewed in the preceding chapters, an inference about the evolution of near-wellbore stress under typical geothermal conditions can be made relative to conventional oil and gas drilling mechanics. Taking a typical high-temperature hot-dry-rock granite reservoir as an example, the near-wellbore stress evolution under drilling-fluid cooling cycles can be summarized as three superimposed processes. (1) As described in Section 3, the high-temperature degradation of granite, together with the brittle–ductile transition and the accumulation of thermal damage near the quartz phase-transition threshold, makes the mechanical properties of the near-wellbore rock markedly different before and after drilling-induced cooling. The high-temperature plastic stage before cooling and the residual-damage stage after cooling should be assigned different strength parameters. (2) As shown in the worked example above, the intrusion of cold fluid sharply reduces the hoop stress around the wellbore and superimposes an additional tensile stress, with a reduction far larger than that of the radial stress, so that the hoop effective stress enters the tensile regime first. (3) As described in the permeability-evolution part of this review, above the threshold temperature the connection of the fracture network causes an order-of-magnitude jump in permeability, and the cooling-induced tensile cracks couple further with thermal-fracturing-enhanced permeability, forming a "cooling–tensile fracturing–lost circulation" feedback. It can therefore be inferred that, under typical geothermal conditions, the controlling factor of wellbore instability is not in-situ stress concentration alone but the superposition of "lithological degradation controlled by the temperature threshold" and "transient tensile stress controlled by the cooling rate". The closer the temperature is to or beyond the phase-transition threshold and the faster the cooling, the more readily the hoop tensile stress exceeds the tensile strength already weakened by thermal damage. This inference is corroborated by the stability-window bounds reviewed in this paper, namely that the temperature difference should be kept within about 250 °C while maintaining a moderate positive overbalance to suppress tensile fracturing; as noted above, these bounds derive from THM numerical models that have not been calibrated against field measurements, so they are indicative rather than prescriptive. The review therefore indicates that, under representative geothermal conditions, wellbore-stability design should place the control of the cooling temperature difference and rate on an equal footing with balancing the wellbore pressure, which constitutes a practically meaningful inference of this review relative to conventional oil and gas drilling mechanics.

6.2 Wellbore instability mechanisms under superposition of mechanical damage and multi-physical fields

Compared to conventional oil and gas drilling, temperature field variations induced by drilling fluid cooling cycles represent the core factor triggering wellbore instability in geothermal drilling [305]. The failure mechanisms primarily arise from coupled macroscopic thermal stress disturbances and microscopic thermal evolution of rock mechanical properties. Temperature differences between drilling fluid and formation first alter near-wellbore stress states through thermal expansion and contraction. Cooling by low-temperature drilling fluid causes rock contraction, generating hoop tensile stresses [79, 88, 91, 287]. High-temperature environments simultaneously trigger nonlinear mutations in rock properties, leading to strength degradation [74, 82, 291, 306]. In crystalline rocks such as granite, intensified thermal motion of crystal grains and differences in thermal expansion coefficients among minerals induce intergranular incompatible deformation and micro-crack propagation [60, 72]. This combination of drilling fluid cooling and high-temperature-induced rock strength reduction forms a dangerous instability synergy. As shown in Fig. 15, cooling contraction and the seepage-induced rise in pore pressure reduce the effective stress, and because the hoop stress decreases far more than the radial stress, the stress circle translates leftward with a shrinking radius. At the same time, high-temperature strength degradation (reduction of c and φ) lowers the shear failure envelope. The two compress the safety margin from opposite directions: tangency of the stress circle with the degraded envelope triggers shear failure, whereas contact of the circle's left edge with the tensile cut-off ($\sigma = \sigma_t$) corresponds to tensile fracturing under cooling-dominated conditions. The relative likelihood of the two modes depends on the combination of the temperature difference and the mud-column support. Particularly in complex geothermal reservoirs, thermally induced additional stresses are more intense. Ignoring this THM coupling mechanism in favor of single mechanical factors severely underestimates wellbore collapse risk. Field cases further reveal the engineering features of wellbore instability under THM coupling. For the IDDP-2 well in the Reykjanes geothermal field in Iceland, a volcanic reservoir dominated by basaltic lavas and hyaloclastites, a comparison between borehole-imaging logs and DEM numerical simulation showed elliptical breakout of the wellbore and extensional fractures induced by thermo-mechanical coupling [307]. In the andesite-hosted Rotokawa geothermal field in the Taupo Volcanic Zone of New Zealand, a similar thermal-stress-induced instability mechanism was confirmed. Massiot et al. [308] directly identified drilling-induced tensile fractures in the andesite reservoir through acoustic borehole imaging. Siratovich et al. [50] further demonstrated through thermal-stimulation experiments that the thermal stress produced by injecting cold water into the andesite reservoir is sufficient to induce micro-crack propagation and significantly raise rock permeability.

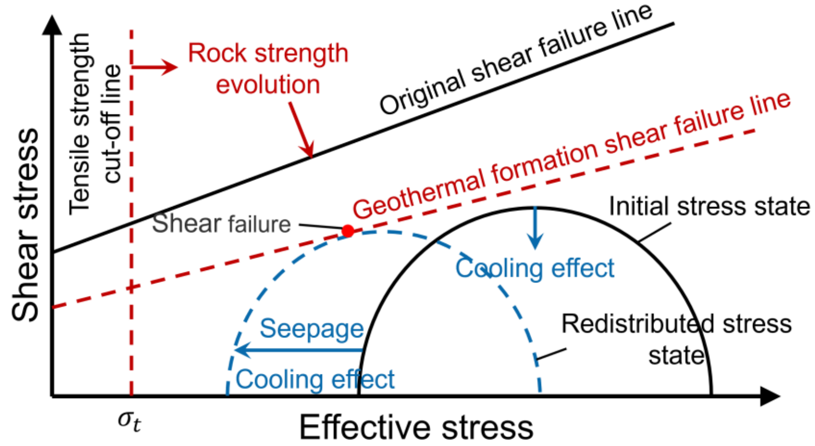

Fig. 15. Schematic of wellbore stress-state evolution and failure modes under THM coupling. The horizontal axis is effective stress and the vertical axis is shear stress. Black solid circle: initial in-situ stress state; blue dashed circle: redistributed stress state after cooling and seepage, with the blue arrow indicating its leftward shift; black solid line: original shear failure envelope; red dashed line: geothermal-condition envelope after high-temperature strength degradation, drawn illustratively and not fitted to a specific dataset, with the red arrow indicating its downward shift; red dot: onset of shear failure; red vertical dashed line at σ_t: tensile cut-off, contact of which by the left edge of the circle corresponds to tensile fracturing

Liu et al. [35] used three-dimensional numerical models to quantify the controlling effect of temperature differences on failure modes. Under small temperature differences, the wellbore tends to experience narrow-band shear failure perpendicular to the well axis. However, with significant temperature increases, intense cooling contraction not only induces tensile fracturing but also causes high-angle shear failure on the wellbore surface, potentially forming combined tangential and axial tensile failure. In fractured formations, thermal effects are more subtle. Heidari et al. [289] showed through simulations that cooling effects not only induce tensile failure but also generate more plastic yield zones in near-wellbore rock matrix. More critically, thermal disturbances significantly increase slip tendencies on inclined fractures. Even natural fractures not directly intersecting the wellbore may activate and undergo shear slip under cooling. Liu et al. [288] further revealed spatiotemporal evolution patterns of wellbore instability using THM coupled models for heterogeneous granite. Fracture opening mechanisms exhibit two temporal stages: early drilling dominated by tensile failure from drilling fluid pressure disturbances, shifting later to shear failure governed by thermal stress and in-situ stress differences. Spatially, fracture aperture exhibits a threshold for wellbore stability. Below 0.005 mm, effects resemble intact formations. At 0.05 mm, drilling fluid invasion saturates, markedly enhancing and stabilizing instability trends. Additionally, increasing horizontal in-situ stress ratios intensifies effective stress concentration at the wellbore, orienting failure locations along principal stress directions. This suppresses tensile failure but significantly heightens shear slip risk on fractures. Yuan et al. [309] further quantified the prediction bias of ignoring damage evolution. The shear displacement of pre-existing fractures predicted by a Weibull stochastic-damage constitutive model is about 40% higher than that of a conventional THM model. The underlying mechanism is that damage-induced stiffness degradation and permeability enhancement jointly weaken the effective normal stress on the fracture surface. This further indicates that neglecting damage in geothermal wellbore-stability assessment systematically underestimates the instability risk.

In-situ stress mechanisms and seepage field characteristics determine instability failure modes. As overburden pressure increases, axial compressive stress at the wellbore rises. This suppresses growth of formation shear stress, thereby reducing shear failure risk to some extent [35]. Seepage effects significantly increase instability complexity. He et al. [310] showed that anisotropic seepage causes sinusoidal or cosine fluctuations in radial and hoop stresses around the wellbore. Particularly in near-wellbore regions, superposition of seepage and thermal stresses markedly alters the rock shear failure envelope, pushing originally stable zones into plastic yield states. Zhang et al. [286] reached similar conclusions in multi-field coupling studies on volcanic rock formations. Ignoring dynamic coupling between fluid seepage and thermal stress while considering only single stress factors significantly underestimates wellbore collapse risk, with calculation errors exceeding 30%.

At the mechanical level, dynamic effects of the drilling process itself cannot be overlooked. Li et al. [311] studied percussion drilling. They found that dynamic bit impacts create significant crushed zones and radial crack networks around the wellbore. Experimental results showed that, compared to conventional rotary drilling, impacts substantially reduce P-wave velocity and tensile strength in granite. This mechanical damage directly increases formation permeability, providing pathways for drilling fluid loss and elevating wellbore instability risk. Additionally, Liu et al. [290] incorporated drill string dynamics. They found that random lateral drill string collisions significantly exacerbate cumulative wellbore damage. Particularly in regions with pre-existing THM damage, impacts cause cracks to propagate along grain boundaries, increasing collapse severity by approximately four times compared to undamaged formations. Engineering cooling measures, while mitigating thermal damage, may introduce new risks. Yang et al. [312] studied the Reelwell drilling method, offering a dialectical thermodynamic perspective. Although the unique double-wall drill pipe design effectively lowers bottom-hole temperature, uncontrolled sustained cooling may induce shear slip on micro-fractures due to excessive rock cooling.

In addition to the instantaneous mechanical instability discussed above, the time-dependent deformation of the wellbore should not be neglected. High-temperature thermal damage markedly reduces the viscosity coefficient and long-term strength of rock, causing it to exhibit pronounced creep: significant rheological deformation can occur even under relatively low deviatoric stress, the strain rate in the steady-state creep stage increases substantially, and the threshold time for entering accelerated creep is markedly shortened [313, 314]. In terms of creep constitutive theory, Zhang et al. [315] improved the conventional Burgers model by introducing a nonlinear Newtonian body, describing the nonlinear characteristics of rock entering the accelerated-creep stage under different temperature conditions and revealing the quantitative relationship between temperature and creep strain rate. For high-temperature environments, Jiang et al. [316] proposed an improved three-dimensional nonlinear Nishihara model that accounts for thermo-mechanical coupling damage, further elucidating how the viscosity coefficient of rock decays with the accumulation of damage at high temperature. In terms of engineering-case validation, Xu et al. [81] carried out real-time high-temperature true-triaxial creep tests over 25–800 °C on HDR from the Gonghe Basin in Qinghai, and found that as the temperature gradient increases, the creep threshold stress of granite decreases significantly. In particular, under the deviatoric stress formed by simulated drilling unloading, the rock around the wellbore is highly prone to large inward radial rheological deformation over time without undergoing instantaneous macroscopic failure. This high-temperature-induced accelerated-creep mechanism is one of the core geomechanical causes of borehole shrinkage and stuck pipe in deep geothermal wells [317, 318].

In summary, wellbore stability in deep geothermal reservoirs involves a dynamic evolution process with multi-physical field coupling. Unlike conventional oil and gas drilling, stability in deep geothermal wells depends not only on mechanical balance between in-situ rock stress and wellbore pressure but also on high-temperature-induced brittle-ductile transitions and pronounced creep characteristics. Therefore, developing dynamic wellbore stability assessment models that account for time effects, thermal damage, and strain rate dependence forms the core theoretical foundation for safe and efficient drilling in deep geothermal resources. Future research on wellbore stability in geothermal drilling should focus on constructing dynamic assessment models that incorporate time-varying effects and thermal damage in surrounding rock. In multi-physics simulation, when constructing a fully coupled THMC model that accounts for chemical effects, physics-informed methods represented by PINN can be explored to improve the efficiency of multi-field coupling inversion while ensuring physical consistency; however, it should be noted that the convergence and computational cost of current PINN on stiff, multi-scale coupled equations remain to be overcome.

7 Synthesis and discussion

The multi-scale framework proposed in Appendix A1 indicates that the temperature thresholds reviewed separately in the preceding chapters are not mutually independent but are manifestations of the same thermal-damage evolution process at different scales. Taking granite reservoirs, currently the most thoroughly studied geothermal reservoir rock, as an example: the roughly threefold contrast in thermal expansion coefficient between quartz and K-feldspar drives grain-boundary mismatch stresses to the micro-crack initiation condition at about 300 °C (Section 3.1); at the rock-sample scale this mineral-scale threshold corresponds to the accelerated strength degradation from 300 °C onward, and at the bit–rock scale it coincides with the 240–360 °C brittle–ductile transition range of PDC cutting (Section 4.1.1). The stress concentration at the cutter tip during rock breaking brings forward the ductility that appears only at about 600 °C in compression tests, so that the mineral-scale softening boundary is translated into the abrupt-transition temperature of the cutting response. The quartz phase transition at 573 °C drives two evolution paths simultaneously: mechanically, cracks shift from intergranular to transgranular; hydraulically, it appears as the order-of-magnitude permeability jump at 573–600 °C (Section 3.2), which supplies the pathway source for losses at the wellbore scale (Section 5). At the wellbore scale during drilling, drilling-fluid cooling reverses the direction of the thermal load: the thermally pre-damaged wellbore wall preferentially undergoes tensile fracturing under rapid cooling contraction, and losses, cooling, and fracturing form a positive feedback loop that keeps accumulating damage; which instability mode appears depends on the relative levels of the wall temperature difference and the drilling-fluid pressure, with an excessive temperature difference triggering tensile fracturing and insufficient column support leading to shear collapse (Section 6). The borehole breakouts recorded by image logs in Iceland's IDDP-2 well can be regarded as the direct field-scale expression of this damage-evolution process that begins with grain-boundary thermal mismatch. The mechanism chain retains the same structure in carbonate and sandstone lithologies while its triggers and thresholds differ (Sections 3.1–3.2), and reasonably complete data across all scales are currently available only for granite.

Within the framework of this mechanism chain, the two controversies addressed in this review can be explained fairly clearly. The net effect of high temperature on deep rock-breaking efficiency is strongly dependent on the temperature–confining-pressure regime: heating at constant confinement is beneficial in net terms, whereas confinement at room temperature is suppressive by an order of magnitude; in deep, highly confined intervals the latter most likely dominates, so the rock-breaking energy fraction obtained under unconfined conditions should be used as an upper bound on downhole energy efficiency. The critical temperature–pressure conditions under which the dominance shifts between temperature gain and confinement suppression, that is, under which the net effect turns from promoting to impeding rock breaking, have not yet been investigated (Section 4.1.1, Regime 4 of the T–σ mechanism map). The selection of rock failure criteria in wellbore-instability assessment likewise admits a tendency drawn from the evidence. This choice directly affects the prediction accuracy of the critical drilling-fluid density: under the measured stress state of $\sigma1 \approx \sigma2 > \sigma3$ and cooling-dominated tensile conditions, the Mogi-Coulomb (or Modified Lade) criterion best fits the design needs of geothermal wellbores; the Mohr-Coulomb criterion, which systematically overestimates instability risk, is appropriate only as a conservative preliminary screen; and the unmodified Drucker-Prager criterion is unsuitable in the tensile regime (Section 6.1).

From the current state of research, the evidentiary bases of the individual links of the mechanism chain are not equal. The mineral-to-rock and rock-to-cutter links are directly supported by acoustic emission, mechanical testing, and cutting comparison experiments, whereas the laboratory-to-in-situ link is systematically constrained by confinement conditions: the permeability threshold is only a lower bound of the in-situ value, and the rock-breaking energy fraction only an upper bound of in-situ efficiency. The rock-to-wellbore link is markedly weaker: on the one hand, the wellbore stability window of about 250 °C temperature difference and about 10 MPa overbalance comes from numerical models and has not been field-calibrated; on the other hand, the error magnitudes of multi-field coupling simplifications (neglecting seepage–thermal coupling underestimates collapse risk by more than 30%, and neglecting damage evolution underpredicts fracture-plane shear displacement by about 40%) are likewise given only by numerical simulation studies, without field calibration. Overall, the qualitative structure of this cross-scale mechanism chain is complete; what remains to be established is the quantitative transfer relations between the links under in-situ conditions. Cross-factor temperature–confinement experiments on rock-breaking energy partitioning, comparative validation of multiple failure criteria under granite geothermal-well conditions, and real-time monitoring of wellbore response while drilling are the three most direct research directions for addressing these limitations, and they dovetail with the prospects in Section 8.1.

8 Conclusions and prospects

This paper systematically reviews advances in the evolution of physical and mechanical properties of deep geothermal reservoir rocks, rock-breaking mechanisms and technologies for deep geothermal well drilling, and wellbore stability during drilling. The main conclusions are as follows:

(1) Deep geothermal well drilling typically encounters high-temperature and high-pressure environments. During heating, the pronounced contrast in thermal expansion coefficients among mineral components (that of quartz being roughly three times that of K-feldspar), together with their anisotropy, causes intense thermal stress concentrations at grain boundaries, triggering rapid initiation and propagation of micro-cracks. For granite, the critical threshold for micro-crack initiation and the onset of a sharp strength decline is about 300 °C; the α/β quartz transition at 573 °C, accompanied by an abrupt volume increase, further drives crack coalescence, and pronounced ductile features appear above about 600 °C. These thresholds are lithology-dependent and must be calibrated piecewise according to the dominant mineral assemblage of the reservoir. This cumulative thermal damage not only significantly reduces rock strength, elastic modulus, and P-wave velocity but also induces a brittle-ductile transition.

(2) In the low-temperature heating stage, matrix thermal expansion under confining pressure occupies pore channels, suppressing permeability. However, once the thermal fracturing threshold is exceeded, fracture network connectivity causes substantial permeability increases, with lithology-dependent threshold temperatures: about 573–600 °C for granite under low-confinement laboratory conditions, about 400 °C for sandstone, and about 340 °C for limestone. Meanwhile, rising temperature reduces rock thermal conductivity due to enhanced phonon scattering, while specific heat capacity typically increases. Cooling cycles from circulating drilling fluids during drilling

further intensify internal thermal stress damage: the higher the heat-transfer coefficient of the cooling medium, the more severe the damage. For example, liquid-nitrogen cooling can increase granite permeability by a factor of 5.24 while reducing compressive strength by 13.6%, significantly weakening the rock's resistance to fracture.

(3) Temperature-induced rock ductility enhancement hinders penetration of conventional PDC bits: the brittle–ductile transition range of granite under PDC cutting is 240–360 °C, markedly lower than the yield temperatures given by conventional compression tests, and ROP declines sharply once this range is exceeded. The energy utilization efficiency of percussive rock breaking is likewise low: simulations and experiments both indicate that only about 7.5%–12.5% of the input energy contributes to actual rock breaking, with most of the remainder dissipated by friction, and the suppression of lateral crack extension by high confining pressure makes the actual downhole efficiency even lower. Consequently, rock-breaking technologies are evolving from single mechanical cutting to axial-torsional coupled composite impact, non-planar cutter point-loading reinforcement, thermal stress assistance, and directed energy methods. Field applications show quantifiable gains: shaped-cutter designs achieved a 20%–50% improvement in drilling performance at the Tauhara geothermal field, and hybrid PDC bits reduced the mean tangential force by about 21%–24% in the ultra-deep high-temperature well Fushenre-1 while effectively suppressing stick-slip vibration.

(4) Geothermal wellbore stability is governed by THM multi-field coupling. Transient tensile thermal stresses induced by drilling fluid cooling represent the core mechanism for wellbore tensile fracturing and fracture-related lost circulation. Numerical studies provide indicative quantitative bounds. Under the conditions assumed in those studies, the wall–fluid temperature difference should be kept within about 250 °C together with a moderate positive overbalance of about 10 MPa to jointly suppress tensile fracturing and shear failure. Neglecting seepage–thermal-stress coupling underestimates wellbore collapse risk by more than 30%, and neglecting damage evolution underpredicts fracture-plane shear displacement by about 40%. None of these figures has been calibrated against field measurements; each reflects the granite properties, wellbore geometry, and stress state assumed in its source study. They are useful for ranking which couplings matter, but a site-specific model is needed before any of them informs a mud-weight or circulation design. Additionally, rheological changes in drilling fluid at high temperatures alter heat transfer efficiency at the wellbore wall, affecting convective heat exchange and accuracy of wellbore temperature field predictions.

8.1 Prospects

Although existing research provides theoretical support for deep geothermal drilling, challenges persist in ultra-deep and magmatic geothermal resource development. Key future directions include:

(1) Existing ROP prediction models adapt poorly to deep heterogeneous formations, and purely data-

driven models lack interpretability; in the downhole high-temperature environment, the limited service life of sensors, together with scarce and noisy real-time data, further constrains the training and online inversion of data-driven models. Future research may embed physical laws such as energy conservation and rock-damage evolution into algorithms in the form of loss functions, so as to achieve physically consistent inversion of formation parameters and operating-condition early warning under limited data; in parallel, high-temperature-resistant measurement-while-drilling and data-assimilation methods should be developed to provide a data basis for real-time decision-making.

(2) Current studies are mostly based on static experimental data and neglect the real-time correction of rock mechanical characteristics by transient fluctuations of the temperature and stress fields during drilling; in particular, systematic rock-mechanics experimental data for the brittle-ductile transition region are lacking, leaving the constitutive models and drillability predictions for this region without a reliable physical basis or training-sample support. Future work needs to supplement systematic experiments within this temperature-pressure region, establish constitutive models that account for strain-rate dependence, thermal-damage accumulation, and dynamic brittle-ductile transition, and intelligently invert the real-time response of bottomhole rock from surface measurement-while-drilling parameters, so as to provide a theoretical basis for the development of geothermal-well-adapted bits and parameter optimization.

(3) Given the intense frictional heat generated by the point contact of non-planar cutters, the ultra-high-temperature stability and impact toughness of PDC cutters need further improvement. Based on digital-twin technology, a comprehensive energy-efficiency evaluation system incorporating bit-rock interaction, multiphase fluid circulation in the wellbore, and heat-transfer processes can be constructed to achieve the coordinated optimization of bit life, drilling cost, and engineering efficiency. However, the solution of fully coupled THM equations remains computationally infeasible on the time scale required for real-time decision-making, so reduced-order models or hybrid physics-data methods need to be developed to support the genuine deployment of digital twins at the drilling site. The same lack of a quantified operating envelope applies to pneumatic hammers, whose temperature and water-influx limits, and the trade-off between loss-free operation and the narrower stability margin of underbalanced drilling, remain unquantified for deep geothermal conditions.

(4) Current studies have not yet established a cross-scale prediction model linking microscopic mineral grain-boundary damage to macroscopic wellbore stability, and the cross-scale parameter-transfer mechanism remains unclear, making it difficult to map microscopic thermal-damage information quantitatively onto wellbore-stability criteria. Future wellbore-stability simulations should focus on the interaction of chemical-potential gradients, anisotropic seepage, and thermal stress under high-temperature and high-in-situ-stress environments, and establish a cross-scale correlation model from microscopic mineral grain-boundary damage to macroscopic wellbore failure, so as to address

engineering challenges such as borehole shrinkage, block falling, and loss-induced instability encountered at real sites.

(5) This paper focuses on the mechanical processes in deep geothermal drilling and does not systematically address chemical-coupling mechanisms such as corrosion and chemical dissolution. At present, research on chemical coupling in deep geothermal drilling is relatively limited and mostly concentrated on reservoir-scale chemical stimulation and the high-temperature degradation of drilling fluids, with little systematic study of the mechanisms of chemical processes during drilling. The following research directions require further in-depth study and systematic review: (i) the long-term effect of mineral dissolution/precipitation on fracture permeability at high temperature; (ii) the influence of silica scaling and carbonate deposition on the wellbore and the near-wellbore fracture zone; (iii) the reaction between the drilling-fluid chemical system and high-temperature rock and its feedback on rock mechanical properties; (iv) the contribution of clay swelling to instability in clay-bearing interlayers; and (v) the wear mechanisms of bit cutters and sealing systems in high-temperature chemical environments. Furthermore, how the near-wellbore fractures and stress state shaped during the drilling stage are transferred to subsequent reservoir stimulation, and coupled with hydraulic-fracture propagation and inter-fracture stress interference, is also an important link connecting drilling mechanics with EGS stimulation, and warrants systematic study in the future.

Nomenclature		P	Rock failure probability
A_b	Bit cutting area	Q	Volumetric flow rate
C_p	Rock specific heat capacity	T_0	Initial rock temperature
D_b	Bit diameter	T_s	Critical rock-surface temperature
dT_i	Average torque per unit time	W	Jet impact coefficient
e_h	Hydraulic aperture	x	Rock-surface displacement
F_r	Critical rock resistance	z	Depth from the rock surface
JRC	Joint roughness coefficient	β	Forchheimer nonlinear fitting coefficient
M	Rock mass	ε_v	Volumetric strain
m_1	Bit mass	$\eta(T)$	Newtonian viscosity
p	Fractional order	μ_f	Fluid dynamic viscosity
T	Temperature	v	Poisson's ratio
T_b	Impact torque	ρ	Fluid density
V_{ROP}	Drilling rate of penetration	σ	Rock uniaxial compressive strength
w	Fracture width	σ_t	Thermal stress on the rock surface
x_b	Bit penetration depth	ϕ	Porosity

α	Linear thermal expansion coefficient
β_T	Volumetric thermal expansion coefficient
ΔT	Temperature change
η	Rock thermal-expansion-coefficient ratio
λ	Thermal conductivity
μ	Viscosity coefficient
ξ	Thermal-diffusion group
ρ_r	Rock density
σ_0	Weibull characteristic strength
σ_r	Rock failure stress
ω	Contact area ratio
C_L	Aspect ratio of spalled chips
D	Thermal diffusivity
dF_i	Average weight on bit per unit time
E	Elastic modulus
F_c	Instantaneous contact force
F_v	Axial impact force
k	Permeability
m	Weibull homogeneity parameter

Abbreviations

HDR	Hot dry rock
THM	Thermo-hydro-mechanical
PDC	Polycrystalline diamond compact
MSE	Mechanical specific energy
RPM	Rotations per minute
DEM	Discrete element method
BP	Back propagation
RSM	Response surface methodology
EGS	Enhanced geothermal systems
THMC	Thermo-hydro-mechanical-chemical
ROP	Rate of penetration
WOB	Weight on bit
UCS	Uniaxial compressive strength
FEM	Finite element method
MLP	Multi-layer perceptron
PINN	Physics-informed neural network

Acknowledgements

This work was supported by the Jilin Provincial Natural Science Foundation (No. 20260102076JC).

Author contributions

Shuaiyi Lu: Conceptualization, Methodology, Investigation, Writing - original draft. Yinlong Ma: Supervision, Funding acquisition, Project administration, Writing - review & editing. Ziwang Yu: Resources. Lianghan Cong: Data curation, Validation, Formal analysis. Lingtao Zeng: Visualization.

Conflict of interest

The authors declare that they have no known competing financial interests or personal relationships that could have appeared to influence the work reported in this paper.

References

[1] Van Oldenborgh GJ, Wehner MF, Vautard R, Otto FE, Seneviratne SI, Stott PA, et al. Attributing and projecting heatwaves is hard: we can do better. Earth's Future. 2022;10:e2021EF002271.

[2] REN21. RENEWABLES 2025 GLOBAL STATUS REPORT. 2025.

[3] Li R, Chen Q, Wang Q. Emerging topic identification in carbon capture utilization and storage (CCUS) for advancing climate action (SDG 13). Renewable Sustainable Energy Rev. 2025;222:115969.

[4] Shan K, Cong L, Yu Z, Ye X. Artificial intelligence empowering geothermal energy development: A full-lifecycle review from exploration to operation. Renewable Sustainable Energy Rev. 2026;226:116468.

[5] Hepburn C, Adlen E, Beddington J, Carter EA, Fuss S, Mac Dowell N, et al. The technological and economic prospects for CO_2 utilization and removal. Nature. 2019;575:87-97.

[6] Mukherji A. Climate change 2023 synthesis report. 2023.

[7] Kumari WGP, Ranjith PG. Sustainable development of enhanced geothermal systems based on geotechnical research – A review. Earth Sci Rev. 2019;199:102955.

[8] Axelsson G, Egilson T, Gylfadóttir SS. Modelling of temperature conditions near the bottom of well IDDP-1 in Krafla, Northeast Iceland. Geothermics. 2014;49:49-57.

[9] Liu J, Shao C, Yang B, Ramadhani Ngata M, Mwangomba M, Josephat S, et al. Advances in enhanced geothermal systems: Integrating laboratory, numerical and field insights. Appl Therm Eng. 2024;249:123350.

[10] Jolie E, Scott S, Faulds J, Chambefort I, Axelsson G, Gutiérrez-Negrín LC, et al. Geological controls on geothermal resources for power generation. Nature Reviews Earth & Environment. 2021;2:324-39.

[11] Montes AC, Ashok P, van Oort E. Stuck Pipe Prediction in Utah FORGE Geothermal Wells. SPE Annual Technical Conference and Exhibition; 2023.

[12] Zulkarnain MB. Stuck Pipe Prediction in Geothermal Well Drilling at Darajat Using Statistical and Machine Learning Application. Proceedings of the 3rd Asia Pacific Conference on Research in Industrial and Systems Engineering. Depok, Indonesia: Association for Computing Machinery; 2020. p. 100–4.

[13] Mati D. Stuck Pipe Prediction And Avoidance: Invocation Of Basic Principle Of Standard Methods, Pre And Post Sticking. Proceedings World Geothermal Congress 2021. Iceland2021.

[14] Qian H, Wang J, Sun Y, Wang Z, Yuan B. Analysis of leakage formation and selection of leaking stoppage methods in geothermal well drilling in Tianjin area. Geol Surv Res. 2016;39:226-30.

[15] Li Z, Xu Y, Wang P, Zong Z. Treatment of Drill Pipe Sticking in SR − 28 Geothermal Well Collapsing Accident. Drilling Engineering. 2011;38.

[16] Browne PRL, Lawless JV. Characteristics of hydrothermal eruptions, with examples from New Zealand and elsewhere. Earth Sci Rev. 2001;52:299-331.

[17] Bhuvankar P, Cihan A, Birkholzer J. A framework to simulate the blowout of CO_2 through

wells in geologic carbon storage. Int J Greenhouse Gas Control. 2023;127:103921.

[18] Bolton RS, Hunt TM, King TR, Thompson GEK. Dramatic incidents during drilling at Wairakei Geothermal Field, New Zealand. Geothermics. 2009;38:40-7.

[19] Anderson I. Blowout blights future of Hawaii's geothermal power. New Scientist Publications Expediting Inc, 200 Meacham Ave, Elmont, NY 11003; 1991. p. 17-17.

[20] Lautze NC, Kim A, Dores D, Brennis T, Ferguson CM, Thomas DM. Outreach Efforts of the Hawai ‘i Groundwater and Geothermal Resources Center. Proceedings World Geothermal Congress2020. p. 1.

[21] Kim K-H, Ree J-H, Kim Y, Kim S, Kang SY, Seo W. Assessing whether the 2017 Mw 5.4 Pohang earthquake in South Korea was an induced event. Science. 2018;360:1007-9.

[22] Grigoli F, Cesca S, Rinaldi AP, Manconi A, López-Comino JA, Clinton JF, et al. The November 2017 Mw 5.5 Pohang earthquake: A possible case of induced seismicity in South Korea. Science. 2018;360:1003-6.

[23] Gombert P, Lahaie F, Cherkaoui A, Contrucci I, de Santis F. Main risks related to deep geothermal energy in the world. World Geothermal Congress (WGC); 2021.

[24] Spada M, Sutra E, Burgherr P. Comparative accident risk assessment with focus on deep geothermal energy systems in the Organization for Economic Co-operation and Development (OECD) countries. Geothermics. 2021;95:102142.

[25] Yuan B, Wood DA. A holistic review of geosystem damage during unconventional oil, gas and geothermal energy recovery. Fuel. 2018;227:99-110.

[26] Jiang O, Cao L, Zhu W, Zheng X. Review of Reservoir Damage Mechanisms Induced by Working Fluids and the Design Principles of Reservoir Protection Fluids: From Oil–Gas Reservoirs to Geothermal Reservoirs. Energies. 2024;17:4895.

[27] Lu W, Wang J, Shang L, Zhang H. Research on geothermal reservoir types classification and formation damage mechanism. Drilling Engineering. 2025;52:98-104.

[28] Pye S. Drilling, Completing, and Maintaining Geothermal Wells in Baca, New Mexico. DOEEEGTP (USDOE Office of Energy Efficiency and Renewable Energy Geothermal; 1980.

[29] Saleh F, Teodoriu C, Salehi S, Ezeakacha C. Geothermal drilling: A review of drilling challenges with mud design and lost circulation problem. Proceedings of 45th Annual Stanford Geothermal Workshop, Stanford University, Stanford, CA; 2020.

[30] Song X, Li G, Huang Z, Shi Y, Wang G, Song G, et al. Review of high-temperature geothermal drilling and exploitation technologies. Gondwana Res. 2023;122:315-30.

[31] Isania F, Elahifar B. Advances in geothermal drilling: A comparative study with oil and gas techniques. Geoenergy Sci Eng. 2025;246:213638.

[32] Zeng D, Lin Y, Lu Y, Zhu D, Li L. Numerical simulation of hole creep shrinkage for composite rock salt layers. Journal of Geomechanics. 2012;18:158-64.

[33] Li S, Fang C, Chen C, Xiang D, Li F, Huang H. Analysis and Research on Borehole Shrinkage Mechanisms and Their Control in Directional Wells in Deep Composite Salt Formations. Lithosphere. 2022;2022.

[34] Albattat R, AlSinan M, Kwak H, Hoteit H. Modeling lost-circulation in natural fractures using semi-analytical solutions and type-curves. Journal of Petroleum Science and Engineering. 2022;216:110770.

[35] Liu W, Chen Z, Li A, Zhu X. The mechanism of wellbore instability in hot dry rock

formations under 3D in-situ stresses. Geoenergy Sci Eng. 2026;256:214147.

[36] Akindipe D, Witter E. 2025 geothermal drilling cost curves update. Proceedings of the 50th Workshop on Geothermal Reservoir Engineering. Stanford (CA): Stanford University; 2025.

[37] Lukawski MZ, Anderson BJ, Augustine C, Capuano LE, Beckers KF, Livesay B, et al. Cost analysis of oil, gas, and geothermal well drilling. Journal of Petroleum Science and Engineering. 2014;118:1-14.

[38] Stober I, Bucher K. Geothermal Energy: From Theoretical Models to Exploration and Development; 2021.

[39] Augustine C, Tester JW, Anderson B, Petty S, Livesay B. A comparison of geothermal with oil and gas well drilling costs. Proceedings of the 31st Workshop on Geothermal Reservoir Engineering: Curran Associates Inc New York, New York; 2006. p. 5-19.

[40] Nkinyam CM, Ujah CO, Asadu CO, Kallon DVV. Exploring geothermal energy as a sustainable source of energy: A systemic review. Unconv Resour. 2025;6:100149.

[41] Ma Y. Deep geothermal resources in China: Potential, distribution, exploitation, and utilization. Energy Geosci. 2023;4:100209.

[42] Li G, Xie Z, Huang Z, Wu X, Zou W, Sun Z, et al. Status and challenges of deep geothermal exploitation and energy storage technology: a comprehensive review. GeoEnergy Communications. 2025;1:5.

[43] Kumari WGP, Ranjith PG, Perera MSA, Li X, Li LH, Chen BK, et al. Hydraulic fracturing under high temperature and pressure conditions with micro CT applications: Geothermal energy from hot dry rocks. Fuel. 2018;230:138-54.

[44] Reinsch T, Dobson P, Asanuma H, Huenges E, Poletto F, Sanjuan B. Utilizing supercritical geothermal systems: a review of past ventures and ongoing research activities. Geotherm Energy. 2017;5:16.

[45] Elders WA, Friðleifsson GÓ, Pálsson B. Iceland Deep Drilling Project: The first well, IDDP-1, drilled into magma. Geothermics. 2014;49:1.

[46] Kelkar S, WoldeGabriel G, Rehfeldt K. Lessons learned from the pioneering hot dry rock project at Fenton Hill, USA. Geothermics. 2016;63:5-14.

[47] Aichholzer C, Duringer P, Orciani S, Genter A. New stratigraphic interpretation of the Soultz-sous-Forêts geothermal wells based on Rittershoffen (URG, France); 2016.

[48] Heap MJ, Kushnir ARL, Gilg H, Wadsworth F, Reuschlé T, Baud P. Microstructural and petrophysical properties of the Permo-Triassic sandstones (Buntsandstein) from the Soultz-sous-Forêts geothermal site (France). Geotherm Energy. 2017;5.

[49] Friðleifsson GÓ, Elders WA, Zierenberg RA, Fowler APG, Weisenberger TB, Mesfin KG, et al. The Iceland Deep Drilling Project at Reykjanes: Drilling into the root zone of a black smoker analog. J Volcanol Geotherm Res. 2020;391.

[50] Siratovich PA, Heap MJ, Villenueve MC, Cole JW, Reuschlé T. Physical property relationships of the Rotokawa Andesite, a significant geothermal reservoir rock in the Taupo Volcanic Zone, New Zealand. Geotherm Energy. 2014;2:10.

[51] Guo Y, Huang L, Li X. Experimental investigation of the tensile behavior and acoustic emission characteristics of anisotropic shale under geothermal environment. Energy. 2023;263:125767.

[52] Elidemir S, Güleç N. Geochemical characterization of geothermal systems in western

Anatolia (Turkey): implications for CO_2 trapping mechanisms in prospective CO_2-EGS sites. Greenhouse Gases Sci Technol. 2017;8:63-76.

[53] Batini F, Brogi A, Lazzarotto A, Liotta D, Pandeli E. Geological features of Larderello-Travale and Mt. Amiata geothermal areas (southern Tuscany, Italy). Episodes. 2003;26:239-44.

[54] Zaigham NA, Nayyar ZA. Renewable hot dry rock geothermal energy source and its potential in Pakistan. Renewable Sustainable Energy Rev. 2010;14:1124-9.

[55] Liu L, Yang L, Shen L, Xiao H. Research progress and prospect of geothermal resources. E3S Web of Conferences. 2023;393:01001.

[56] Yang S-Q, Ranjith PG, Jing H-W, Tian W-L, Ju Y. An experimental investigation on thermal damage and failure mechanical behavior of granite after exposure to different high temperature treatments. Geothermics. 2017;65:180-97.

[57] Yin W, Zhao Y, Feng Z. Experimental research on the permeability of fractured-subsequently-filled granite under high temperature-high pressure and the application to HDR geothermal mining. Renewable Energy. 2020;153:499-508.

[58] Baoping X, Jinchang Z, Yangsheng Z. Key technologies of hot dry rock drilling during construction. Chinese Journal of Rock Mechanics and Engineering. 2011;30:2234-43.

[59] Umam MF, Purba DP, Adityatama DW, Campen B. Drilling manpower and equipment transfer from petroleum to geothermal industry: a preliminary study on skill assessment. The 6th Indonesia International Geothermal Convention & Exhibition (IIGCE)2018. p. 5-8.

[60] Kumari W, Ranjith P, Perera M, Shao S, Chen B, Lashin A, et al. Mechanical behaviour of Australian Strathbogie granite under in-situ stress and temperature conditions: An application to geothermal energy extraction. Geothermics. 2017;65:44-59.

[61] Fei Y. Thermal Expansion. Mineral Physics & Crystallography1995. p. 29-44.

[62] Zhang P, Wang C, Gao Z, Wang Z, Zhou C, Wang F. Combined effects of high temperature and lithology on the tensile mechanical damage and fracture surface morphology of reservoir rocks. Bull Eng Geol Environ. 2024;83:226.

[63] Bauer SJ, Handin J. Thermal expansion and cracking of three confined water-saturated igneous rocks to 800°C. Rock Mech Rock Eng. 1983;16:181-98.

[64] Aryanpour M, Falamaki A, Vakili AH. Effects of elevated temperature on mineralogical/microstructural changes and mechanical responses of clay soil. Physics and Chemistry of the Earth, Parts A/B/C. 2023;132:103493.

[65] Wang F, Konietzky H. Thermo-Mechanical Properties of Granite at Elevated Temperatures and Numerical Simulation of Thermal Cracking. Rock Mech Rock Eng. 2019;52:3737-55.

[66] Glover PWJ, Baud P, Darot M, Meredith PG, Boon SA, LeRavalec M, et al. α/β phase transition in quartz monitored using acoustic emissions. Geophys J Int. 1995;120:775-82.

[67] Guo P, Zhang P, Bu M, Wang J, Zheng X, He M. Microcracking behavior and damage mechanism of granite subjected to high temperature based on CT-GBM numerical simulation. Comput Geotech. 2023;159:105385.

[68] Hu J, Xie H, Gao M, Li C, Sun Q. Damage mechanism and heat transfer characteristics of limestone after thermal shock cycle treatments based on geothermal development. Int J Rock Mech Min Sci. 2022;160:105269.

[69] Fulignati P. Clay Minerals in Hydrothermal Systems. Minerals2020. p. 919.

[70] Pytte AM, Reynolds RC. The Thermal Transformation of Smectite to Illite. In: Naeser ND,

McCulloh TH, editors. Thermal History of Sedimentary Basins. New York, NY: Springer New York; 1989. p. 133-40.
[71] Wang Y, Peng J, Wang L, Xu C, Dai B. Micro-macro evolution of mechanical behaviors of thermally damaged rock: A state-of-the-art review. J Rock Mech Geotech Eng. 2024;16:2833-53.
[72] Zhu D, Li Y, Huang W, Hu X. Experimental study on physico-mechanical responses and energy characteristics of granite under high temperature and hydro-mechanical coupling. Case Stud Therm Eng. 2024;63:105245.
[73] Gautam P, Verma A, Jha M, Sharma P, Singh T. Effect of high temperature on physical and mechanical properties of Jalore granite. J Appl Geophys. 2018;159:460-74.
[74] Deng S, Zhang Y, Yan X, Yang S, Li C, Peng H. Experimental study on P-wave response characteristics of hot dry rock under high temperature and high confining pressure. Geomech Energy Environ. 2023;36:100514.
[75] Zhao H, Yin G, Li X. Experimental study of characteristics of tensile burned gritstone. Rock Soil Mech. 2010;31:1143-275.
[76] Nasseri MHB, Schubnel A, Young RP. Coupled evolutions of fracture toughness and elastic wave velocities at high crack density in thermally treated Westerly granite. Int J Rock Mech Min Sci. 2007;44:601-16.
[77] Liu S, Xu J. Mechanical properties of Qinling biotite granite after high temperature treatment. Int J Rock Mech Min Sci. 2014;71:188-93.
[78] Gao W, Zhao J, Wang H. Rock physics experiment and rock physical modeling of hot dry rock under high temperature. J Min Sci Technol. 2023;8:758-67.
[79] Yan C, Deng J, Yu B, Li W, Chen Z, Hu L, et al. Borehole Stability in High-Temperature Formations. Rock Mech Rock Eng. 2014;47:2199-209.
[80] Wan Z, Zhao Y, Zhang Y, Wang C. Research status quo and prospection of mechanical characteristics of rock under high temperature and high pressure. Procedia Earth Planet Sci. 2009;1:565-70.
[81] Xu Z, Zhong X, Zhang S, Wang Y, Liu K, Liu X, et al. Experimental study on mechanical damage and creep characteristics of Gonghe granite under real-time high temperature. Geothermics. 2024;123:103100.
[82] Wang Z, Chen F, Dong Z, Li H, Shi X, Xu Z, et al. Study on the influence of temperature on the damage evolution of hot dry rock in the development of geothermal resources. Geoenergy Sci Eng. 2024;241:213171.
[83] Ge Z, Zhang H, Zhou Z, Cao S, Zhang D, Liu X, et al. Experimental study on the characteristics and mechanism of high-pressure water jet fracturing in high-temperature hard rocks. Energy. 2023;270:126848.
[84] Wong LNY, Liu Z. Thermal shock in rocks: A review of mechanisms, impacts, and applications in underground engineering. J Rock Mech Geotech Eng. 2025;17:8172-97.
[85] Xi Y, Wang H, Li J, Dong W, Li H, Guo B. Experimental comparison of mechanical properties and fractal characteristics of geothermal reservoir rocks after different cooling treatments. Energy Rep. 2022;8:5158-76.
[86] Kim K, Kemeny J, Nickerson M. Effect of Rapid Thermal Cooling on Mechanical Rock Properties. Rock Mech Rock Eng. 2014;47:2005-19.

[87] Li Q, Yin T, Li X, Zhang S. Effects of rapid cooling treatment on heated sandstone: a comparison between water and liquid nitrogen cooling. Bull Eng Geol Environ. 2020;79:313-27.
[88] Brotóns V, Tomás R, Ivorra S, Alarcón JC. Temperature influence on the physical and mechanical properties of a porous rock: San Julian's calcarenite. Eng Geol. 2013;167:117-27.
[89] Garrido ME, Petnga FB, Martínez-Ibáñez V, Serón JB, Hidalgo-Signes C, Tomás R. Predicting the uniaxial compressive strength of a limestone exposed to high temperatures by point load and Leeb rebound hardness testing. Rock Mech Rock Eng. 2022;55:1-17.
[90] Fan L, Li H, Xi Y. Evaluation of the effects of three different cooling methods on the dynamic mechanical properties of thermal-treated sandstone. Bull Eng Geol Environ. 2022;81:154.
[91] Zhu H, Jiao Z, Zhao P, Tang X, Chen S, Tao L. Physico-mechanical properties of granite after thermal treatments using different cooling media. J Rock Mech Geotech Eng. 2025;17:3619-31.
[92] Feng G, Wang X, Kang Y, Zhang Z. Effect of thermal cycling-dependent cracks on physical and mechanical properties of granite for enhanced geothermal system. Int J Rock Mech Min Sci. 2020;134:104476.
[93] Liu B, Xie H, Hu J, Liu J, Li B, Li C. Failure mechanism of hot dry rock under the coupling effect of thermal cycling and direct shear loading path. Int J Rock Mech Min Sci. 2024;176:105695.
[94] Zhu Z, Yang S, Wang R, Xie J, Tian N, Tian H, et al. Experimental investigation on the physical-thermal properties of Nanan granite after air and water cooling for deep geothermal heat extraction. Renewable Energy. 2024;223:119963.
[95] Xu XL, Gao F, Shen XM, Jin CH. Research on mechanical characteristics and micropore structure of granite under high-temperature. Yantu Lixue/Rock and Soil Mechanics. 2010;31:1752-8.
[96] Sun Y, Xie L, He B, Gao C, Wang J. Effects of effective stress and temperature on permeability of sandstone from CO_2-plume geothermal reservoir. J Rock Mech Geotech Eng. 2016;8:819-27.
[97] Peng H, Zhao Z, Chen W, Chen Y, Fang J, Li B. Thermal effect on permeability in a single granite fracture: Experiment and theoretical model. Int J Rock Mech Min Sci. 2020;131:104358.
[98] Yasuhara H, Kinoshita N, Ohfuji H, Takahashi M, Ito K, Kishida K. Long-term observation of permeability in sedimentary rocks under high-temperature and stress conditions and its interpretation mediated by microstructural investigations. Water Resour Res. 2015;51:5425-49.
[99] Tian W-L, Yang S-Q, Wang J-G, Zeng W. Numerical simulation of permeability evolution in granite after thermal treatment. Comput Geotech. 2020;126:103705.
[100] Yasuhara H, Kinoshita N, Ohfuji H, Lee DS, Nakashima S, Kishida K. Temporal alteration of fracture permeability in granite under hydrothermal conditions and its interpretation by coupled chemo-mechanical model. Appl Geochem. 2011;26:2074-88.
[101] Jiang C, Xu L, Chen Y, Liu W, Wang B, Liu P, et al. Thermal behavior of minerals in shale and its influence on evolution of gas-flow channels under thermal shock. Gas Sci Eng. 2024;121:205183.
[102] He B, Xie L, Liu X, Liu J, Elsworth D. Mechanistic controls on permeability evolution

in thermally-upgraded low-maturity oil shales: Application of machine learning outputs. Unconv Resour. 2025;6:100133.

[103] Rehman M, Hafeez MB, Krawczuk M. A Comprehensive Review: Applications of the Kozeny–Carman Model in Engineering with Permeability Dynamics. Arch Comput Methods Eng. 2024;31:3843-55.

[104] Ran Q, Li S. Study on dynamic models of reservoir parameters in the coupled simulation of multiphase flow and reservoir deformation. Pet Explor Dev. 1997;24:61-5.

[105] Tapponnier P, Brace WF. Development of stress-induced microcracks in Westerly Granite. International Journal of Rock Mechanics and Mining Sciences & Geomechanics Abstracts. 1976;13:103-12.

[106] Gautam PK, Verma AK, Singh TN, Hu W, Singh KH. Experimental investigations on the thermal properties of Jalore granitic rocks for nuclear waste repository. Thermochim Acta. 2019;681:178381.

[107] Xu Y, Yao W, Wang S, Xia K. Investigation of the Heat-Treatment Effect on Rock Fragmentation Characteristics Using the Dynamic Ball Compression Test. Rock Mech Rock Eng. 2020;53:2095-108.

[108] Chen S, Yang C, Wang G. Evolution of thermal damage and permeability of Beishan granite. Appl Therm Eng. 2017;110:1533-42.

[109] Deng S, Xiong F, Liu Y, Jiang Q. Temperature-dependent permeability model of granite after thermal treatment based on energy dissipation theory and fractal theory. Rock Mech Rock Eng. 2023;56:6321-35.

[110] Lima MG, Vogler D, Querci L, Madonna C, Hattendorf B, Saar MO, et al. Thermally driven fracture aperture variation in naturally fractured granites. Geotherm Energy. 2019;7.

[111] Vidana Pathiranagei S, Gratchev I, Sokolowski KA. Investigation of the microstructural characteristics of heated sandstone by micro-computed tomography technique. Environ Earth Sci. 2022;81.

[112] Zhang Y, Sun Q, Cao L, Geng J. Pore, mechanics and acoustic emission characteristics of limestone under the influence of temperature. Appl Therm Eng. 2017;123:1237-44.

[113] Kong L, Yin Z, Chen Y, Dong Z, Xu J. Pore Structure Evolution and Failure Mechanism of Limestone in the Taiyuan Formation of the Ordos Basin under High Temperature. ACS Omega. 2024;9:10177-89.

[114] Liang B, Gao HM, Lan YW. THEORETICAL ANALYSIS AND EXPERIMENTAL STUDY ON RELATION BETWEEN ROCK PERMEABILITY AND TEMPERATURE. Chinese Journal of Rock Mechanics & Engineering. 2005;24:2009-12.

[115] Zhang J, Hu Z, Liu D, Qiu J, An R. Thermal-induced damage mechanisms and permeability evolution in gneiss for deep mining applications. Front Earth Sci. 2025;13:1603348.

[116] Li M, Zhang B, Wu Z, Luo S, Lu J, Zhang D, et al. A novel permeability calculation model to simultaneously quantify the impacts of pore and fracture with full feature size. Int J Min Sci Technol. 2025;35:609-18.

[117] Liu J, Bai X, Elsworth D. Evolution of pore systems in low-maturity oil shales during thermal upgrading—Quantified by dynamic SEM and machine learning. Pet Sci. 2024;21:1739-50.

[118] Ma Y, Li Y, Gan Q, Zhi S. Permeability evolution due to combined thermal stress and in-situ stress during fractured geothermal reservoir production. Geothermics. 2023;115:102831.
[119] Zimmerman RW, Al-Yaarubi A, Pain CC, Grattoni CA. Non-linear regimes of fluid flow in rock fractures. Int J Rock Mech Min Sci. 2004;41:163-9.
[120] Yao C, Shao Y, Yang J, Huang F, He C, Jiang Q, et al. Effects of non-darcy flow on heat-flow coupling process in complex fractured rock masses. J Nat Gas Sci Eng. 2020;83:103536.
[121] Forchheimer P. Wasserbewegung. Ver Dtsch Ing. 1901;45:1782-8.
[122] Liu Z, Li S, Liu R, Zheng C. Nonlinear Flow Properties of Newtonian Fluids through Rough Crossed Fractures. CMES - Computer Modeling in Engineering and Sciences. 2023;136:1427-40.
[123] Tan J, Rong G, Li C, Zhou J-Q, Tang H. Thermal Effect Promotes Non-Darcian Flow in Heated Rock Fractures. Rock Mech Rock Eng. 2023;56:7599-617.
[124] Liu Y, Zhang Y, Cheng Y, Zhou L. Experimental investigation on non-linear flow and convective heat transfer of damaged multi-fractured rock. Appl Therm Eng. 2025;264:125466.
[125] Yin Q, Liu R, Jing H, Su H, Yu L, He L. Experimental Study of Nonlinear Flow Behaviors Through Fractured Rock Samples After High-Temperature Exposure. Rock Mech Rock Eng. 2019;52:2963-83.
[126] Luo J, Zhu Y, Guo Q, Tan L, Zhuang Y, Liu M, et al. Experimental investigation of the hydraulic and heat-transfer properties of artificially fractured granite. Sci Rep. 2017;7:39882.
[127] Kumari WG, Ranjith PG. Experimental and Numerical Investigation of the Flow Behaviour of Fractured Granite under Extreme Temperature and Pressure Conditions. Sustainability2022. p. 8587.
[128] Li J, Ye L. Investigations of Water Flow Behaviors Induced by Local Temperature Variations through a Single Rough Fracture for the Enhanced Geothermal Systems. J Therm Sci. 2024;33:1055-64.
[129] Rutqvist J, Freifeld B, Min KB, Elsworth D, Tsang Y. Analysis of thermally induced changes in fractured rock permeability during 8 years of heating and cooling at the Yucca Mountain Drift Scale Test. Int J Rock Mech Min Sci. 2008;45:1373-89.
[130] Ghassemi A, Nygren A, Cheng A. Effects of heat extraction on fracture aperture: A poro–thermoelastic analysis. Geothermics. 2008;37:525-39.
[131] Zou L, Jing L, Cvetkovic V. Roughness decomposition and nonlinear fluid flow in a single rock fracture. Int J Rock Mech Min Sci. 2015;75:102-18.
[132] Rong G, Yang J, Cheng L, Zhou C. Laboratory investigation of nonlinear flow characteristics in rough fractures during shear process. J Hydrol. 2016;541:1385-94.
[133] Cunningham D, Auradou H, Shojaei-Zadeh S, Drazer G. The Effect of Fracture Roughness on the Onset of Nonlinear Flow. Water Resour Res. 2020;56:e2020WR028049.
[134] Javadi M, Sharifzadeh M, Shahriar K, Mitani Y. Critical Reynolds number for nonlinear flow through rough-walled fractures: The role of shear processes. Water Resour Res. 2014;50:1789-804.
[135] Wang B, Yang W, Zhang X, Yang Y, Zhang L, Yao J. Flow behavior of a rough single rock fracture under high-temperature, high-stress, and high-seepage pressure coupling conditions. Int J Min Sci Technol. 2025;35:1789-807.
[136] Hu J, Xie H, Sun Q, Li C, Liu G. Changes in the thermodynamic properties of alkaline

granite after cyclic quenching following high temperature action. Int J Min Sci Technol. 2021;31:843-52.
[137] Gao X, Zhang Y, Cheng Y, Yu Z, Huang Y. Impact of fractures with multi-scale aperture variability on production observations of geothermal reservoir units. J Hydrol. 2022;615:128693.
[138] Isaak DG. High-temperature elasticity of iron-bearing olivines. J Geophys Res: Solid Earth. 1992;97:1871-85.
[139] Seipold U. Temperature dependence of thermal transport properties of crystalline rocks — a general law. Tectonophysics. 1998;291:161-71.
[140] Gibert B, Seipold U, Tommasi A, Mainprice D. Thermal diffusivity of upper mantle rocks: Influence of temperature, pressure, and the deformation fabric. J Geophys Res: Solid Earth. 2003;108.
[141] Sun Q, Zhang W, Zhu Y, Huang Z. Effect of High Temperatures on the Thermal Properties of Granite. Rock Mech Rock Eng. 2019;52:2691-9.
[142] Chen C, Zhu C, Zhang B, Tang B, Li K, Li W, et al. Effect of Temperature on the Thermal Conductivity of Rocks and Its Implication for In Situ Correction. Geofluids. 2021;2021:6630236.
[143] Förster A, Fuchs S, Förster HJ, Norden B. Ambiguity of crustal geotherms: A thermal-conductivity perspective. Geothermics. 2021;89:101937.
[144] Abdulagatova Z, Abdulagatov IM, Emirov VN. Effect of temperature and pressure on the thermal conductivity of sandstone. Int J Rock Mech Min Sci. 2009;46:1055-71.
[145] Pashuk EG, Ramazanova AE, Abdulagatov IM. High-pressure thermal conductivity, speed of ultrasonic measurements and derived elastic modulus of sandstones with different porosity. Geothermics. 2025;125:103195.
[146] Emirov SN, Aliverdiev AA, Zarichnyak YP, Emirov RM. Studies of the Effective Thermal Conductivity of Sandstone Under High Pressure and Temperature. Rock Mech Rock Eng. 2021;54:3165-74.
[147] Seipold U, Huenges E. Thermal properties of gneisses and amphibolites — high pressure and high temperature investigations of KTB-rock samples. Tectonophysics. 1998;291:173-8.
[148] Ji M, Wei S, Wei Z, Feng L, Liao Y, Yuan R, et al. Characterization of rock thermophysical properties and factors affecting thermal conductivity− A case study of Datong Basin, China. Journal of Groundwater Science and Engineering. 2024;12:4.
[149] Liu M, Yang Y, Liu F, Wang J, Song H, Zhang J, et al. Thermal disturbance anisotropy and structural stability in deep multimineral granular systems: A discrete element method study. Geothermics. 2025;132.
[150] Albert K, Schulze M, Franz C, Koenigsdorff R, Zosseder K. Thermal conductivity estimation model considering the effect of water saturation explaining the heterogeneity of rock thermal conductivity. Geothermics. 2017;66:1-12.
[151] Yu Z, Ye X, Zhang Y, Gao P, Huang Y. Experimental research on the thermal conductivity of unsaturated rocks in geothermal engineering. Energy. 2023;282.
[152] Pribnow D, Williams CF, Sass JH, Keating R. Thermal conductivity of water-saturated rocks from the KTB Pilot Hole at temperatures of 25 to 300°C. Geophys Res Lett. 1996;23:391-4.

[153] Waples D, Waples J. A Review and Evaluation of Specific Heat Capacities of Rocks, Minerals, and Subsurface Fluids. Part 1: Minerals and Nonporous Rocks. Nat Resour Res. 2004;13:97-122.
[154] Sun Q, Lü C, Cao L, Li W, Geng J, Zhang W. Thermal properties of sandstone after treatment at high temperature. Int J Rock Mech Min Sci. 2016;85:60-6.
[155] Wen H, Lu J-h, Xiao Y, Deng J. Temperature dependence of thermal conductivity, diffusion and specific heat capacity for coal and rocks from coalfield. Thermochim Acta. 2015;619:41-7.
[156] Becattini V, Motmans T, Zappone A, Madonna C, Haselbacher A, Steinfeld A. Experimental investigation of the thermal and mechanical stability of rocks for high-temperature thermal-energy storage. Appl Energy. 2017;203:373-89.
[157] Drury MJ. Thermal diffusivity of some crystalline rocks. Geothermics. 1987;16:105-15.
[158] Tiskatine R, Bougdour N, Idoum A, Bazgaou A, Oaddi R, Ihlal A, et al. Experimental investigation on rock thermal properties under the influence of temperature. Thermochim Acta. 2023;720:179424.
[159] Vosteen H-D, Schellschmidt R. Influence of temperature on thermal conductivity, thermal capacity and thermal diffusivity for different types of rock. Physics and Chemistry of the Earth, Parts A/B/C. 2003;28:499-509.
[160] Miao SQ, Li HP, Chen G. Temperature dependence of thermal diffusivity, specific heat capacity, and thermal conductivity for several types of rocks. J Therm Anal Calorim. 2014;115:1057-63.
[161] Merriman J, Hofmeister A, Roy D, Whittington A. Temperature-dependent thermal transport properties of carbonate minerals and rocks. Geosphere. 2018;14.
[162] Finger JT, Blankenship DA. Handbook of best practices for geothermal drilling. Sandia National Lab.(SNL-NM), Albuquerque, NM (United States); 2012.
[163] Friðleifsson G, Elders W, Zierenberg R, Weisenberger T, Harðarson B, Stefánsson A, et al. The drilling of the Iceland Deep Drilling Project geothermal well at Reykjanes has been successfully completed. Completion Report, Iceland, February. 2017;1.
[164] Winkler D. Utah FORGE: Well 16A(78)-32: Summary of Drilling Activities. In: Swearingen L, editor.: Energy and Geoscience Institute at the University of Utah; 2021.
[165] Raymond D, Knudsen S, Blankenship D, Bjornstad S, Barbour J, Schen A. PDC bits outperform conventional bit in geothermal drilling project. Transactions - Geothermal Resources Council. 2012;36:307-15.
[166] Sebastian H. Custom PDC Bits Significantly Increase Drilling Performance in Tauhara Geothermal Drilling Project. Proceedings of the World Geothermal Congress; 2020.
[167] Miyazaki K, Ohno T, Karasawa H, Imaizumi H. Performance of polycrystalline diamond compact bit based on laboratory tests assuming geothermal well drilling. Geothermics. 2019;80:185-94.
[168] Ford R, Fanti D, Freeman A, Prakash S, Panayirci M, Gjertsen O, et al. Drill Bits For Hard-Rock And Geothermal Wells: Roller-Cone Bit Performance Quantified and Fixed-Cutter Bit Lessons Learned. Geothermal Resources Council Transactions; 2023.
[169] Pearce R, Pink T. Drilling for superhot geothermal energy: A technology gap analysis. Cascade Institute: Victoria, BC, Canada. 2024.

[170] Yang Y, Huang K, Song D, Chen X, Chen H, Chen L. The study on tooth failure and fixation strength of cone bits under high temperature. Eng Fail Anal. 2020;110:104444.
[171] Ren H, Tian H, Yu H, Zhou C, Yang D, Liu Q, et al. Development and application of tri-cone bit suitable for the drilling of high-temperature geothermal wells. Natural Gas Industry. 2021;41.
[172] Zhou Y, Wang R, Hu J, Lei X. High-temperature wear mechanism of roller cone bit spiral seal. Wear. 2023;532-533:205112.
[173] Al Hammadi Y, Al Harbi A, Hermawirawan L, Aboulkheir A, Akl B, Amer R. Hybrid Bit Technology: Transforming Tricone-Bit Drilling to New Levels. Abu Dhabi International Petroleum Exhibition & Conference2018.
[174] Zhu X, Dan Z. Numerical simulation of rock breaking by PDC bit in hot dry rocks. Nat Gas Ind B. 2019;6:619-28.
[175] Liu W, Zhu X, Jing J. The analysis of ductile-brittle failure mode transition in rock cutting. Journal of Petroleum Science and Engineering. 2018;163:311-9.
[176] Dai X, Huang Z, Shi H, Wu X. Experimental investigation on the PDC cutter penetration efficiency in high-temperature granite. Geothermics. 2022;98:102281.
[177] Zhang W, Wang Z, Shi Z, Xu P, Chang Z. Influence Mechanism of High Temperature on Drilling Rate and Hardness of Sandstone. Nat Resour Res. 2022;31:2589-601.
[178] Saksala T, Gomon D, Hokka M, Kuokkala V-T. Numerical and experimental study of percussive drilling with a triple-button bit on Kuru granite. Int J Impact Eng. 2014;72:56-66.
[179] Saksala T. Numerical study of the influence of hydrostatic and confining pressure on percussive drilling of hard rock. Comput Geotech. 2016;76:120-8.
[180] Li Y, Peng J, Zhang P, Huang C. Hard Rock Fragmentation in Percussion Drilling Considering Confining Pressure: Insights from an Experimental Study. Int J Rock Mech Min Sci. 2021;148:104961.
[181] Xiong C, Huang Z, Shi H, Yang R, Dai X, He W. 3D Cutting Force Model of a Stinger PDC Cutter: Considering Confining Pressure and the Thermal Stress. Rock Mech Rock Eng. 2021;54:5001-22.
[182] Rafatian N, Miska S, Ledgerwood LW, Ahmed R, Yu M, Takach N. Experimental study of MSE of a single PDC cutter interacting with rock under simulated pressurized conditions. SPE Drill Complet. 2010;25:10-8.
[183] Dai X, Chen P, Huang T. Investigation on the rock failure characteristics and reliability of hybrid drill bits combing shaped PDC cutters and roller-cone elements. Geoenergy Sci Eng. 2024;239:212976.
[184] Cai C, Cao W-Y, Yang X-P, Xie Q-G, Li B-R, Tan Z-B, et al. Rock breakage and temperature rising of rock cutting after high-temperature treatment. Pet Sci. 2025;22:1289-306.
[185] Zhao JC, Li Y, Zhao YS, Feng ZJ, Zhang Y. Study on impact grinding law of granite under the conditions of high temperature and high pressure. Meitan Xuebao/Journal of the China Coal Society. 2010;35:904-9.
[186] Song H, Shi H, Chen Z, Li G, Ji R, Chen H. Numerical study on impact energy transfer and rock damage mechanism in percussive drilling based on high temperature hard rocks. Geothermics. 2021;96:102215.
[187] Liu Q, Huang T. Impact rock-breaking mechanisms and energy transfer laws of conical

tooth bits in hot dry rocks. Pet Explor Dev. 2025;52:1053-63.
[188] Holtzman B, Groebner N, Mittal T. Quench-Spallation Drilling: A Novel Drilling Head Designfor Routine Heat Mining Above the Brittle-Ductile Transition. Proceedings of the 48th Workshop on Geothermal Reservoir Engineering, Stanford, CA, USA2023. p. 6-8.
[189] Aldannawy Ha, Rouabhi A, Gerbaud L. Percussive Drilling: Experimental and Numerical Investigations. Rock Mech Rock Eng. 2022;55:1555-70.
[190] Xi Y, Wang H-Y, Zha C-Q, Li J, Liu G-H, Guo B-Y. Numerical simulation of rock-breaking and influence laws of dynamic load parameters during axial-torsional coupled impact drilling with a single PDC cutter. Pet Sci. 2023;20:1806-27.
[191] Kazi A, Riyaz M, Tang X, Staack D, Tai B. Specific cutting energy reduction of granite using plasma treatment: A feasibility study for future geothermal drilling. Procedia Manuf. 2020;48:514-9.
[192] Li Y, Peng J, Huang C, Lian M, Xu T, Zhang Y, et al. Multi-fractured stimulation technique of hydraulic fracturing assisted by the DTH-hammer-induced impact fractures. Geothermics. 2019;82:63-72.
[193] Sun Z, Mu Z, Huang Z, Li G, Popov Y, Wu X, et al. Hard rock drilling characteristics under axial-torsional isofrequency impact: Insights for improving efficiency of deep energy mineral excavation. Geoenergy Sci Eng. 2024;240:213089.
[194] Shi J, Yang Z, Li G, Qiu Z, Mu Z, Sun Z, et al. Investigations on optimal parameters for enhancing penetration efficiency during axial-torsional coupled impact drilling in hard rock. Geoenergy Sci Eng. 2025;247:213668.
[195] Shi H, He S, Xiong C, Huang Z, He W, Li G. Development and application of a hybrid PDC bit for drilling the high temperature granite formation in the deep geothermal exploration well Fushenre-1. Energy Geosci. 2026;7:100467.
[196] Rickard W, Bailey A, Pahler M, Cory S. 39th Workshop on Geothermal Reservoir Engineering 2014 : Stanford, California, USA, 24 - 26 February 2014 ; Vol. 2. Workshop on Geothermal Reservoir Engineering ; 39. Red Hook, NY, Stanford, Calif: Curran; 2014.
[197] Huang Z, Wu X, Li R, Zhang S, Yang R. Mechanism of drilling rate improvement using high-pressure liquid nitrogen jet. Pet Explor Dev. 2019;46:810-8.
[198] Dai X, Huang Z, Wu X, Zhao H, Shi H. Fluid-solid-thermal coupling analysis of rock failure under the joint action of cutting and jet impingement. Geothermics. 2021;94:102092.
[199] Dai X, Huang Z, Wu X, Shi H, Xiong C. Failure Analysis of High-Temperature Granite Under the Joint Action of Cutting and Liquid Nitrogen Jet Impingement. Rock Mech Rock Eng. 2021;54:6249-64.
[200] Augustine CR. Hydrothermal spallation drilling and advanced energy conversion technologies for engineered geothermal systems: Massachusetts Institute of Technology; 2009.
[201] Song X, Lyu Z, Li G, Sun B. Model evaluation and experimental validation of thermal jet drilling for geothermal energy. Geothermics. 2019;77:151-7.
[202] Wang M, Zhang S, Josue EGN. Hydrothermal Spallation Drilling Technology: An Alternative Method of Geothermal Energy Development. Proceedings of the 2017 2nd International Conference on Electrical, Automation and Mechanical Engineering (EAME 2017): Atlantis Press; 2017. p. 302-5.
[203] Gallucci M. Altarock melts rock for geothermal wells: Millimeter waves could help us

dig deeper and faster than with traditional drills - [News]. IEEE Spectr. 2020;57:8-9.

[204] Bonneville A, Cladouhos T, Petty S, Schults A, Sorlie C. Toward Super Hot EGS: The Newberry Deep Drilling Project. Proceedings of the GRC Transactions, Reno, NV, USA. 2018:14-7.

[205] Houde M, Woskov P, Lee J, Oglesby K, Bigelow T, Garrison G, et al. Unlocking deep superhot rock resources through millimeter wave drilling technology. Transactions—Geothermal Resources Council. 2021:2068-83.

[206] Quaise E. Quaise Energy Achieves Drilling Milestone with Millimeter Wave Technology — Marks New Era for Superhot Geothermal. Houston, TX: BusinessWire; 2025.

[207] Mu Z, Li G, Huang Z, Du T SH. Status and development trend of vibration-impact ROP improvement technologies. Oil Drilling & Production Technology. 2020;42:253-60.

[208] Huang J, Zeng B, He Y, Wang X, Qian L, Xia C, et al. Numerical study of rock-breaking mechanism in hard rock with full PDC bit model in compound impact drilling. Energy Rep. 2023;9:3896-909.

[209] Rossi E, Saar M, Rudolf von Rohr P. The influence of thermal treatment on rock- bit interaction: a study of a combined thermo- mechanical drilling (CTMD) concept. Geotherm Energy. 2020;8:1-22.

[210] Wang W, Liu G, Li J, Zha C, Lian W, Gao R. Numerical investigation on rock-breaking mechanism and cutting temperature of compound percussive drilling with a single PDC cutter. Energy Sci Eng. 2021;9:2364-79.

[211] Zhu X, Luo Y, Liu W, Yang F, Li Z, Lu D. Rock cutting mechanism of special-shaped PDC cutter in heterogeneous granite formation. Journal of Petroleum Science and Engineering. 2022;210:110020.

[212] Chen P, Dai X, Shao F, Ozbayoglu E, Liu W, Wang J. Review of PDC cutter – Rock interaction: Methods and physics. Geoenergy Sci Eng. 2023;228:211995.

[213] Rahmani R, Pastusek P, Yun G, Roberts T. Investigation of Geometry and Loading Effects on PDC Cutter Structural Integrity in Hard Rocks. IADC/SPE International Drilling Conference and Exhibition2020.

[214] Chen P, Meng M, Miska S, Yu M, Ozbayoglu E, Takach N. Study on integrated effect of PDC double cutters. Journal of Petroleum Science and Engineering. 2019;178:1128-42.

[215] Shao Z, Wang Y, Tang X. The influences of heating and uniaxial loading on granite subjected to liquid nitrogen cooling. Eng Geol. 2020;271:105614.

[216] Lyu Z, Song X, Li G. Numerical analysis of characteristics of reaction in hydrothermal jet drilling for geothermal energy. Geothermics. 2019;77:62-74.

[217] Zhang S, Huang Z, Wang H, Li G, Sepehrnoori K, Wu X, et al. Experimental study on the rock-breaking characteristics of abrasive liquid nitrogen jet for hot dry rock. Journal of Petroleum Science and Engineering. 2019;181:106166.

[218] Su S, Hou P, Gao F, Liang X, Ding R, Cai C. Changes in mechanical properties and fracture behaviors of heated marble subjected to liquid nitrogen cooling. Eng Fract Mech. 2022;261:108256.

[219] Samuel A, Rickard WM, Rivas E, Atalay S, Moore J, Self J, et al. Improvement in rate of penetration in FORGE drilling through real time MSE analysis and improved PDC technology. PROCEEDINGS, 47th Workshop on Geothermal Reservoir Engineering2022. p. 1-8.

[220] Al-asadi A. Advancing Geothermal Drilling Through Enhanced Mechanical Specific Energy Equation and Machine Learning Validation: University of Wyoming; 2024.

[221] Yost K, Valentin A, Einstein HH. Estimating cost and time of wellbore drilling for Engineered Geothermal Systems (EGS) – Considering uncertainties. Geothermics. 2015;53:85-99.

[222] Najjarpour M, Jalalifar H, Norouzi-Apourvari S. Fifty years of experience in rate of penetration management: Managed pressure drilling technology, mechanical specific energy concept, bit management approach and expert systems - A review. Journal of Petroleum Science and Engineering. 2022;208:109184.

[223] Teale R. The concept of specific energy in rock drilling. International journal of rock mechanics and mining sciences & geomechanics abstracts: Elsevier; 1965. p. 57-73.

[224] Meng C, Jiajun L, Guodong J, Yongheng C. Optimize method of drilling parameter of compound drilling based on mechanical specific energy theory. Petroleum Drilling Techniques. 2014;42:66-70.

[225] Ji Z, Shi H, Li G, Song H. Improved drifting oscillator model for dynamical bit-rock interaction in percussive drilling under high-temperature condition. Journal of Petroleum Science and Engineering. 2020;186:106772.

[226] Rauenzahn RM, Tester JW. Rock failure mechanisms of flame-jet thermal spallation drilling—theory and experimental testing. International Journal of Rock Mechanics and Mining Sciences & Geomechanics Abstracts. 1989;26:381-99.

[227] Weibull W. A statistical theory of the strength of materials. Proc Am Math Soc. 1939.

[228] Swenson D, Stovall J. PARMILA. Los Alamos national Laboratory internal Memorandum. MP-3-19, January; 1968.

[229] Walsh SD, Lomov IN, Wideman TW, Potter JM. Size dependent spall aspect ratio and its effects in thermal spallation. Int J Rock Mech Min Sci. 2014;70:375-80.

[230] Hu X, Song X, Li G, Shen Z, Lyu Z, Shi Y, et al. An analytical model to evaluate the heating conditions for drilling in hard rock using an innovative hydrothermal spallation method. Appl Therm Eng. 2018;142:709-16.

[231] Capik M, Yilmaz AO, Yasar S. Relationships between the drilling rate index and physicomechanical rock properties. Bull Eng Geol Environ. 2017;76:253-61.

[232] Yenice H, Özdoğan MV, Özfırat MK. A sampling study on rock properties affecting drilling rate index (DRI). J Afr Earth Sci. 2018;141:1-8.

[233] Okoroafor ER, Smith CM, Ochie KI, Nwosu CJ, Gudmundsdottir H, Aljubran M. Machine learning in subsurface geothermal energy: Two decades in review. Geothermics. 2022;102:102401.

[234] Yazitova A, Yagiz S. Performance analysis of drilling machines based on rock properties and machine's specifications. Bull Eng Geol Environ. 2024;83:37.

[235] Yehia T, Gasser M, Ebaid H, Meehan N, Okoroafor ER. Comparative analysis of machine learning techniques for predicting drilling rate of penetration (ROP) in geothermal wells: A case study of FORGE site. Geothermics. 2024;121:103028.

[236] Zhai W, Feng B, Liu S, Jia Z, Jiang Z, Liu Z, et al. A shallow machine learning method based on geothermal drilling data: A case study of well 58–32 at the U.S. FORGE site. Geothermics. 2025;127:103239.

[237] Mantegazini DZ, Nascimento A, Mathias MH, Romero Guzman OJ, Reich M. Optimization of Rate of Penetration and Mechanical Specific Energy Using Response Surface Methodology and Multi-Objective Optimization. Applied Sciences. 2025;15:1390.

[238] Auriol J, Kazemi N, Niculescu S-I. Sensing and computational frameworks for improving drill-string dynamics estimation. Mech Syst Signal Process. 2021;160:107836.

[239] Kong M, Zhang Z, Zhao C, Chen H, Ma X, Zou Y. Rock Mechanical Properties and Breakdown Pressure of High-Temperature and High-Pressure Reservoirs in the Southern Margin of Junggar Basin. Geofluids. 2021;2021:1116136.

[240] Dupriest FE, Koederitz WL. Maximizing Drill Rates with Real-Time Surveillance of Mechanical Specific Energy. SPE/IADC Drilling Conference2005.

[241] Anemangely M, Ramezanzadeh A, Mohammadi Behboud M. Geomechanical parameter estimation from mechanical specific energy using artificial intelligence. Journal of Petroleum Science and Engineering. 2019;175:407-29.

[242] Amani M, Al-Jubouri M. An experimental investigation of the effects of ultra-high pressure and temperature on the rheological properties of water-based drilling fluids. SPE International Conference and Exhibition on Health, Safety, Environment, and Sustainability?: SPE; 2012. p. SPE-157219-MS.

[243] Collins IR, Cano Floriano D, Paevskiy I, Wee J, Boek ES, Mohammadi MK. Transition from oil & gas drilling fluids to geothermal drilling fluids. Geoenergy Sci Eng. 2024;233:212543.

[244] Wang F, Tan X, Wang R, Sun M, Wang L, Liu J. High temperature and high pressure rheological properties of high-density water-based drilling fluids for deep wells. Pet Sci. 2012;9:354-62.

[245] Mohamed A, Salehi S, Ahmed R. Significance and complications of drilling fluid rheology in geothermal drilling: A review. Geothermics. 2021;93:102066.

[246] Altun G, Osgouei AE, Serpen U. Controlling rheological and fluid loss properties of sepiolite based muds under elevated temperatures. Proceedings World Geothermal Congress, Bali, Indonesia, April2010. p. 25-9.

[247] Qu Y, Zhang W, Ren H, Yuan Y, Zhou X, Yang G, et al. Investigation of the correlation between molecular structures with high-temperature and salt resistance for acrylamides polymer in drilling fluid. J Dispersion Sci Technol. 2024;45:1364-72.

[248] Tian M, Yang C, Huang Q, Wang R, Su X, Xu P, et al. Synthesis and Evaluation of High-Temperature-Resistant and Environmentally Friendly Polymer Filter Loss Additives. Polymers (Basel). 2025;17.

[249] Bai J, Wang S, Chen Q, Li Y, Xie C, Zhang J, et al. High-temperature resistant drilling fluid of Sodium-based rectorite modified by organic laponite. Geothermics. 2023;111.

[250] Santoyo E, Garcia A, Espinosa G, Santoyo-Gutiérrez S, González-Partida E. Convective heat-transfer coefficients of non-Newtonian geothermaldrilling fluids. J Geochem Explor. 2003;78-79:249-55.

[251] Mao L, Zhang Z. Transient temperature prediction model of horizontal wells during drilling shale gas and geothermal energy. Journal of Petroleum Science and Engineering. 2018;169:610-22.

[252] Fomin S, Hashida T, Chugunov V, Kuznetsov AV. A borehole temperature during drilling

in a fractured rock formation. Int J Heat Mass Transfer. 2005;48:385-94.

[253] Zhang Z, Xiong Y, Pu H, Peng G, Wang J. Borehole temperature distribution when drilling fluid loss occurs in the two-dimensional area at the bottom-hole during drilling. J Nat Gas Sci Eng. 2020;83:103523.

[254] Mao L, Liu Y, Wei C, Chen X, Yang S. Temperature prediction of geothermal drilling considering the drilling fluid thermophysical parameters. Renewable Energy. 2024;237:121489.

[255] Zhang Z, Xiong Y, Guo F. Analysis of Wellbore Temperature Distribution and Influencing Factors During Drilling Horizontal Wells. J Energy Res Technol. 2018;140.

[256] Yuan Y, Li W, Bian L, Lei J. A Prediction Model for Pressure and Temperature in Geothermal Drilling Based on Physics-Informed Neural Networks. Electronics. 2024;13:3869.

[257] Xie J, Zhang J, Cheng Y, Zhou J, Li X, Li X, et al. Real-Time prediction of wellbore temperatures in deep shale gas drilling using a combination of PINN and heat transfer models. Appl Therm Eng. 2025;279:127984.

[258] Elmousalami H, Sakr I. Artificial intelligence for drilling lost circulation: A systematic literature review. Geoenergy Sci Eng. 2024;239:212837.

[259] Xu C, Zhang H, Kang Y, Zhang J, Bai Y, Zhang J, et al. Physical plugging of lost circulation fractures at microscopic level. Fuel. 2022;317:123477.

[260] Diehl T, Kraft T, Kissling E, Wiemer S. The induced earthquake sequence related to the St. Gallen deep geothermal project (Switzerland): Fault reactivation and fluid interactions imaged by microseismicity. J Geophys Res: Solid Earth. 2017;122:7272-90.

[261] Henriques C, Dahi Taleghani A. An evaluation of fiber-based lost circulation material for fracture plugging using simulations. Geoenergy Sci Eng. 2023;229:212144.

[262] Kibikas W, Chang C, Bauer SJ, Nakagawa S, Dobson P, Kneafsey T, et al. Time-dependent thermal degradation of lost circulation materials in geothermal systems. Geothermics. 2024;121:103038.

[263] Feng Y, Gray KE. Modeling Lost Circulation Through Drilling-Induced Fractures. SPE J. 2017;23:205-23.

[264] Pang H, Chen M, Wang H, Jin Y, Lu Y, Li J. Lost circulation pattern in the vug-fractured limestone formation. Energy Rep. 2023;9:941-54.

[265] Zhao L, Yuan C, Shan K, Gao M, Long X, Xu M, et al. Expandable profile liner technology for mitigating lost circulation and wellbore instability in geothermal drilling. Renewable Sustainable Energy Rev. 2025;209:115109.

[266] Vidal J, Genter A, Chopin F. Permeable fracture zones in the hard rocks of the geothermal reservoir at Rittershoffen, France. J Geophys Res: Solid Earth. 2017;122:4864-87.

[267] Liu W, Li A, Zhu X. The mechanism of wellbore instability in high-temperature fractured granite formation. Energy. 2024;299:131425.

[268] Zhang G, Tang M, He S, Kong L, Yao G, Guo X, et al. Wellbore-formation transient temperature distribution considering heat transfer by fluid seepage while drilling in horizontal well. Geoenergy Sci Eng. 2025;251:213886.

[269] Guenot A, Maury V. Practical Advantages Of Mud Cooling Systems For Drilling. SPE Drill Complet. 1995;10:42-8.

[270] Zhu Z, Wang C, Guan Z, Lei W. Thermal Characteristics of Borehole Stability Drilling in Hot Dry Rock. ACS Omega. 2021;6:19026-37.

[271] Yang Y, Wang Q, Yang F, Hu D, Lu Y, Zhou H. Thermo-mechanical analysis of wellbore stability in ultra-deep formations. J Rock Mech Geotech Eng. 2025.

[272] Wu B, Liu T, Zhang X, Wu B, Jeffrey RG, Bunger AP. A Transient Analytical Model for Predicting Wellbore/Reservoir Temperature and Stresses during Drilling with Fluid Circulation. Energies. 2018;11:42.

[273] Suo Y, Dong M, Fu X, He W, Pan Z. Experimental and numerical simulation research on hot dry rock wellbore stability under different cooling methods. Geothermics. 2024;119:102977.

[274] Chen G, Ewy RT, Yu M. Analytic solutions with ionic flow for a pressure transmission test on shale. Journal of Petroleum Science and Engineering. 2010;72:158-65.

[275] Ma T, Chen P. A wellbore stability analysis model with chemical-mechanical coupling for shale gas reservoirs. J Nat Gas Sci Eng. 2015;26:72-98.

[276] Zhou X, Ghassemi A. Finite element analysis of coupled chemo-poro-thermo-mechanical effects around a wellbore in swelling shale. Int J Rock Mech Min Sci. 2009;46:769-78.

[277] Ghassemi A, Tao Q, Diek A. Influence of coupled chemo-poro-thermoelastic processes on pore pressure and stress distributions around a wellbore in swelling shale. Journal of Petroleum Science and Engineering. 2009;67:57-64.

[278] Gao J, Deng J, Yan W, Feng Y, Wang H, Xia Y. Utilize an Integrated Geomechanical Wellbore Model to Analyze the Horizontal Borehole Failure Regions of Laminated Heterogeneous Shale Formation. 50th US Rock Mechanics/Geomechanics Symposium2016.

[279] Tang Z, Li Q, Yin H. The influence of solute concentration and temperature of drilling fluids on wellbore failure in tight formation. Journal of Petroleum Science and Engineering. 2018;160:276-84.

[280] Yan X, Li M, Xu C, Deng S, Kang Y, Jing H, et al. A new insight into failure mechanism of granular plugging zone for wellbore strengthening in deep fractured reservoirs based on force chains energy dissipation. Eng Geol. 2025;352:108067.

[281] Sonmez A, Kok MV, Bal B, Bagatir G, Gucuyener IH. Comprehensive approach to torque and lost circulation problems in geothermal wells in terms of drilling fluid. Geothermics. 2021;95:102126.

[282] Xiao D, Hu Y, Wang Y, Deng H, Zhang J, Tang B, et al. Wellbore cooling and heat energy utilization method for deep shale gas horizontal well drilling. Appl Therm Eng. 2022;213:118684.

[283] Li X, Yang H, Wei Y, Feng Y, Yang H, Yan W, et al. Wellbore instability in naturally fractured formations: Experimental study and 3D numerical investigation. Gas Sci Eng. 2024;124:205265.

[284] Magzoub MI, Salehi S, Hussein IA, Nasser MS. Loss circulation in drilling and well construction: The significance of applications of crosslinked polymers in wellbore strengthening: A review. Journal of Petroleum Science and Engineering. 2020;185:106653.

[285] Pašić B, Gaurina-Međimurec N, Davorin M. Wellbore instability: Causes and consequences. Rudarsko-Geološko-Naftni Zbornik. 2007;19.

[286] Zhang M, Wen J, Xu Z, Xu Z, Feng J, Zhao X. Study of borehole stability of volcanic rock formation with the influence of multiple factors. J Pet Explor Prod Technol. 2024;14:3367-82.

[287] Liu W, Li A, Zhu X. The wellbore instability mechanism in hot dry rock drilling.

Geoenergy Sci Eng. 2023;231:212298.

[288] Liu W, Chen Z, Li A, Zhu D. Mechanism of wellbore instability while drilling in fractured hot dry rock formations. Natural Gas Industry. 2025;45.

[289] Heidari S, Li B, Jacquey AB. Finite element modeling of wellbore stability in a fractured formation for the geothermal development in northern Quebec, Canada. Geoenergy Sci Eng. 2023;231:212350.

[290] Liu W, Chen Z, Li A, Zhu X. Wellbore instability in hot dry rock drilling under multi-field coupling---new insights from drilling string impact. Energy. 2025;334:137786.

[291] Suo Y, Dong M, He W, Fu X, Pan Z. Modeling wellbore instability in hot dry rock under various temperature conditions. Unconv Resour. 2023;3:275-83.

[292] Aslannezhad M, Kalantariasl A, Keshavarz A. Borehole stability in shale formations: Effects of Thermal-Mechanical-Chemical parameters on well design. J Nat Gas Sci Eng. 2021;88:103852.

[293] Al-Ajmi AM, Zimmerman RW. Stability analysis of vertical boreholes using the Mogi–Coulomb failure criterion. Int J Rock Mech Min Sci. 2006;43:1200-11.

[294] Li X, Jaffal H, Feng Y, El Mohtar C, Gray KE. Wellbore breakouts: Mohr-Coulomb plastic rock deformation, fluid seepage, and time-dependent mudcake buildup. J Nat Gas Sci Eng. 2018;52:515-28.

[295] Valley B, Evans K. Stress State At Soultz-Sous-Forêts to 5 km depth from wellbore failure and hydraulic observations2007.

[296] Ma X, Dong W, Hu D, Zhou H. Mechanical properties of granite at high temperature subjected to true triaxial compression. Int J Rock Mech Min Sci. 2023;164:105313.

[297] Mogi K. Fracture and flow of rocks under high triaxial compression. Journal of Geophysical Research (1896-1977). 1971;76:1255-69.

[298] Meng M, Chen P, Ren R. Statistic evaluation of failure criteria in wellbore stability with temperature effects. Fuel. 2019;252:730-52.

[299] Colmenares LB, Zoback MD. A statistical evaluation of intact rock failure criteria constrained by polyaxial test data for five different rocks. Int J Rock Mech Min Sci. 2002;39:695-729.

[300] Wong T-f, Baud P. The brittle-ductile transition in porous rock: A review. J Struct Geol. 2012;44:25-53.

[301] Byerlee JD. Brittle-ductile transition in rocks. Journal of Geophysical Research (1896-1977). 1968;73:4741-50.

[302] Ewy RT. Wellbore-Stability Predictions by Use of a Modified Lade Criterion. SPE Drill Complet. 1999;14:85-91.

[303] Hoek E, Brown ET. The Hoek–Brown failure criterion and GSI – 2018 edition. J Rock Mech Geotech Eng. 2019;11:445-63.

[304] Maurer V, Gaucher E, Grunberg M, Koepke R, Pestourie R, Cuenot N. Seismicity induced during the development of the Rittershoffen geothermal field, France. Geotherm Energy. 2020;8.

[305] Aadnoy BS, Ong S. Introduction to special issue on Borehole Stability. Journal of Petroleum Science and Engineering. 2003;38:79-82.

[306] Zhao Y, Feng Z, Xi B, Wan Z, Yang D, Liang W. Deformation and instability failure of

borehole at high temperature and high pressure in Hot Dry Rock exploitation. Renewable Energy. 2015;77:159-65.

[307] Peter-Borie M, Loschetter A, Merciu IA, Kampfer G, Sigurdsson O. Borehole damaging under thermo-mechanical loading in the RN-15/IDDP-2 deep well: towards validation of numerical modeling using logging images. Geotherm Energy. 2018;6.

[308] Massiot C, McNamara DD, Nicol A, Archibald G, Townend J. Fracture geometries and processes in andesites at Mt Ruapehu, New Zealand: implications for the fracture modelling of the Rotokawa Geothermal Field. 34th GOCAD Meeting, France; 2014.

[309] Yuan C, Wei Z, Ma Z, Gao Y, Xu J, Tang K. Rock damage and fault reactivation mechanisms under initial perturbation in enhanced geothermal systems. Energy Geosci. 2026;7.

[310] He S, Zhou J, Chen Y, Li X, Tang M. Research on wellbore stress in under-balanced drilling horizontal wells considering anisotropic seepage and thermal effects. J Nat Gas Sci Eng. 2017;45:338-57.

[311] Li Y, Peng J, Bo K, Huang C, Zhang Y, Zhang P. Analysis on the mechanical properties of granite rock near the wellbore after percussive drilling and AWJ perforation. Journal of Petroleum Science and Engineering. 2020;184:106489.

[312] Yang H, Li J, Zhang H, Jiang J, Guo B, Gao R, et al. Thermal behavior prediction and adaptation analysis of a reelwell drilling method for closed-loop geothermal system. Appl Energy. 2022;320:119339.

[313] Verma S, Sirdesai NN, Goel MD. Comprehensive review on the impact of high temperatures and dynamic loading on rocks in construction materials. Physics and Chemistry of the Earth, Parts A/B/C. 2025:103934.

[314] Li X, Chai B, Qi C, Shao Z. Macro-meso fracture mechanical mechanisms of creep in brittle rocks after high-temperature heat treatment. Chinese Journal of Underground Space and Engineering. 2025;21:1514-24.

[315] Zhang L, Wei X, Zhang Y. The creep model based on nonlinear Newton body under different temperature conditions. Sci Rep. 2023;13:4822.

[316] Jiang H, Yin W, Zhang K, Zhang F. Three-dimensional nonlinear Nishihara creep-Ubiquitous joint model considering high temperature effect. Therm Sci Eng Prog. 2025;61:103528.

[317] Xi B, He S, Wu Y, Chen Z, Cui J. Rheological deformation and failure laws of boreholes in granite under thermo-mechanical coupling and its application in deep hole drilling of hot dry rock for geothermal energy exploitation. IOP Conf Ser: Earth Environ Sci. 2020;570:032045.

[318] Merzouki J, Poulachon G, Rossi F, Ayed Y, Abrivard G. Method of Hole Shrinkage Radial Forces Measurement in Ti6Al4V Drilling. Procedia CIRP. 2017;58:629-34.